910013 C
GADR 55
VOLUME 2

CONSOLIDATED DESIGN REPORT FOR THE MODEL FSV-1 SHIPPING CASK

CONFIGURATIONS E, F and G

GENERAL ATOMICS

910013 C
GADR 55
VOLUME 2

CONSOLIDATED DESIGN REPORT FOR THE MODEL FSV-1 SHIPPING CASK

CONFIGURATIONS E, F and G

List of Effective Pages
For Volume II

Page Number	Page Count	Revision
i to ii	2	C
iii to iv	2	N/C
1-1 to 1-13	13	N/C
2-1 to 2-66	66	N/C
2-66a to 2-66e	5	N/C
2-67 to 2-190	124	N/C
3-1 to 3-22	22	N/C
4-1 to 4-12	12	N/C
5-1 to 5-19	19	N/C
6-1 to 6-29	29	N/C
7-1 to 7-18	18	N/C
7-19	1	C
7-20 to 7-23	4	N/C
7-24	1	C
7-25 to 7-27	3	N/C
7-28	1	C
8-1 to 8-13	13	N/C
9-1 to 9-2	2	N/C
Total Pages (Volume II)	337	

See Volume I for List of Effective Pages for Volume I.

TABLE OF CONTENTS

TABLE OF CONTENTS (Continued)

SECTION 1.0

GENERAL INFORMATION

1.1. INTRODUCTION

Volume II of GADR 55 provides a description and an evaluation of Model FSV-1 in Configurations E, F and G as shown in Table 1-1.

Volume I of the GADR 55 provides a description and an evaluation of Model FSV-1 packaging in Configurations A, B, C and D. Some evaluations and diagrams that apply to configurations E, F and G may be found in Volume I of GADR-55.

1.2. PACKAGE DESCRIPTION

The Model FSV-1 in Configuration E is designed and evaluated for the transport of spent nuclear fuel elements from the Fort St. Vrain High-Temperature Gas-Cooled Reactor. Configurations F and G are designed and evaluated for the transport of large quantities of solid, nonfissile, irradiated and contaminated hardware. These packages have a loaded weight of approximately 47,600 pounds and the maximum weight of the cavity contents is 4430 pounds. The length of the package, with the impact limiter installed is 229.45 inches with a maximum diameter of 46.7 inches at the impact limiter. The remaining 196.6 inches of the package has a diameter of 28 inches. These configurations have been grouped together since the impact limiter is used in each of these shipping configurations.

1.2.1. Packaging

Model FSV-1 in Configurations E, F and G all use the same cask body and impact limiter as shown on GA Technologies Inc. drawings GADR 55-2-1 Issue C, GADR 55-2-2 Issue A, and GADR 55-2-3 Issue B. Only Model FSV-1 in Configuration E uses the inner container as shown on the above referenced

TABLE 1-1
MODEL FSV-1A CASK AND CONFIGURATIONS
CONFIGURATIONS E THROUGH G

Configuration	Reference Drawings	Authorized Contents	Allowable Weight-Cask Cavity	Allowable Weight-Contents	Remarks
E	70086F, Rev. 7 (a) 1501-003, Rev. C (b) 70296F, Rev. 2 (a) GADR55-2-1 Issue C GADR55-2-2 Issue A GADR55-2-3 Issue B	Irradiated fuel elements with graphite body-1.4 kg of U 235 and 11.3 kg thorium - wt 300 lb	4430 lb	1800 lb	Requires impact limiter Requires inner container Loaded wt 47,600 lb
F	70086F, Rev. 7 1501-003, Rev. C 70296F, Rev. 2 GADR55-2-1 Issue C GADR55-2-2 Issue A GADR55-2-12 Issue C GADR55-2-13 Issue A	Solid, nonfissile, irradiated and contaminated hardware	4430 lb	Depends on spacer up to 2800 lb	Inner container not required. Wt of burial canister with shield plug is 1635 lb Loaded wt 47,600 lb
G	70086F, Rev. 7 1501-003, Rev. C 70296F, Rev. 2 GADR55-2-1 Issue C GADR55-2-2 Issue A GADR55-2-12 Issue C GADR55-2-13 Issue A	Solid, nonfissile, irradiated and contaminated hardware	4430 lb	900 lb	Requires impact limiter Inner container not required. Wt of burial canister plus spacer with supplemental shielding is 3530 lb Loaded wt 47,600 lb

(a) National Lead Company drawing.
(b) General Atomics drawing.

910013 NC

drawings and Fig. 1-1. Configuration F uses a burial canister with a suitable spacer and a shield plug that provides supplemental shielding as shown on Fig. 1-2. Configuration G uses the same burial canister and shield plug as the Configuration F, and in addition uses a spacer that provides supplemental shielding as shown on Fig. 1-3.

1.2.2. Operational Features

Model FSV-1 package has a smooth external surface that simplified decontamination. Lifting attachments on the package consist of sockets rather than trunnions since sockets are less likely to be damaged in a manner that would impair any safety function of the package. Tie-down of the package to the rear support on the transport semitrailer is by means of four (4) socket head cap screws which are installed into threaded inserts located in the base of the cask body. This attachment arrangement prevents any damage that is likely to impair any safety function of the package.

1.2.3. Contents of Packaging

The contents of Model FSV-1 in Configuration E consist of six spent fuel elements from the Fort St. Vrain, High Temperature Gas-Cooled Reactor. Each fuel element is a hexagonal graphite block approximately 31 inches long and 14 inches across the flats. Each fuel element has a weight of approximately 300 pounds and contains a maximum of 1.4 kilograms of 93.5% enriched uranium and about 11.3 kilograms of thorium, with a thorium/uranium ratio of at least 8.1/1.

The contents of Model FSV-1 in Configurations F and G consist of solid, nonfissile, irradiated and contaminated hardware. Examples of such reactor hardware include, but are not limited to, control rods, fuel channels, poison curtains, shrouds, power range monitors, and miscellaneous structures.

9-L.

FIGURE WITHHELD UNDER 10 CFR 2.390

FIGURE WITHHELD UNDER 10 CFR 2.390

Figure 1-2

FIGURE WITHHELD UNDER 10 CFR 2.390

FIGURE WITHHELD UNDER 10 CFR 2.390

FIGURE WITHHELD UNDER 10 CFR 2.390

FIGURE WITHHELD UNDER 10 CFR 2.390

Configurations F and G
Cask with Burial Canister

FIGURE WITHHELD UNDER 10 CFR 2.390

FIGURE WITHHELD UNDER 10 CFR 2.390

SECTION 2.0

STRUCTURAL EVALUATION

2.0 STRUCTURAL EVALUATION

2.1. STRUCTURAL DESIGN

2.1.1. Discussion

Principal structural components of Model FSV-1 in Configurations E, F and G are the cask body with the outer closure, the inner container with the inner closure and the impact limiter which protects the closure end of the package. These components are shown on the design drawings located in Section 1.0.

Configurations F and G use a burial canister in place of the inner container. This component is shown on the design drawing located in Section 1.

2.1.2. Design Criteria

Model FSV-1 was designed to comply with all regulatory requirements in effect at the time of application for a certificate of compliance. An initial application was submitted to the U.S. Atomic Energy Commission in April 1969. This application described and evaluated the basic package without the impact limiter. A later application, submitted to the U.S. Nuclear Regulatory Commission in August 1977, described and evaluated the package with an impact limiter and with modified inner and outer closures used in Configurations E, F and G.

Table 2-1 lists the structural conditions analyzed. The sections where the analyses are presented are also listed.

TABLE 2-1
GADR 55, VOLUME II CROSS-REFERENCE TO 10CFR71 REQUIREMENTS

	Section
Normal Conditions of Transport:	
Heat (Differential Thermal Expansion)	2.6.1
Cold (Differential Thermal Expansion)	2.6.1
Pressure	2.5.2, 2.6.3
Vibration	2.6.2
Water Spray - not significant for this type of packaging-	
Free Drop	
- Bottom	2.6.4.1
- Side	2.6.4.2
Penetration - not significant for this type of packaging-	
Hypothetical Accident Conditions	
Free Drop	
- End	2.7.1.1
- Side	2.1.4, 2.7.1.2
- Bottom Corner	2.7.1.10
Puncture	2.7.2
Thermal (Differential Thermal Expansion)	2.6.1
Water Immersion - not significant for this type of packaging-	
Package Standards	
Load Resistance	2.5.1
External Pressure	2.5.2

910013 NC

blank page

blank page

2.1.3. Plywood Impact Limiter

The impact limiter was designed to fit and protect Model FSV-1 in Configurations E, F and G during the hypothetical accident conditions.

This impact limiter, described in Figure 2-1, is made up with sufficient 3/4-in. plywood circular sections glued together to absorb the kinetic energy of the cask when dropped from a 30-ft height. These plywood sections are then glued in turn to an aluminum cylinder and end cap which serve as load carrying members. The combined limiter fits snugly over the closure end of the cask body and is secured in place by a retaining ring.

2.1.4. Impact Limiter Loads Analysis

Considerations pertaining to the structural evaluation of the impact limiter are discussed below for the side drop case. The impact loads, although complex, were examined firstly from a most probable standpoint and secondly, discussed from the viewpoint of a later time increment.

The first loading is that of a side drop inducing an uncapping moment by the crushing force that is not balanced by direct reaction loads. This uncapping moment must be balanced by two internally generated forces producing an opposing moment. The internal compressive reacting load is generated by the resulting upper cap-half pressure loading. Lower opposing tension loading is assumed to act over the projected hollow aluminum cylinder arc sector that reacts the compressive plywood crush force. Obviously, this plywood crushing force is not at right angles to the required tension force. These tension forces could be realized but this arrangement is too overly conservative. This is evidenced in light of the

FIGURE 2-1

PLYWOOD IMPACT LIMITER

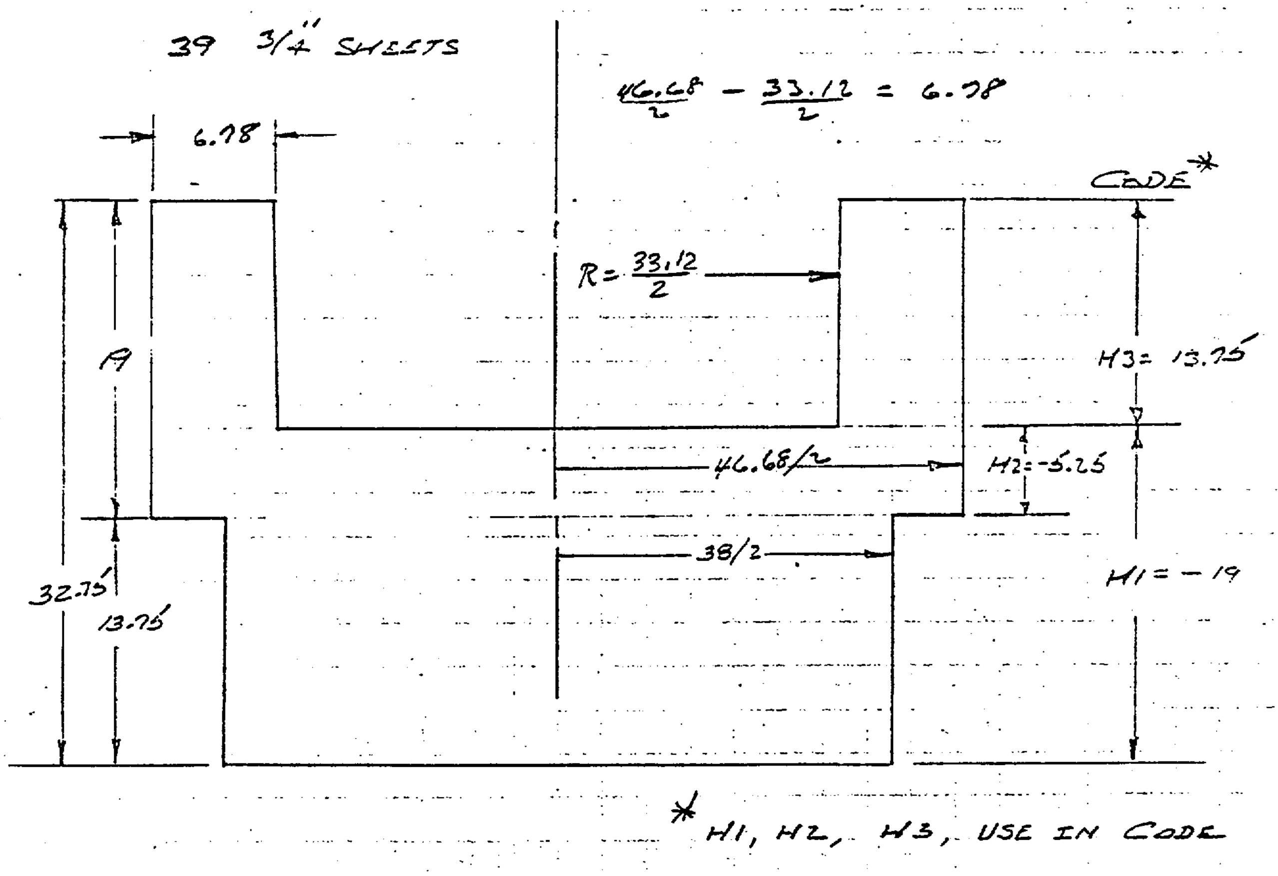

low tension/normal force ratio of 0.049. This in itself is conservative as the assumed arc sector over which the tension force is generated is in reality just about half of the actual projected aluminum cyliner width. Any tension load tails off as the full diameter is approached. A judicious use of approximately 8% of the referenced static friction factor was found to be required for generation of the tension force. This is felt to be the total tension force; resulting in no net tension force required by the tie down studs.

A second consideration of impact limiter reaction loading to the side drop case is that due to a jamming action. This action, initially, is similar to that first discussed. The difference, however, is that the uncapping moment now is considered to be reacted by the upper outer edge and lower inner edge loads. This loading is difficult to analyze but appears to cause local yielding of the upper outer cylinder edge. The resulting yielding allows a redistribution of stress by spreading the applied load over a greater edge or band area. This action tends to induce cylinder bending along with the cylinder hoop tension stress. At some later time interval, the cask body section 'rotates' downward (with respect to the impact limiter cap) since the lower cask body section is free. This rotation causes a reversing affect on the internal reaction loading. But now the plywood crushing load is redistributed.

The upcapping moment is reduced somewhat and must be reacted by forces similar to those first discussed.

A most probable occurrence is that the resulting reaction loads are a combination of both the above schemes; compression-tension (tension supplied by friction forces) and jamming. It is felt however that greater emphasis be placed upon the former loading consideration.

Diagram Depicting Loading Considerations

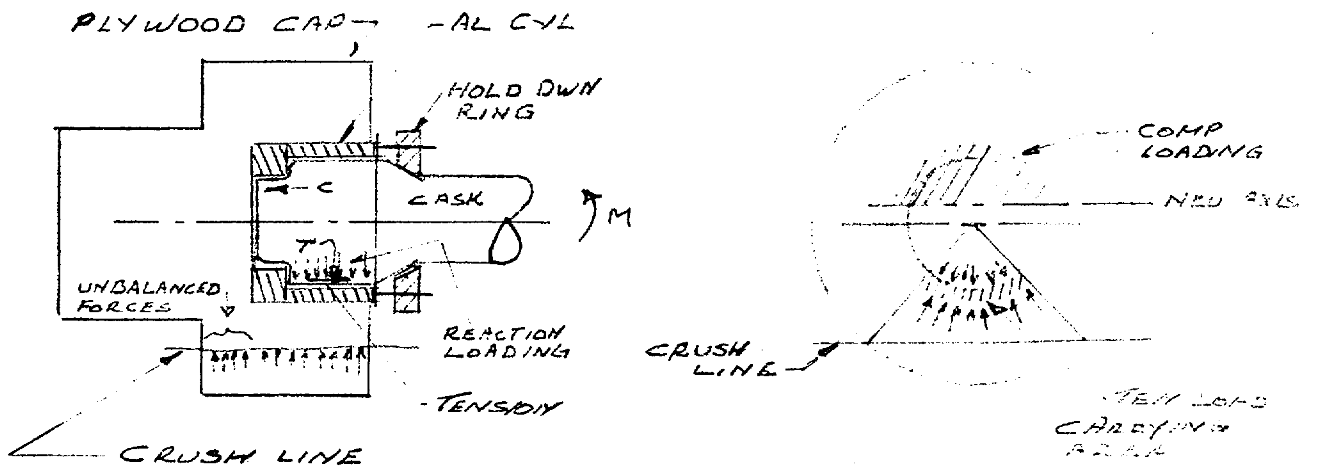

FRICTION SCHEME

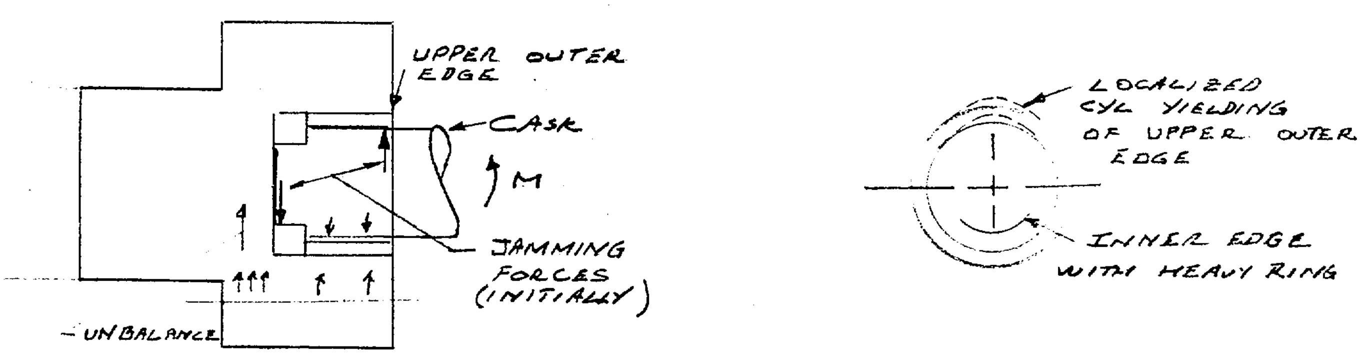

JAMMING SCHEME

910013 NC

2.1.5. Impact Limiter Loads Analysis 30-ft Side Drop

The sketch below shows an axial view of a 90° ground impact with a plywood crush average of 3.925 in. (58%).

$$\sigma_{58\%} = 3500 + 1118(58-50) = 12{,}444 \text{ Psi}$$

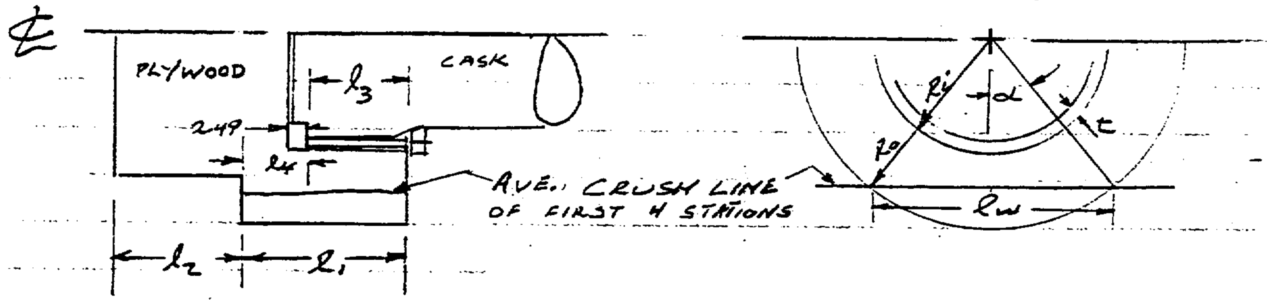

ℓ_1 = 19.0 in.

ℓ_2 = 13.75

ℓ_3 = 11.26

ℓ_4 = 7.74

R_i = 16.56 in.

R_o = 23.34 in.

t = 1.0 in.

$$\alpha = \cos^{-1} \frac{R_o - 3.925}{R_o} = \cos^{-1} \frac{23.34 - 3.925}{23.34} = \underline{33.71}$$

$$= \underline{(0.5884 \text{ Rad})}$$

$$\ell w = 2 R_o \sin\alpha = 2 (23.34) \sin 33.71 \quad \underline{25.91 \text{ in.}}$$

2.1.5.1 Unbalanced Load Over Length ℓ_4 (crush < 50% over ℓ_4)

$$P_u = q\,\ell w\,(\ell_4 - 2.49) = 3500\,(25.91)\,5.25 = \underline{4.761 \times 10^5 \text{ lb}}$$

2.1.5.2 Cylinder Moment at Ring (ℓ_4) (Ring Bottom)

$$\mu = P_u \frac{2.49 + \ell_4}{2} + \ell w \frac{2.49^2}{2} (12{,}444) = \underline{3.446 \times 10^6 \text{ in. lb}}$$

2.1.5.3 Cylinder Bending Stress

$$I_{cy} = \pi/4\,(R^4 - (R - t)^4) =$$

$$= \pi/4\,(16.56^4 - 15.56^4) = \underline{13{,}026 \text{ in.}^4}$$

$$\sigma_B = \mu / I_{cy} = 3.446 \times 10^6\,(16.56)/13{,}026 = \underline{4381 \text{ psi}}$$

2.1.6 Impact Limiter Neutral Axis and Inertia Calculations

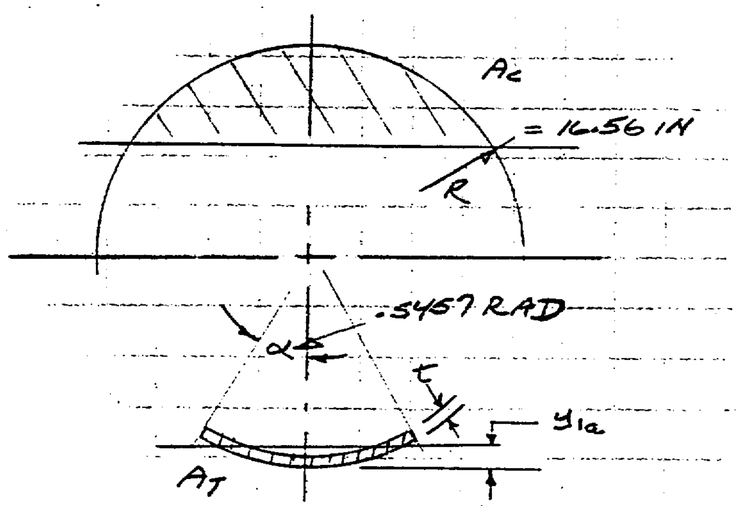

End View Looking into Impact Limiter Showing
Load Areas for Neutral
Axis Calculation

Coarse cross hatched upper sections reacts compression force; the lower aluminum arc sector determined from 50% plywood crush and supplies the required tension to react the uncapping moment.

$$A_T = \alpha t\ (2R - t),\ I_{y_{oT}} = I_{y_{(R-y_{1a})}},\ y_T = (R - y_{1a})$$

2.1.6.1 Sector Centroidal Axis:

$$y_{1a} = R\left\{1 - \frac{2\ \text{Sin}\alpha}{3\alpha}\left(1 - \frac{t}{R} + \frac{1}{2 - t/R}\right)\right\}$$

$$I_{y_{(R-y_{1a})}} = R^3 t\left\{\left(1 - \frac{3t}{2R} + \frac{t^2}{R^2} - \frac{t^3}{4R^3}\right) x \left(\alpha + \sin\alpha\ \cos\alpha - \frac{2\ \sin^2\alpha}{\alpha}\right)\right\}$$

$$+ \frac{t^2\ \sin^2\alpha}{3R^2\alpha\ (2-t/R)}\ (1 - t/R + t^2/6R^2)\Big)$$

Equation development for the compressive area is expanded on the following pages due to the greater complexity involved.

The tension area properties are noted below and need only be transferred about the neutral axis developed in the following pages. The lower tension area is

$$A_T = 0.5757 \times 1 \times (2 \times (16.56) - 1) = \underline{17.52788 \text{ in.}^2}$$

and

$$I_y = I_{y_{1a}} = \text{below} = \underline{9.866 \text{ in.}^4}$$

$$y_T = \text{below} = \underline{15.28 \text{ in.}}$$

2.1.6.2 Where Numerics are Substituted into Previous Equations

$$I_{y_{oT}} = 16.56^3 \ (1) \left\{ \left(1 - \frac{3(1)}{2\ 16.50} + \frac{1}{16.56^2} - \frac{1^3}{4(16.56)^3} \right) x \right.$$

$$\left(0.5457 + \sin 0.5457 \cos 0.5457 - \frac{2 \sin^2 0.5457}{0.5457} \right)$$

$$+ \frac{1^2 \sin^2 0.5457}{3\ (16.56)^2\ 0.5457\ (2 - 1/16.56)} \left(1 - \frac{1}{16.56} \right.$$

$$\left. \left. + \frac{1}{6\ (16.56)^2} \right) \right\}$$

$$= (4541.308) \ \{0.913012\ (0.0020610) + 0.00030935\ (0.94022)\}$$

$$(4541.308) \quad (0.00188192 \quad + \quad 0.000290858)$$

$$(4541.308) \quad (0.00217257)$$

$$I_{y_{oT}} = 9.866 \text{ in.}^4$$

$$y_{1a} = 16.56 \left\{1 - \frac{2 \sin 0.5457}{3\ (0.5457)} \left(1 - \frac{1}{16.56} + \frac{1}{2 - 1/16.56}\right)\right\}$$

$$= 16.56\ \{1 - 063407\ (1.4552)\}$$

$$= 16.56\ (0.0773) = \underline{1.28036 \text{ in.}}$$

$$R - y_{1a} = 16.56 - 1.28 = \underline{15.28 \text{ in.}}$$

The lower tension inertia is calculated as

$$I_{T_{NA}} = I_o + A_T\ \bar{y}_T^2$$

$$= 9.866 + 17.528\ (24.478)^2 = \underline{10{,}512 \text{ in.}^4}$$

2.1.6.3 Neutral Axis Calculations

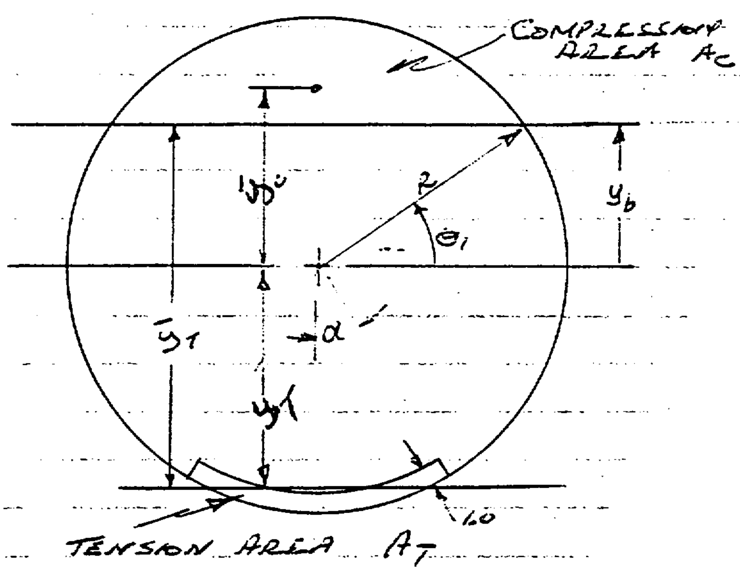

$$\bar{Y}_c = \frac{2\int_0^{x=\sqrt{R^2 - y_o^2}} \int_{y_b}^{\sqrt{R^2 - x^2}} dxydy}{2\int_0^{x} \int_{y_b}^{\sqrt{R^2 - x^2}} dx\ dy}$$

$$\bar{y} = \frac{2/3\ (R^2 - y_h^2)^{3/2}}{R^2 \sin^{-1} \frac{\sqrt{R^2 - y^2}}{R} - y_b \sqrt{R^2 - y^2}}$$

An iteration scheme was used to determine (y_b) the neutral axis for the tension/compression areas, i.e.,

$A_c\ (y_c - y_b) = A_T\ (y_T + y_b)$; by assuming a value for 'y_b' then calculating '$\bar{y}$'. 'A_T' and 'Y_t' are known and fixed as is R with y_b = 9.198

'A_c' calculated 142.611, $y_b + y_T$ = 24.478. 'y_c' was calculated 3.0085

$$142.611(3.0085) \stackrel{?}{=} 17.528\ (15.28 + 9.198)$$

$$429.045 \stackrel{?}{=} 429.050 \quad \text{o.k.}$$

with 'y_b' evaluated, 'θ' may be calculated along with I_{yc} about the neutral axis

2.1.6.4 Compressive Area Section Properties

$$I_1 = 2\int y^2\, x\, dy = 2\int y^2 (R^2 - y^2)^{1/2}\, dy$$

where $y = R \sin\theta$

$dy = R \cos\theta\, d\theta$

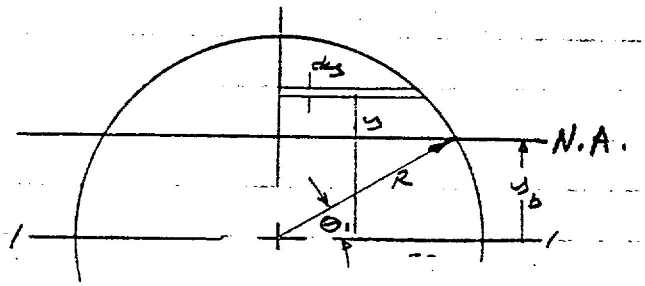

$$I_1 = 2\int_{\theta_1}^{\pi/2} R^2 \sin^2\theta \sqrt{R^2 - R^2 \sin^2\theta}\,(R \cos\theta\, d\theta)$$

$$= \frac{R^4}{8}(\pi = 2\theta_1 + \sin 2\theta_1 - 4 \sin^3\theta_1 \cos\theta)$$

I_1 = 21,787 in.^{4}

$$I_{NA} = I_{yc} = I_1 - A_c(y_b + y_c)^2 + A_c\, y_b^2$$

$$= 21{,}787 - 142.611\ [(9.198 + 3.0085)^2 - 3.0085^2]$$

$$= 21{,}787 - 142.611\ [149 - 9.05] = \underline{1829}$$

2.1.6.5 Total Section Inertia

Combining I_{y_c} and $(I_{y_{OT}} + A_T\, \bar{y}_T^2)$

$$I_{y_b} = I_{y_c} + I_{y_{OT}} + A_T\, \bar{y}_T^2$$

1829 + 9.87 + 17.528 24.478^2 = 12,341 in.^{4}

2.1.7 Impact Limiter Loads Analysis

If moment is reacted over the cylinder/cap and hollow sector of the cylinder

$$\sigma = M\, C_{NA}/I_{y_b}\ ,$$

$$C_{NA} = R_{it}\ \bar{y} = 16.56 + 9.20 = \underline{25.76\ \text{in.}}$$

Tension

$$\sigma_T = 3.446 \times 10^6\ 25.76/12{,}341 = \underline{7195\ \text{psi}}$$

Compression

$$\sigma_c = 3.446 \times 10^6\ (16.56 - 9.20)/12{,}341 = \underline{2055\ \text{psi}}$$

2.1.7.1 Impact Limiter - Stud Loads

Pull down load derived from moment:

$$F(\bar{y}_c + y_T) = M \qquad \bar{y}_c + y_T = \text{centroid/centroid distance}$$

$$y = 12.2065 + 15.28 = 27.49\ \text{in.}$$

$$F = M/(y) = 3.446 \times 10^6/27.49 = \underline{125{,}355\ \text{lb}}$$

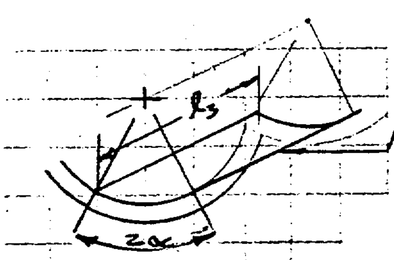

Inside Bearing Area of Aluminum Cylinder

Normal Force F_N Aluminum Cylinder/Stainless Steel

Av crush 3.925; 2α = 1.1768 rad; $\sigma_{59\%}$ 12,444 psi

$$F_N = R\ (2\alpha)\ \ell_3\ q = (15.56)\ 1.1768\ (11.26)\ 12{,}444 = \underline{2.566 \times 10^6\ \text{lb}}$$

$$F/F_N = 125{,}355/2.566 \times 10^6 = \underline{0.049}$$

Coefficient of function for friction force calculation was taken from the table below which is lifted from "Marks Mechical Engineering Handbook 4th Ed. pg. 234, Table 3.

	Hard Steel	Mild Steel	Platinum	Nickel	Copper	Brass	Alumninum	Glass	Tin	Lead
Hard steel	0.39									
Mild steel	0.41	0.41								
Platinum	0.40	0.43	0.45							
Nickel	0.43	0.43	0.39	0.39						
Copper	0.55	0.53	0.50	0.56	0.60					
Brass	0.54	0.51	0.56	0.50	0.62	0.63				
Aluminum	0.65	0.61	0.80	0.75	0.70	0.71	0.94			
Glass	0.61	0.72	0.57	0.73	0.68	0.87	0.85	0.94		
Tin	0.79	0.77	0.86	0.90	0.88	0.75	0.91	0.94	1.11	
Lead	1.96	1.93	2.07	2.15	1.95	2.11	2.00	2.40	2.20	3.30

The coefficient of friction, μ, for mild steel and aluminum, which is representative of the impact limiter aluminum cylinder and the stainless steel cask is seen to be 0.61.

The friction force F_R that may be realized is:

$$F_R = \mu F_N = 0.61 \times 2.566 \times 10^6 = \underline{1.565 \times 10^6\ \text{lb}}$$

$F_{req'd}$ = <u>125,355 lb</u>

Margin:

$F_R/F_{req'd} = 15.65/1.25 = \underline{12.5}$

or approximately 8% of the available friction force is required. Therefore, the tie-down studs provide no net tension load due to the 90° side drop.

However, rotational axial loads do not depend on friction and the loads must be taken up by the hold down studs. Rotational loads are calculated as follows:

2.1.7.2 Centripetal Force Due to Rotation: Assuming total kinetic translational energy is converted to rotational energy:

$$KE = 1/2\ M\ v^2 = 1/2\ I\ \omega^2 \qquad {}_oI = I + M\ (L/2)^2$$

$$v = \sqrt{2gh} = \sqrt{2\ (386.4)\ 360} = \underline{5.275 \times 10^2}\ \text{in./sec}$$

$$I = 1/12\ M\ \ell^2 + M\ (\ell/2)^2$$

$$= 1/12\ (120)\ 210^2 + (120)\ 105^2 = \underline{1.764 \times 10^6}\ \text{lb sec}^2\ \text{in.}$$

$$\omega^2 = M\ v^2/I = 120\ (5.275 \times 10^2)^2/1.764 \times 10^6 = \underline{18.93}\ \text{rad}^2/\text{sec}^2$$

Centrifugal Acceleration

$$n_z = \ell\ \omega^2/g = 210\ (18.93)/386.4 = \underline{10.29}\ g$$

Centripetal Force on Studs

$$F = n_z W = 10.29\ (1060) = \underline{10,910}\ \text{lb total}$$

Stud Load = F/n = 10,910/6 = 1,820 lb/stud

Stud Stress F/A_R = 1820/0.1257 = 14,480 psi

Studs: 1/2 - 13 - A_R = 0.1257 in.² root area

Impact Limiter Insert Strength

Per 'Keensert' Catalog No. 200-A, minimum shear contact area x ult shear of the particular material

Shear ultimate = 60% tension ultimate* | 300°F (6061-T6) 10,000 hr

= 0.6 x 37,400 = 22,440 psi

Pull Out Strength of Insert

Calculated Pull Out Strength = Minimum Shear Stud Engage Area x Minimum Ult Shear Strength of Parent Mat

= 0.7172 (22,400) = 16,065 lb

Pull Out Margin

Pull out/applied = 16,065/1820 = 8.8

2.1.8 Impact Limiter Retaining Ring

Material: 6061-T6 Al. alloy

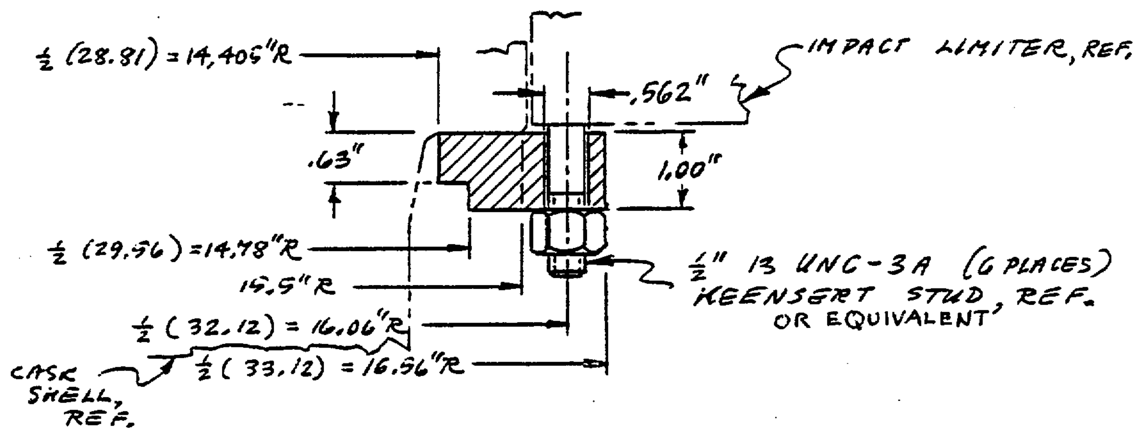

SECTION PROPERTIES

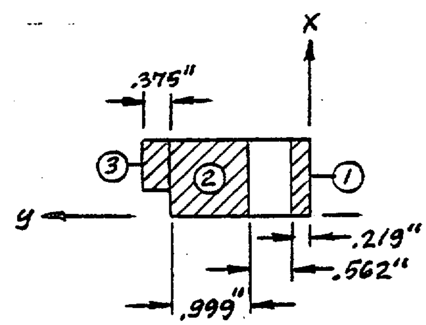

$I_{xo} = \frac{1}{12} b h^3$

Item	A	x	x²	Ax	Ax²	Ixo	Ax² + Ixo	y	Ay
1	0.219	0.50	0.25	0.1095	0.05475	0.01825	0.07300	0.1095	0.02398
2	0.999	0.50	0.25	0.4995	0.24975	0.08325	0.33300	1.2805	1.27922
3	0.23625	0.685	0.4692	0.1618	0.11085	0.00781	0.11866	1.9675	0.46482
Σ	1.45425	--	--	0.7708	0.41535	0.10931	0.52466	--	1.76802

$(\bar{x})\ (\Sigma A) = \Sigma(AX) = (\bar{x})\ (1.45425) = 0.7708\ ;\ \bar{x} = \underline{0.53005\text{ in.}}$

$I_{NA} = \Sigma(Ax^2 + Ixo) - (\bar{x})\ (\Sigma(AX)) = 0.52455 - (0.530050\ (0.7703)$

$= \underline{0.1161\text{ in.}^4}$

$(\bar{y})\ (\Sigma A) = \Sigma\ (Ay) = (\bar{y})\ (1.45425) = 1.76802;\ \bar{y} = \underline{1.21576\text{ in.}}$

$R = 1/2\ (33.12) - \bar{y} = 16.56 - 1.21576 = \underline{15.344\text{ in.}}$

2.1.8.1 Inertia Load

$$10{,}350\text{ lb} \sim \frac{10{,}350}{2\pi\ (15.344)} = \underline{107\text{ lb/in.}}$$

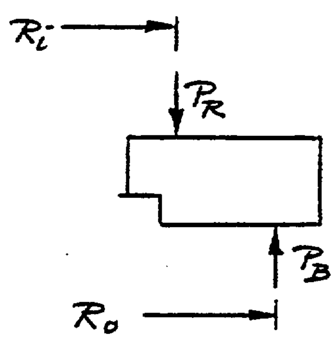

$R_i = 1/2\ [14.405 + 15.5] = \underline{14.9525\text{ in.}}$

$R_o = \underline{16.06\text{ in.}}$

Moment arm $= R_o - R_i$

$= 16.06 - 14.9525$

$= \underline{1.1075\text{ in.}}$

$M = (107)\ (1.1075) = \underline{118.5\text{ in. lb/in.}}$

Ring bending moment due to couple on section moment = MR

$= (118.5)\ (15.344) = \underline{1818\text{ lb in.}}$

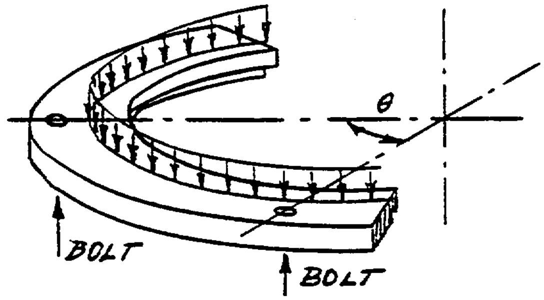

Ring stress due to redistribution of bolt load as indicated on sketch:

Assume for simplicity a straight beam uniformly loaded and fixed at both ends.

$L = \theta R = (160)\ \pi/180\ (15.344) = \underline{16.07 \text{ in.}}$

$p = \underline{107 \text{ lb.in.}}$

$M_{max} = 1/12\ p\ L^2 = 1/12\ (107)\ (16.07)^2 = \underline{2310 \text{ in. lb}}$

Total ring bending moment = 1818 + 2310 = 4128 in. lb

$$\sigma = \frac{M_c}{I} = \frac{(4128)\ (0.53005)}{0.1161} = \underline{18{,}846 \text{ psi}};\ < \sigma_{yield} = 30{,}000 \text{ psi}$$

2.1.8.2 Bolt Preloading

Maximum nut installation torque specified = 12 ft lb

$T = 12 \text{ ft lb} = 12 \times 12 = \underline{144 \text{ in. lb}}$

13 UNC: coarse threads (1/2 in. diam)

With a friction factor of F = 0.15 a K-value of K = 0.098585 is found from Table I of "Bolt Torque Factors," by R. H. Lipp, Design News, March 8, 1971 issue.

$$P = \text{axial load of bolt} = \frac{T}{K} = \frac{144}{0.098585} = 1461 \text{ lb}$$

Total axial load = 6P = 6 x 1461 = $\underline{8764 \text{ lb}}$

Bolt stress area: A = <u>0.1416 in.²</u>

$$\sigma_{bolt} = \frac{1461}{0.1416} = \underline{10,315 \text{ psi}}$$

Bolt preloading total = 8764 lb is less than inertia load 10,350 lb: Impact limiter will slide forward a small amount during rotation of cask.

Ring stress for preloading of bolts to 12 ft lb:

$$\sigma = (18.846)\ \frac{8,764}{10,350} = \underline{15,958 \text{ psi}};\ < \sigma_{yield} = 30,000 \text{ psi}$$

2.1.9 Impact Limiter Equation Development.

Two degrees of freedom: vertical translation and pitch rotation about c.g.

Translation: Upward force - gravity force = m x appar't access.

$$F(u) - m\ g = m\ \ddot{y}_c$$

Expressed in terms of the tip or contact point

$$y_{tip} = y_c - \ell \cos\theta$$

Rates and acceleration may be calculated

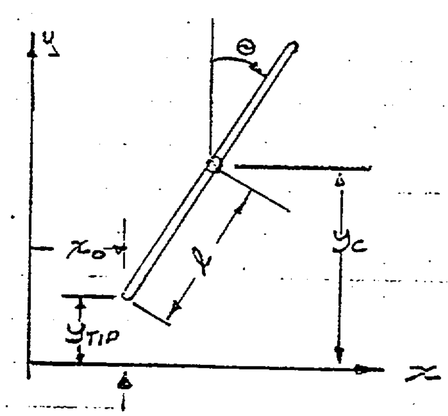

F(u) = crush force

$$\dot{y}_{tip} = \dot{y} + \ell \dot{\theta} \sin\theta$$

and

$$\ddot{y}_{tip} = \ddot{y}_c + \ell\ddot{\theta} \sin\theta + \ell\dot{\theta}^2 \cos\theta$$

Solving for $\ddot{y}_c$ and replacing $\ddot{y}_{tip}$ with $-\ddot{u}$

$$\ddot{y}_c = -\ddot{u} - \ell (\ddot{\theta} \sin\theta + \dot{\theta}^2 \cos\theta)$$

So that the force Eq. (1) may be written:

$$F(u) - mg - m \quad \ddot{u} - \ell (\ddot{\theta} \sin\theta + \dot{\theta}^2 \cos\theta) \qquad (2)$$

In similar fashion the horizontal force is described as:

$$F(x) = m \ddot{x}_{cg}$$

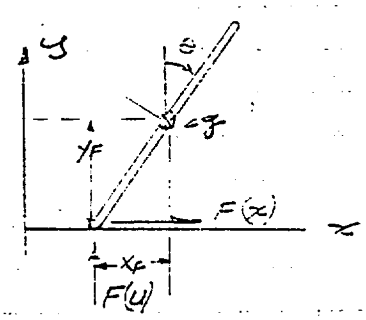

where $x_{cg} = x_o + \ell \sin\theta$

$$\dot{x}_{cg} = \ell \dot{\theta} \cos\theta$$

$$\ddot{x} = \ell \ddot{\theta} \cos\theta - \ell \dot{\theta}^2 \sin\theta$$

Then upon substituting

$$F(x) = m \ell (\ddot{\theta} \cos\theta - \dot{\theta}^2 \sin\theta)$$

The pitch rotation equation is described:

$$M = I\,\ddot{\theta}$$

In terms of previously described forces

$$F(u)\,X_F - F(x)\,Y_F = I\,\ddot{\theta} \qquad (3)$$

where the arms X_F and Y_F are variables and functions of crush distances and are described shortly.

Substituting the previously developed F(x) expression into the moment equation (3) above leads to :

$$F(u)\,X_F - m\ell\,(\ddot{\theta}^2 \cos\theta\,Y_F = \ddot{\theta}^2 \sin\theta)\,Y_F = I\,\ddot{\theta}$$

or

$$F(u)\,X_F + m\,\ell\,\dot{\theta}^2 \sin\theta\,Y_F = \ddot{\theta}\,(I + m\ell\,Y_F \cos\theta)$$

Solving for $\ddot{\theta}$ yields:

$$\ddot{\theta} = \frac{F(u)\,X_F + m\,\ell\,Y_F\,\dot{\theta}^2 \sin\theta}{(I + m\,\ell\,Y_F \cos\theta)}$$

This term may then be substituted into the vertical force expression repeated below.

$$F(u) - mg = m\,[-\ddot{u} - \ell\,(\ddot{\theta}\,\sin\theta + \ddot{\theta}\,\cos\theta)]$$

from which $\ddot{u}$ is described.

$$\underline{\ddot{u} = g - F(u)/m - \ell\,(\dot{\theta}^2\,\cos\theta + \ddot{\theta}\,\sin\theta)}$$

The arms, X_F and Y_F of the torque equation are described below.

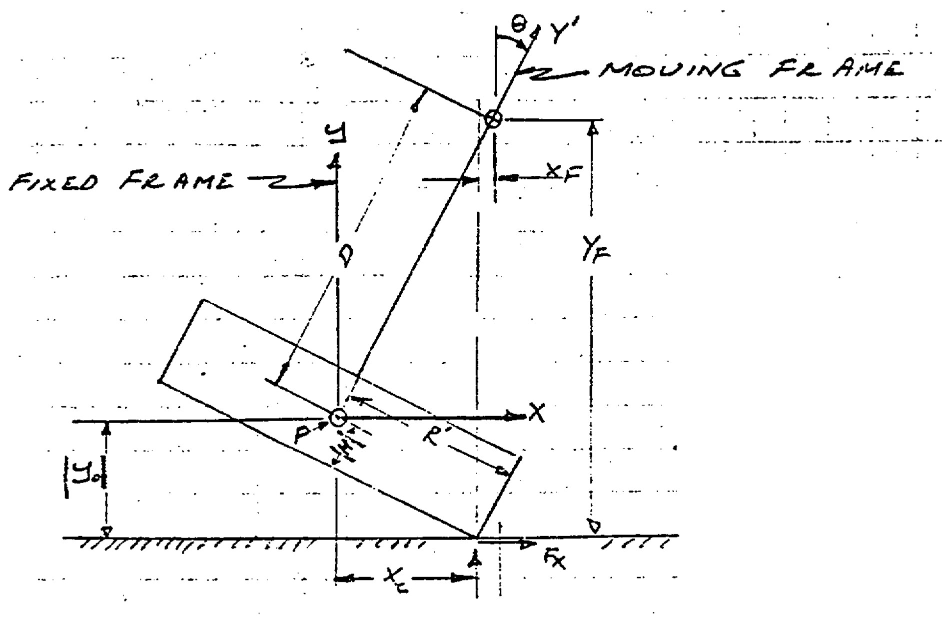

X_F = D sinθ − X_c

Y_F = D cosθ + R sinθ + |H| cosθ

X_c = distance X from reference point P to centroid of contact area

Initial contact, time = 0

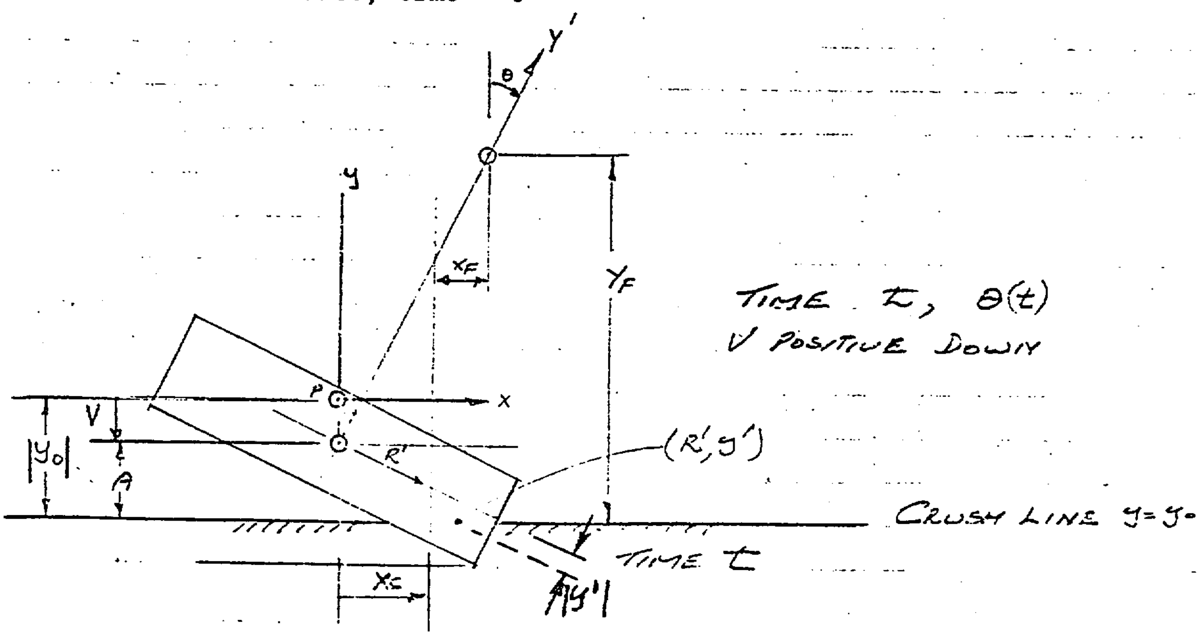

For a point (R', y') on the crush line (y = y_o);

Dimension A = R' sinθ − y' cosθ = − y_o − V

Solving for: $R' = \dfrac{y_o + V - y' \cos\theta}{-\sin\theta}$

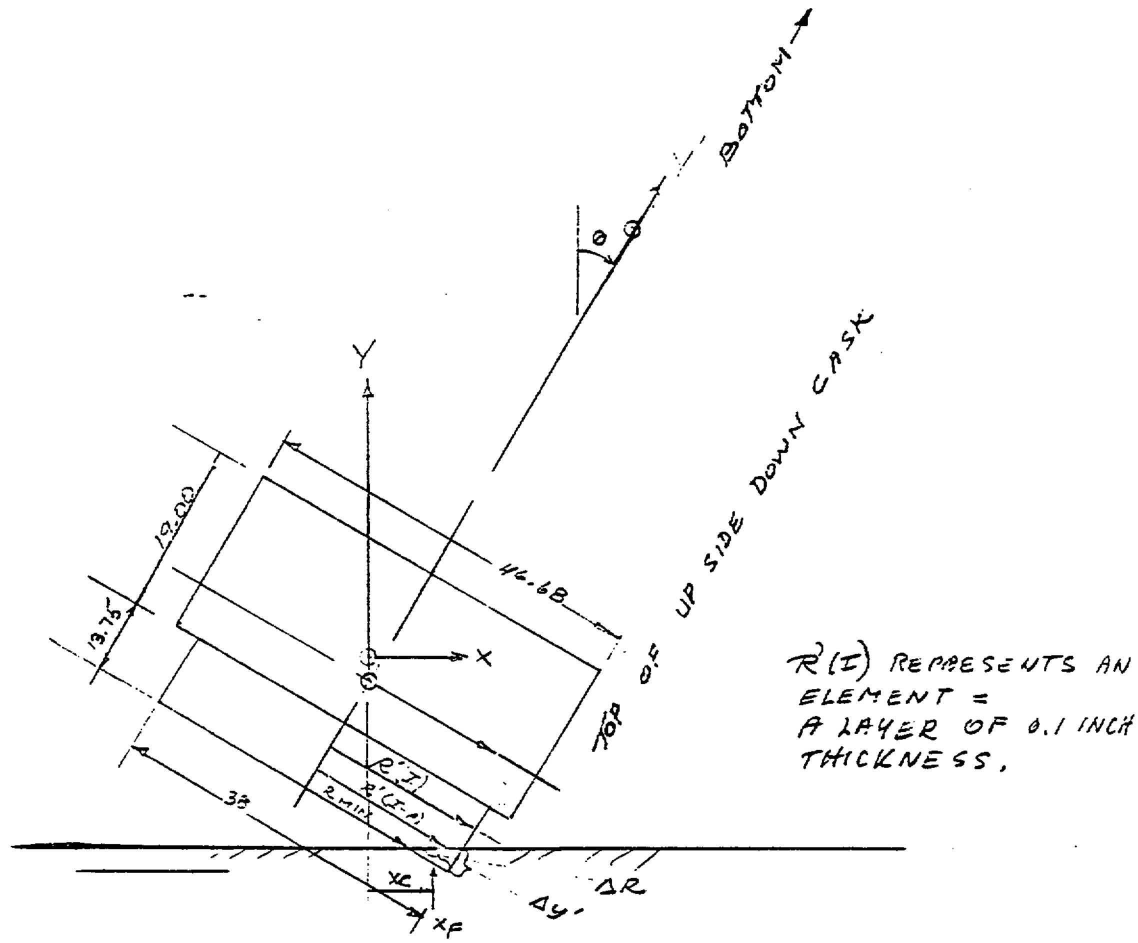

R'(I) represents an element of the radius vector at preassigned incremental depths. These vector elements begin at the top and continue every 0.1 in. towards the bottom of the plywood impact limiter.

When the radius vector equals the radius magnitude the point is saved and differenced with the minimum radius. Both of these radii are the 'ground-radius' coincident points. This allows a ΔR calculation and knowing the other coordinate, y (depth), a Δy calculation. The impact area is next calculated with the action arm X_F passing through the centroid of the area. The resulting forces and moments are then calculated and integrated; the process repeated over the ensuing time steps till $\theta = 90°$ or $F(u) = 0$.

2.1.9.1 Impact Limiter Axial Shear Loads

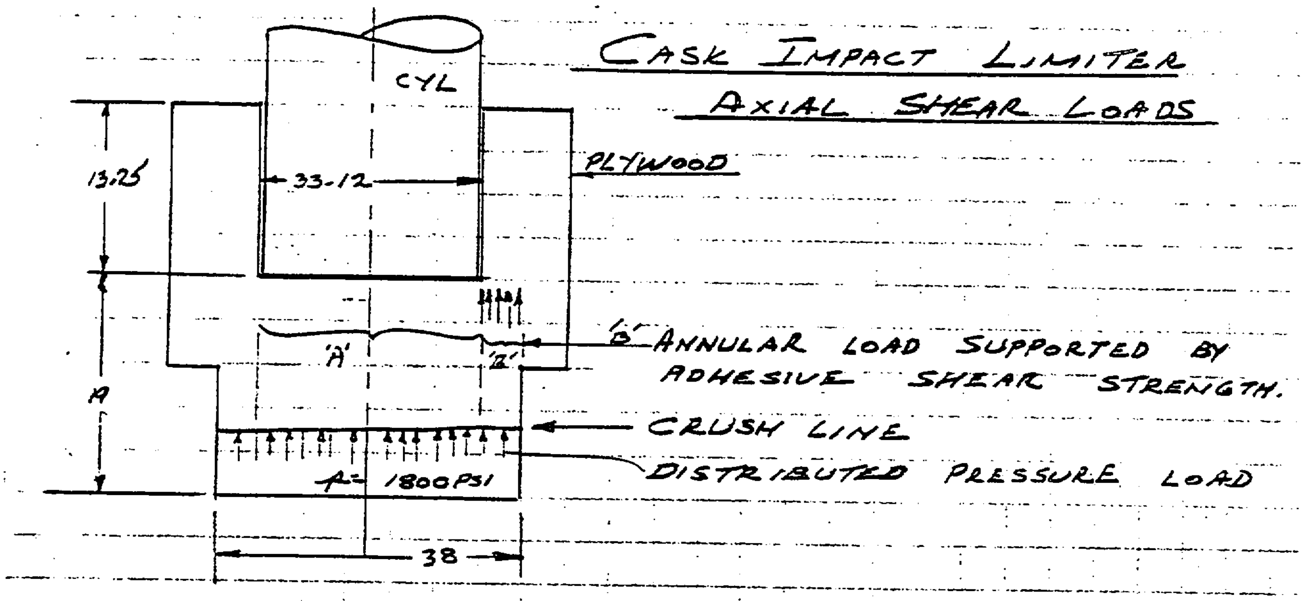

'A' central area supported by cylinder top
'B' annular section contributing to glue shear

Crush $\Delta = PE/A\sigma$ = 120 (386) 360 / (π 38² x 1800) = 8.17 in.

% = 8.17/19 < 50% $\therefore$ σ = 272.6 in.²

$$\text{Average Acceleration} = \pi \times \frac{38^2}{4} \times \frac{1{,}800}{46{,}000} = 44 \text{ g}$$

Area B = A = 0.25 π (38² − 33.12²) = 272.6 in.²

Shear load: $F_{S_{cy}} = p\,A_B$ = 1800 (272.6) = 490,680 lb

Shear Stess-Adhesive

$$\sigma_{S_{AD}} = F_{S_{cy}} / \pi\, D \cdot \ell$$

ℓ is glued length wood shear is ignored

490,680 / (π)(33.12) (13.75) = 342 psi

342 < 1000 psi

Reference Roark 5th Ed., Table 38

2.1.9.2 Impact Limiter Plywood Shear and Bending Stress

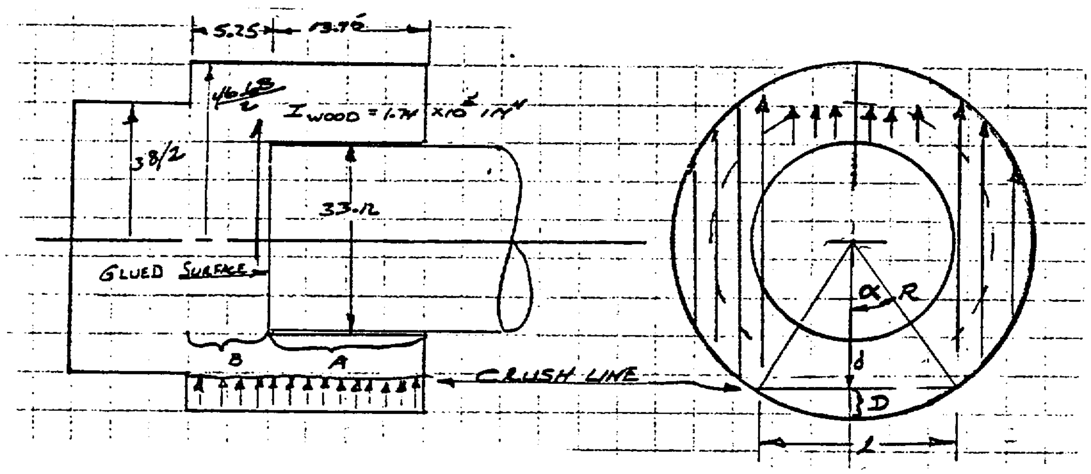

D_{max} (Estimated) = 4.49 in.

$\ell = 2R \sin(\cos^{-1} d/R)$

$= (23.34) \sin(\cos^{-1} 18.85/23.34 = \underline{27.527 \text{ in.}}$

B Contact Area = $\ell \cdot B = s$

$= 27.527\ (5.25) = \underline{144.5 \text{ in.}^2}$

Section B sees uniform σ_{11} = 3500 psi

Crush/diam percent very small.

Load on Section 'B': $F_B = \sigma_{11}\ S = 3500\ (144.5) = 5.058 \times 10^5$ lb

Shear Stress:

$$\sigma_S = F_B/(\pi\ D_o^2/4) = 5.058 \times 10^5/(\pi\ 46.68^2/4) = \underline{296\ \text{psi}}$$

Per Engineering Material Handbook C. L. Mantell allowable wood shear 1000 psi.

Bending Stress (wood):

$$\sigma_B = \frac{M_c}{I_{wood}} = \frac{5.058 \times 10^5\ (5.25)}{2}\ \frac{(23.34)}{1.74 \times 10^5} = 180\ \text{psi}$$

Per same reference: tension perpendicular to grain: 340 psi

Margin: 340/180 = 1.9

2.1.9.3 Impact Plate Lateral Loading

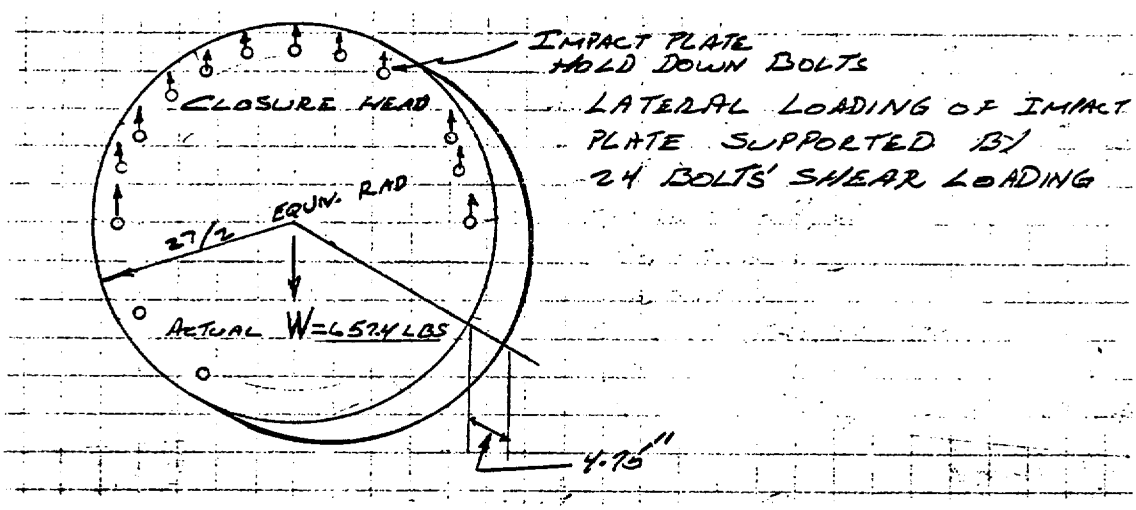

Impact Plate does not move. Impact plate lateral loads supported by bolt shear.

Lateral Load: $L_L = \mu_y \sin\theta \, W = \mu_s \, W$

$$L_L = 272.1\ (657.4) = \underline{178{,}770\ \text{lb}}$$

Bolt Shear: $\sigma_S = L_L/(24)(0.8920) = \underline{8350\ \text{psi}}$

2.1.9.4 Shield Lid Lateral Load

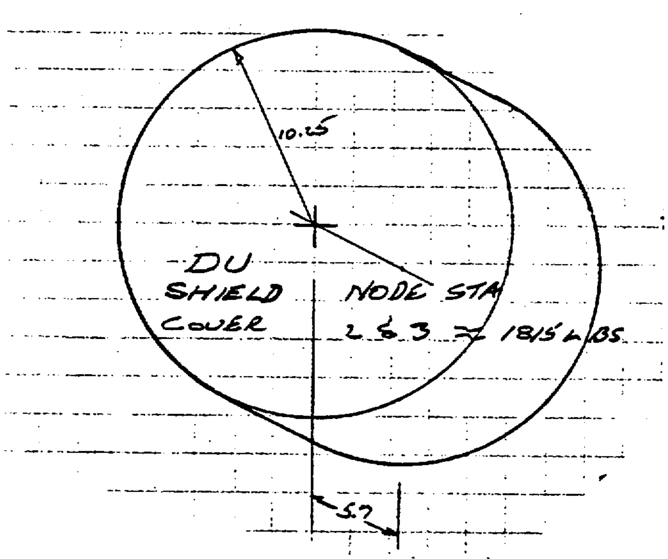

Rad = 10-1/4 in.

t = 5.7 in.

w = 1815 lb

n_y = 2721.1 gs

$P = Wn_y = 1815\ (272.1) = \underline{4.939 \times 10^5\ \text{lb}}$

$$(D_1 - D_2) = 20\text{-}5/8 - 20\text{-}1/2 = 1/8 = 0.125 \text{ in.}$$

$$K_D = D_1 D_2/(D_1 - D_2) = (20\text{-}5/8 \times 20\text{-}1/2)/0.125 = \underline{3382.5 \text{ in.}}$$

$$C_E = 2\,\frac{1 - \nu^2}{E} = 2\,\frac{1 - 0.3^2}{30 \times 10^6} = \underline{6.067 \times 10^{-8}}$$

(E stainless and uranium = 30.10^6)

$$\sigma_c = 0.798 \left[\frac{4.939 \times 10^5 \times 10^8}{5.7 \times 3382.5 \times 6.067} \right]^{1/2} = \underline{16{,}400 \text{ psi}}$$

$$\sigma_{yield} = 31{,}500 \text{ psi at } 300°F$$

2.2. WEIGHTS AND CENTERS OF GRAVITY

A summary of the weights of Model FSV-1 in Configurations E, F and G is presented in Table 2-2. Model FSV-1 in Configurations E, F and G has been evaluated for the normal conditions of transport and hypothetical accident conditions while containing a total weight of 4430 pounds. This total weight consists of 2630 pounds for the inner container and 1800 pounds for the radioactive contents.

TABLE 2-2
ALLOWABLE WEIGHTS

	Configuration E	Configuration F	Configuration G
Cask Body	43,160	43,160	43,160
Inner Container	2,630	not used	not used
Burial Canister/Spacer	not used	2,195	3,525
Contents-Allowable Weight	1,800	2,235	905
Total	47,590	47,590	47,590

The center of gravity of Model FSV-1 in Configurations E, F and G is located 109 inches from the bottom of the package.

2.2.1. Weight Calculations - Model FSV-1 Configurations E, F, and G

2.2.1.1. Outer Closure

ASSUME BOLTS ARE IN PLACE AND NEGLECT HOLES AND BOLT HEADS

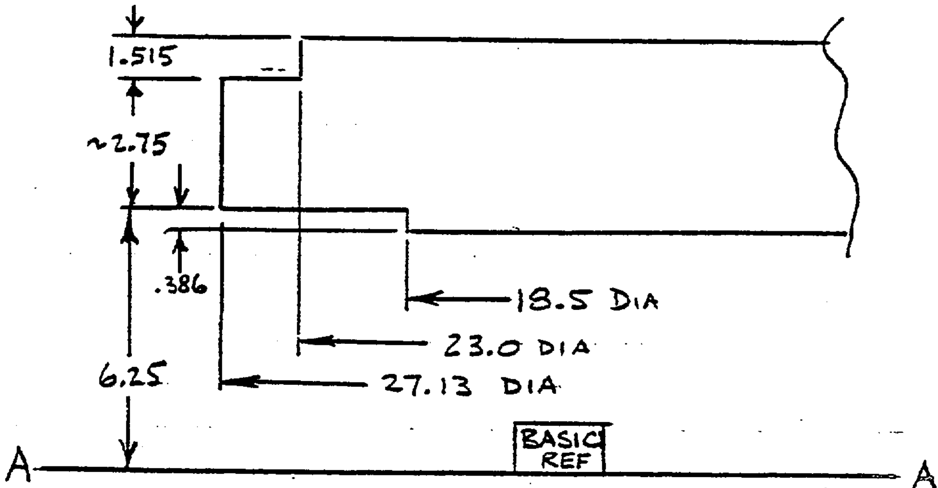

				V		y	Vy
TOP	23d	$\pi d^2/4 (1.515)$	=	629.4 in^3	X	−9.76	= −6143.
MIDDLE	27.13d	$\pi d^2/4 (2.75)$	=	1589.7 in^3	X	−7.63	= −12130.
BOTTOM	18.5d	$\pi d^2/4 (.386)$	=	103.8 in^3	X	−6.06	= −629.
				2322.9			−18,902.
				X 0.283			X 0.283
		WT	=	657.4 LB			M = −5349. IN-LB

2.2.1.2 Cask Body

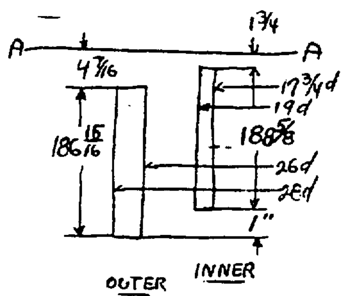

28d 613 in²
-26d -530
83 in² × 186 15/16 = 15,500 in³ × +97 29/32 = +1,511,000.
(outer) wt .29 × 4500 lbs M = .29 × +439,000

19d 283.5 in²
-17¾d -247
36.5 in² × 188 5/8 = 6870 in³ × +96.06 = +660,000
(inner) wt = .29 × 1990 lbs M = .29 × 191,200 "lb

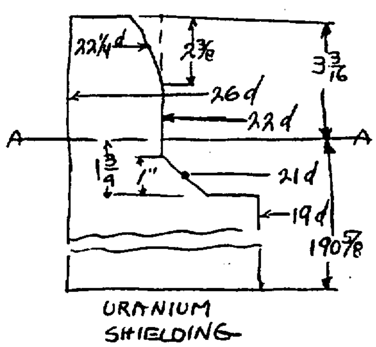

26d 530 in² × 193 13/16 = +102,750 in³ × +93 23/32 = +9,639,000.
-19d -283.5 × 188⅞ = -53,500 × +96 3/16 = -5,150,000
-21d -346 × 1 = - 346. × +1¼ = - 432
-22d -380 × 1 9/16 = - 594 × -1/32 = + 19
-22¼d -389 × 2⅜ = - 925 × -2 = + 1850
-55,365 -5,148,563
+ 47,385 +4,481,437
.683 .683
URANIUM wt 32,400 lbs M = +3,060,000"

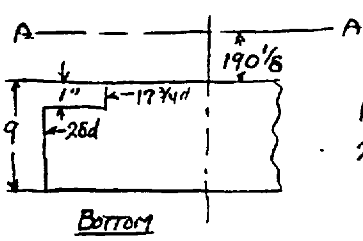

17¾d 247 in² × 1 = 247 in³ × +190⅝ = +47,100
28d 613 × 8 = 4904 × +195⅛ = +960,000
+ 5151 + 1,007,100

wt = .29 × 1494 lbs M = .29 × 292,060 in-lb

2.2.1.2 Cask Body (Continued)

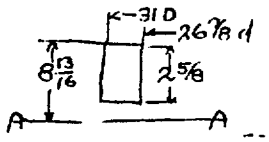

31d +752 in²
26 7/8d −568
184 × 2 5/8 = 483 in³ × −7 1/2" = −3622
.29 .29
wt = 140 lbs M = −1050 in lbs

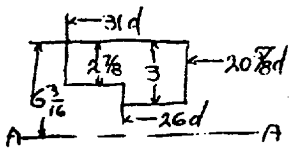

31d +752 in² × 2 7/8 = 2160 in³ × −4 3/4" = −10,250.
26d +530 × 1/8 = 66 × −3 1/4 = − 216.
+2226 −10,466
−20 7/8d −335 × 3 = −1005 × −4 11/16 = +4850
+1221 in³ −5616.
.29 .29
wt = 354. lbs M = −1628 in lbs

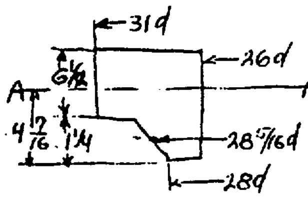

31d 752 in² × 6.5 = 4880. × −1/16 = −305.
28 9/16d 630 × 1 1/4 = 787 × +3 13/16 = +3000.
+5667 +2695
−26d −530 × 7 3/4 = −4100 × +9/16 = −2300
+1567 in³ +395.
.29 .29
wt = 455 lbs M = +114 in lbs

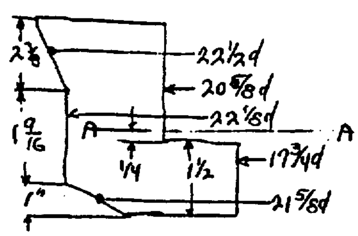

22 1/2d 397 in² × 2 3/8 = 942 in³ × −2 1/4 = −2120
22 1/8d 385 × 1 9/16 = 601 × −9/32 = −169
21 5/8d 367 × 1 = 367 × +1 1/4 = +458
+1910 −1831
−20 5/8d −335 × 3 7/16 = −1154 × −1 15/32 = +1670
−17 3/4d −247 × 1 1/2 = −370 × +1 = −370
−1524 +1300
+386 −531
.29 .29
wt = 112 lbs W = −154 in lbs

910013 NC

2.2.1.3. Inner Closure

DEPLETED URANIUM

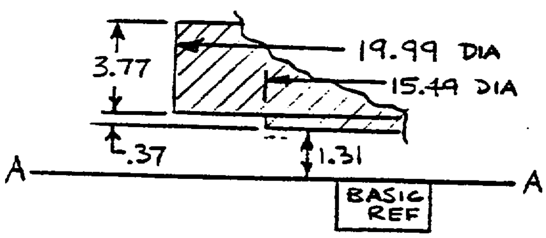

				V	y	Vy
TOP	19.99 d	313.8 in²	x 3.77 =	1183.2 in³	x −3.565 =	−4218.1
BOTTOM	15.49 d	188.4	x .37 =	69.7	x −1.4975 =	−104.4
HOLES	−18(.94)(3.77)(.75)		=	−47.8	x −3.565 =	+170.5
				1205.1		4152.
				X.683		X.683
				WT.= 823.1 LBS		M = −2835.3 IN-LB

SHELL

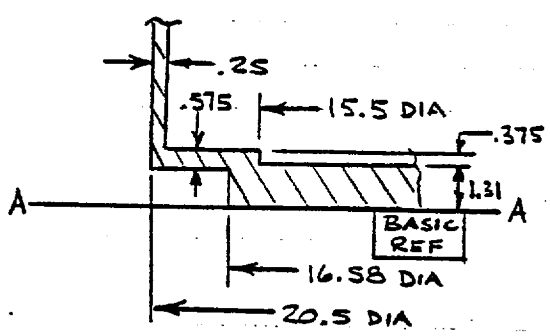

				V	y	Vy
TOP PLATE	20.5d	330 in²	X .25 =	82.5 in³	X −5.585 =	−460.9
CYLINDER	20.25 π X .25		X 4.46 =	70.9	X −3.355 =	−238.
BOTTOM PLATE	16.58d	215.9 in²	X 1.31 =	282.8	X −.655	−185.3
RING AT BOTTOM	20d	314.2	X .575 =	180.6	X 1.3975	−252.4
	−15.5d	188.7	X .575 =	−108.5	X 1.3975	+151.6
BOLTS & SLEEVES	16(3.77)(.75)(.92)		=	41.6	X −3.355	−139.6
				550.		−1124.6
				X .29		X .29
				WT = 159.5 LBS		M = −326.1 IN-LB

TOTALS

WT = 982.6 LBS   M = −3162

2.2.1.4. Inner Container

CONTAINER BODY

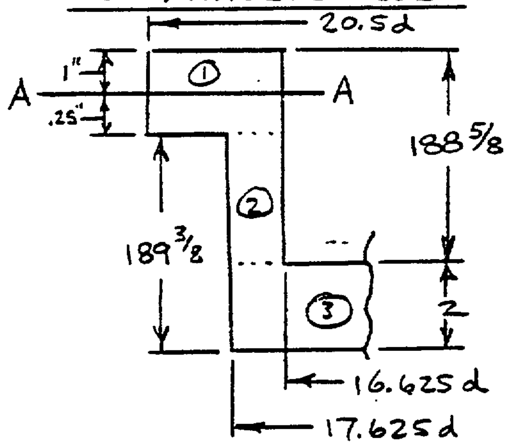

		V	y	Vy
1	$\frac{\pi}{4}(\overline{20.5}^2 - \overline{16.625}^2)(1.25)$ =	141.2 in³	X -.375 =	-53
2	$\pi/4(\overline{17.625}^2 - \overline{16.625}^2)(187.375)$ =	5040.4 in³	X +93.94 =	473,495
3	$\pi/4(17.625)^2(2)$ =	488. in³	X +188.625 =	92040
		5669.6		565,482
		X .29		X .29
		WT = 1644.2 LB		M = 163,990 IN-LB

CONTENTS OF CONTAINER

300# x 6 = 1800 LB x 93.844 = 168,919 IN-LB

2.2.1.5. Impact Limiter

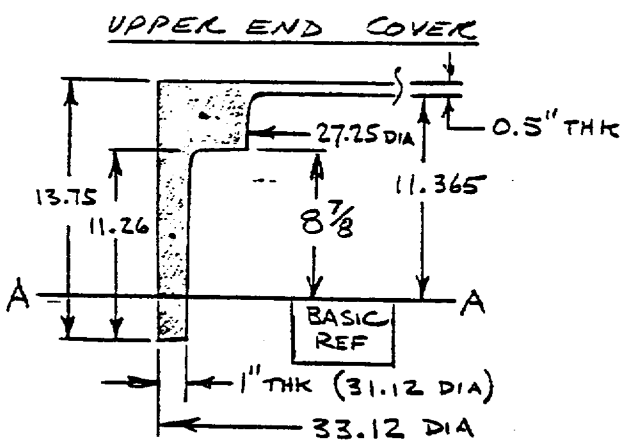

			V		y	Vy
OUTER	32.12 d	$\pi d(11.26)(1)$	= 1136.2	in^3	X -3.245	= -3687.
TOP	27.25	$\pi d^2/4 (0.5)$	= 291.6	in^3	X -11.615	= -3387.
REMAINDER	27.25	$\pi(30.185)(2.935)(2.49)$	= 693.0	in^3	X -10.12	= -7013.
			2120.8			-14087
			X .098			X .098
			WT = 207.8 LB			M = -1380.5 IN-LB

2.2.1.5. Impact Limiter (Continued)

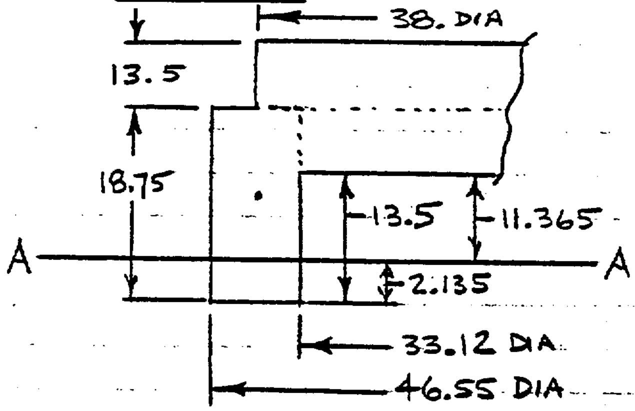

				V		y	Vy
OUTER	39.835d	$\pi d(6.715)(18.75)$	=	15,757	in^3	X −7.24	= −114078.
TOP	38d	$\pi d^2/4\ (13.5)$	=	15,311	in^3	X −23.365	= −357,742
INNER	33.12d	$\pi d^2/4\ (5.25)$	=	4523	in^3	X −13.99	= −63,277
				35,591			−535,097.
				X .0208			X .0208

ALUMINUM SHEATH

				V		y		Vy
BOTTOM PLATE	39.835d	$\pi d(6.715)(0.25)$	=	210.1	in^3	X +2.26	=	+ 474.8
TOP PLATE	46.55d	$\pi d^2/4\ (0.25)$	=	425.5	in^3	X −27.24	=	−11,590.
CYLINDER	46.63d	$\pi d(.06)(32.75)$	=	287.9	in^3	X −13.99	=	−4027.
MTG RING (90-H1501-106)	30.97d	$\pi d(.63)(2.16)$	=	132.4	in^3	X 2.8	=	+370.7
	31.34d	$\pi d(.37)(1.78)$	=	64.8	in^3	X 3.3	=	+214.
				1120.7 in^3				−14,558
				X .098				X .098
				109.8 LB				−1427

TOTALS FOR IMPACT LIMITER ASSEMBLY WT = 1057.9 LB M = −13,938

$$C.G. = \frac{-13,938}{1057.9} = 13.18 \text{ ABOVE A-A}$$

OR 17.18 BELOW TOP

2.2.1.6. Weight Summary

E. SUMMATION

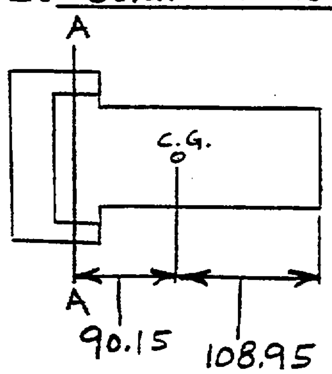

	WT	MOMENT
HEAD	657.	- 5349.
CASK	140.	- 1050.
	354.	- 1628.
	455.	+ 114.
	112.	- 154.
	4500.	+ 439,000.
	1990.	+ 191,200.
	32,400.	+ 3,060,000.
	1494.	+ 292,060.
CONT LID	983.	- 3162.
CONT BODY	1644	+ 163,990.
CONTENTS	1800.	+ 168,919.
IMPACT LIMITER	1058	- 13938

CASK TOTAL (LOADED) 47,587 LB 4,290,002 IN-LB

DISTANCE FROM A-A = 4,290,002/47,587 = 90.15"

C.G. IS 108.95" FROM BOTTOM OF CASK

2.2.2. Weight Calculations - Configurations F and G

Configurations F and G use the same burial canister.

Burial canister body	980 lb
Closure plug	655
total	1635 lb

2.2.2.1. Configuration F Spacer

The proposed spacer consists of six (6) steel tubes that are 4.75 inches in diameter, have a wall thickness of 0.125 inches and are 179.5 inches long.

Spacer	560 lb

2.2.2.2. Configuration G Spacer

This spacer is shown in Section 1. on drawing GADR 55-2-13 provides supplemental shielding.

Spacer with shielding	1890 lb

2.2.2.3. Weight Summary

The total allowable weight in the cask body for Model FSV-1 in Configurations E, F and G is 4430 lb and the allowable weight of any radioactive contents is 4430 lb less the weight of the burial canister and the spacer.

For Configuration F:

Total allowable	4430 lb
Burial canister	-1635
Spacer	-560
Radioactive contents	2235 lb

For Configuration G:

Total allowable	4430 lb
Burial canister	-1635
Spacer	-1890
Radioactive contents	905 lb

2.3 MECHANICAL PROPERTIES OF MATERIALS

2.3.1. Depleted Uranium (0.2% Mo)

Shielding Sleeve - Cask Body:

Density: 18.9 grams/cc or 0.683 lb/in.^{3}

Mechanical Properties:	Room Temperature	250°F
Ultimate Tensile Strength	60,000 to 100,000 psi	
Yield Strength	25,000 to 45,000 psi (tension)	73,000 psi (compression)
Reduction in Area	10% to 40%	
Elongation	8% to 15%	
Modulus of Elasticity	$24\ (10)^6$ psi	22.73×10^6
Poisson's Ratio	0.21	
Shear Modulus	$12\ (10)^6$ psi	
Hardness	Rockwell B 65 to 90	

Melting Point:	2070°F	
Thermal Expansion:	6.5 $(10)^{-6}$ in./in./°F	

Shielding Desk - Inner Closure:
Same properties as above except:

Ultimate Tensile Strength	75,900 psi	59,200 psi
Yield Strength (tension)	41,500 psi	36,300 psi
Modulus of Elasticity	23.3×10^6 psi	21.1×10^6 psi

2.3.2. Stainless Steel Pipe, Type 304 per ASTM Spec. A-351, Grade CF-8

Physical Properties:	Room Temp.	250°F	300°F
Density	0.287 $lb/in.^3$		
Melting Range	2550° to 2650°		
Modulus of Elasticity	28×10^6 psi	27.4×10^6 psi	27.1×10^6 psi
Specific Heat (32° to 212°F)	0.12 Btu/lb/°F		

Thermal Conductivity:

At 200°F	9.4 $Btu/hr/ft^2/°F/ft$
At 1000°F	12.5 $Btu/hr/ft^2/F/ft$

Mean Coefficient of Thermal Expansion:

32° to 212°F	9.6 in./in./°F x 10^{-6}
32° to 600°F	9.9 in./in./°F x 10^{-6}
32° to 1000°F	10.2 in./in./°F x 10^{-6}

Mechanical Properties:	Room Temp. (72°F)	250°F	300°F
Ultimate Tensile Strength	70,000 psi		
Yield Strength	30,000 psi	23,700 psi	22,500 psi
Elongation	35%		
Reduction of Area (approx.)	60%		
Hardness	R_B-88		

2.3.3. Stainless Steel Forgings, Type 304 per ASTM Spec. A-182, Grade F-304

Physical Properties:

Same as 2.3.2. above:

Mechanical Properties:

Ultimate Tensile Strength	70,000 psi
Yield Strength	30,000 psi
Elongation	40%
Reduction of Area	50%
Hardness (approx.)	R_B-88

2.3.4. ASTM A579 Alloy Steel [HY140(T)]

Physical Properties:	Room Temp.	300°F
Density	0.285 lb/in.^{3}	
Modulus of Elasticity	29.5 x 10^6 psi	28.5 x 10^6 psi
Ultimate Tensile Strength	150,000 psi	140,000 psi
Yield Strength	140,000 psi	130,000 psi
Elongation	15%	

2.3.5. 6061-T6 Aluminum Alloy

Modulus of Elasticity at 300°F	10.4×10^6 psi
Ultimate Tensile Strength at 300°F	35,000 psi
Yield Strength at 300°F	30,000 psid
Elongation at 300°F	20%

2.3.6. Douglas Fir Plywood

Crushing Stress parallel to Grain	3500 psi
Crushing Stress perpendicular to Grain	1800 psi
Shear stress allowable (Ref. 12, Table 38)	1000 psi
Tensile strength perpendicular to Grain (Ref. 13)	340 psi

The crushing stress remains nearly constant up to approximately 50% reduction of the original thickness. Beyond approximately 50% the crushing stress increases rapidly.

For the structural evaluation the lower of either the adhesive strength or the wood shear stress parallel to the grain was used for the shear stress allowable.

2.3.7. Uranium Welds

All uranium welding will be accomplished using single V-butt joints and inert direct current tungsten arc welding. The inert gas used for shielding and trailing shields shall be of welding grade argon. The filler and base metals shall be depleted uranium.

2.3.8. Stainless Steel Welds (Refs. 1 and 2)

All stainless steel welds will be in accordance with the "Rules for Construction of Nuclear Vessels" (Ref. 1). All of the welding procedures and welders will be qualified in accordance with "Welding Qualifications" (Ref. 2).

2.3.9. Seals (Refs. 3, 4 and 27)

a) Seal Assemblies, Gask-O-Seal, Parker Seal Company.
Material: Parker Compound S455-70 Silicone rubber or equivalent.

Outer Closure Seal - GA Technologies Inc. Drawing 1501-108, Issue C - o.d. = 23.63 and i.d. = 21.34
Inner Closure Seal - GA Technologies Inc. Drawing 1501-093, Issue D - o.d. = 18.72 and i.d. = 16.62

b) All metal O-rings shall be self-energized for use in bolted flange assemblies. These O-rings will be made of silver plated Inconel tubing. Service temperature is -320° to +1300°F. The following metal O-rings have been selected for sealing the Model FSV-1 in Configurations E, F, and G.

Cask Center Plug Seal - United Aircraft Products, Inc. Cat. No. U-6420-02813-SEA; o.d. = 2.81, i.d. = 2.56, Tube Diameter = 0.125.
Cask Purge Connection Cover Seal - United Aircraft Products, Inc. Cat. No. U-6420-02630-SEA; o.d. = 2.63, i.d. = 2.38; Tube Diameter = 0.125.

c) All elastomer O-rings shall be molded per AMS Specification 3304 of silicone rubber. Service temperature for this material is

-100° to +500°F. The material will resist temperatures up to 700°F for short periods. The compression force used to install these O-rings will be as recommended by the manufacturer (Ref. 4). The following silicone rubber O-rings have been selected for sealing Model FSV-1 in Configurations E, F, and G.

Cask Center Plug Seal - Parco No. PRP-568-236 (or equivalent) o.d. = 3.500; i.d. = 3.25, Diameter = 0.125.

Cask Helium Connection Cap Seal - Parco No. PRP-568-233 (or equivalent) o.d. = 3.125; i.d. = 2.875; Diameter = 0.125.

2.3.10 Fasteners (Refs. 5, 6, 7)

a) The bolts used in the assembly of the inner container are high alloy steel per AMS 5737, which corresponds to SA-453, Grade 660 in Ref. 1. These bolts are heat treated to 130 ksi/min ultimate tensile strength. The 1/2-in. size used in fastening the inner closure to the container body has a minimum ultimate axial tensile strength of 18,400 lb.

b) The bolts of the inner closure are threaded into "screw-lock" inserts made of Type 18-8 stainless steel (per AMS-7245B) wire having an ultimate tensile strength of approximately 200,000 psi. These "screw-lock" inserts meet military specification for locking torque and vibration. The internal thread conforms to thread form standards issued by the Department of Commerce (Ref. 6).

c) The bolts used in the assembly of the outer closure to the cask body alloy steel per AMS 5737 with the following physical properties for the 1-1/4-7 UNC size:

Tensile Strength, min.	130,000 psi
Yield Strength, min.	95,000 psi

2.3.11 <u>Adhesives</u>

The assemblies formed by laminating the plywood and then bonding the laminated plywood to the aluminum end cap are structurally important.

The plywood sheets have been laminated with Resorcinol resin to provide a waterproof joint that is stronger than the wood. Resorcinol is recommended by the American Plywood Association for structural assemblies fabricated in the field designed to withstand adverse environmental conditions.

An epoxy (Furane Epibond 1210/9861) is used between the aluminum end cap and plywood to provide a structural bond with a minimum shear strength of 1200 psi at 230°F for the maximum (130°F ambient) temperature condition. This particular expoxy was selected because it bonds well to diverse materials and retains sufficient strength at elevated temperatures.

2.3.12 <u>Note</u>:

The original analysis for Model FSV-1 in Configurations E, F and G was completed using 4340 Low Alloy Steel for the outer closure. Because the large billet of 4340 could not be heat treated properly to guarantee the required material conditions, the material was changed to ASTM A579 [HY140(T)]. Table 2-3 compares the properties of the two materials. Third column lists test

TABLE 2-3

COMPARISON OF 4340 AND ASTM A579 OUTER CLOSURE MATERIAL

Physical Properties	4340	ASTM A579 (Nominal)	ASTM A579 (Actual)
Density, $lb/in.^3$	0.285	0.285	
Modulus of Elasticity, psi			
At room temperature	--	29.5×10^6	
At 300°F	29.0×10^6	28.5×10^6	
Ultimate Tensile Strength, psi			
At room temperature	175,000	150,000	171,000
At 300°F	--	140,000	164,500
Yield Strength, psi			
At room temperature	165,000	140,000	160,500
At 300°F	150,000	130,000	154,300
Elongation, %			
At room temperature	17	15	16.5
At 300°F	18		13.

data from the actual material that was used for fabrication of the parts. An analytical check, using the data in column 2, showed the alternate material to be adequate for all conditions covered in the structural evaluation.

2.4. GENERAL STANDARDS FOR ALL PACKAGES

2.4.1. Iron-Uranium Eutectic Prevention (Reference 8)

Investigations have shown that uranium combines with stainless steel by solid state diffusion at temperatures above 1000°F. The iron-uranium eutectic melts at 1337°F so that if the two materials are in intimate contact at this temperature a molten alloy will be formed (Ref. 8).

Other investigations have shown that uranium in contact with stainless steel will penetrate the stainless steel by solid state diffusion in 24 h of 1400°F. At 1355°F there was no attack on the stainless steel.

Recent tests of stainless steel--uranium--stainless steel assemblies where the surfaces of the stainless steel next to the uranium were spray coated with a 0.005-in. thick coating of copper showed this coating to be an effective barrier to diffusion between the stainless steel and uranium at temperatures of up to 1750°F (Ref. 8). All surfaces of stainless steel in contact with the depleted uranium shielding will be coated with 0.005-in. thick copper coating for Model FSV-1 cask.

2.4.2. Positive Closure

Twelve (12) high strength socket head cap screws, torqued to 20 ft-lb are used to secure the inner closure to the inner container body. The inner container is transported within the cask body which is closed by the outer closure. The outer closure is secured to the cask body with twenty four (24) high strength socket head cap screws.

2.4.3. Lifting Devices

Model FSV-1 in Configurations E, F and G are lifted by means of two sockets installed in machined recesses located in the enlarged diameter section of the closure end of the cask body. A dedicated lifting device with a ball located on each arm is used to lift the package. The sockets are removable and can be replaced if damaged in anyway.

2.4.4. Tiedown Devices

During transport Model FSV-1 in Configurations E, F and G is attached to the rear support on the semitrailer by four (4) high strength socket head cap screws which are installed in threaded holes located in the base of the cask. The upper end of the package rests on a saddle mounted on the semitrailer and is restrained by a semicircular strap.

2.5. STANDARDS FOR TYPE B AND LARGE QUANTITY PACKAGING

2.5.1. Load Resistance

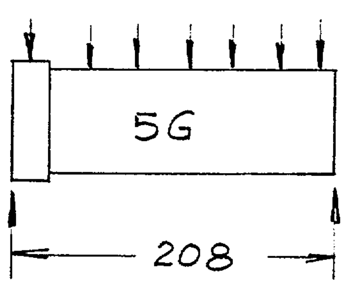

5g - Uniformly Distributed

WT = 46024 lb

W = 5(46024) = 230,120 lb

$$\text{Max at center} = \frac{W\ell}{8} = \frac{230120}{8}(208) = 6{,}000{,}000 \text{ in. lb}$$

Assume only outer shell is stressed

o.d. = 28" i.d. = 26" $I = \frac{\pi}{4}(R^4 - r^4) = \frac{\pi}{4}(14^4 - 13^4) = \underline{7750} \text{ in.}^4$

$$Z = \frac{7750}{14} = 554 \text{ in.}^3$$

$$S_b = \frac{M}{Z} = \frac{6{,}000{,}000}{554} = \underline{\underline{10{,}800 \text{ psi}}} \text{ ok, less than } 30{,}000 \text{ psi}$$

2.5.2 External Pressure

25 psig Roark XVI Case 3c (Stability)

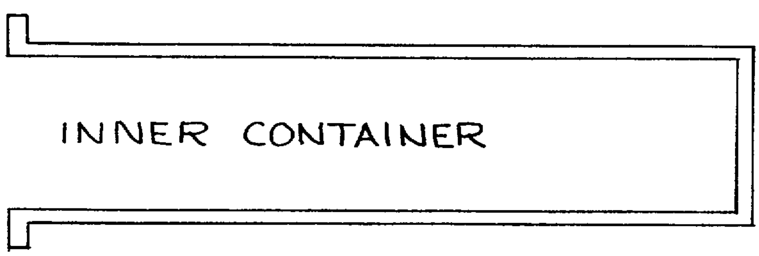

17-5/8 OD - 16-5/8 ID - 1/2 wall - 190-5/8 long

$$p^1 = \frac{1}{4}\,\frac{E}{1-\nu^2}\,\frac{t^3}{r^3} = \frac{1}{4}\,\frac{30(10^6)}{(1-.09)}\,\frac{(1/2)^3}{(8.31)^3} = \underline{1795} \text{ psi}$$

2.6. NORMAL CONDITIONS OF TRANSPORT

2.6.1 Differential Thermal Expansions

2.6.1.1 Clearances

The cask and its container assemblies are stainless steel and uranium constructions. No lead is present and thus there are no problems associated with voids of this kind, which vary greatly in volume with changes in temperatures and also shift in position within the cask. The uranium is monolithic and jacketed by the steel. The dimensional proportions of the cask shielding cylinder uranium require that there be minimal clearances for machining and assembly purposes. These clearances are a substantial part of the differential expansions which developed in several of the cases examined. Materials and the associated gaps are identified on Fig. 2-2.

2.6.1.2 Coefficients of Expansion

Coefficient of thermal expansion used for uranium is 6.5×10^{-6} in./in. °F. This value is obtained from records of the NL Albany plant and refer specifically to as-cast 0.2% molybdenum uranium - unalloyed composition.

Stainless Steel values are from Section III, Table N-426 of the Nuclear Code, as follows:

Figure 2-2. Location of Gaps and Materials for
FSV-1, Configurations E, F and G

FIGURE WITHHELD UNDER 10 CFR 2.390

A = instantaneous values at given temperature

B = mean coefficient (from 70°F to indicated temperature)

A	B	Temp °F
9.11	9.11	70
9.73	9.47	300
10.43	9.82	600
10.90	10.05	800

2.6.1.3 Temperature Distribution

Temperature distribution through the cask under hypothetical accident and fire conditions has been obtained from memorandum III, a part of the specification, dated 18 April 1968, and titled "Heat Transfer Calculations for PSC Fuel Shipping Cask". Heat generation rates were chosen in each case to give the maximum differential temperatures.

2.6.1.4 Cases Investigated

The following cases are investigated relative to axial and to radial differential expansions and contractions for the two uranium bodies contained within the stainless steel structure.

Case 1 - 30 minutes after start of fire (1101 Btu/hr fuel rate)
Case 2 - 10 hours after start of fire (2322 Btu/hr fuel rate)
Case 3 - start up - cask 70° - container and inner shell 240°
Case 4 - Immersion in water 70° - container and inner shell 240°
Case 5 - Low temp. - 40° whole cask - No container
Case 6 - Low temp. - 40° cask - Container and inner shell 240°

2.6.1.5 Analysis of Uranium Shielding in Cask Body

In the calculations + is a clearance or gap
- is an interference (based on original 0 gap)

The various negative (-) dr or dl values thus indicate the minimum initial clearances at 70°F required to prevent interference and stressed conditions. These requirements are reflected in the drawings.

The maximum values required for such clearances for the cask itself are:

Gap 12 = -0.0322 from case 2

Gap 23 = -0.015 from case 2

Gap 34 = -.03670 from case 3

Length container = -0.309 from case 6

Interferences - to be prevented by suitable mfg. clearances.

Case 1

T_1 = 1120° T_3 = 430° Tθ = 70° T_4 = 370°

Gap 12 Assume $T_2 = T_3$ for max. diff.

$dr=(13")(T_1 - T\theta)(10.05)10^{-6} - (13")(T_2 - T_0)(6.5)10^{-6}$

$= 0.137 - 0.0304 = +$ 0.1066" SS > U gap

Gap 23 Assume $T_2 = T_3$ for min. clearance

$dr=(9.5")(T_2 - T_0)(6.5)10^{-6} - (9.5")(T_3 - T_0)(9.6)10^{-6}$

$= 0.0222 - 0.328 = -$ 0.0106 U < SS Interference

Gap 34 Assume T_4 = 370° from 2322 Btu/hr fuel rate

$dr=(8\text{-}7/8")(T_3 - T_0)(9.6)10^{-6} - (8\text{-}13/16")(T_4 - T_0)(_9.5)10^{-6}$

= 0.0306 - 0.0251 = + 0.0055 gap

Length of U. Assume $T_2=T_3$ for max. differential

$dl=(194\text{-}1/8)(T_1-T_0)(10.05)10^{-6} - (194\ 1/8)(T_3-T_0)(6.5)10^{-6}$

= 2.05 - 0.455 = 1.595" expansion SS > U gap

Container shows gap.

Case 2

T_1 = 220° T_3 = 340° T_0 = 70° T_4 = 370°

GAP 12 Assume $T_2=T_3$ for min. clearance

$dr=(13")(T_1 - T_0)(9.4)10^{-6} - (13)(T_2 - T_0)(6.5)10^{-6}$

= 0.0183 - 0.0228 = -0.0045 U > SS Interference

Gap 23 Assume $T_2=T_1$ for min. clearance

$dr=(9.5")(T_2 - T_0)(6.55)10^{-6} - (9.5)(T_3 - T_0)(9.47)10^{-6}$

= 0.00925 - 0.0243 - 0.015 U < SS Interference

Gap 34 Assume T_4 = 370°

$dr=(8\text{-}7/8")(T_3 - T_0)(8.47)10^{-6} - (8\text{-}13/16)(T_4 - T_0)(9.47)10^{-6}$

= 0.0227 - 0.025 = 0.0023 Interference

Case 3 Cask at original dimen. T_4 = 241° T_0 = 70° T_3 = 70°

Gap 34 $dr=0-(8\text{-}13/16)(T_4-T_0)(9.7)10^{-6}$

= - 0.0367" container increase - interference

Length Container

$dl = (187\text{-}5/8)(T_4 - T_0)\ (9.7)10^{-6}$

$= -0.309$ container increase Interference

Case 4

$T_1 = 70^o$ T_2 assumed $= T_3 = 450°$ $T_0 = 70°$ $T_4 = 240°$

Gap 12 $= 0 - (13)(T_2 - T_0)\ (6.5)10^{-6}$

$= 0 - 0.0322 = -.0322$ SS < U Interference

Gap 23 $= 0$

Gap 34 = negligible

Length Container - in time same as case 3

Case 5

$T_1 = T_2 = T_3 = 40°$ $T_0 = +70$

Gap 12 $dr = (13)(T_1 - T_0)(9.11)10^{-6} - (13)(T_1 - T_0)(6.5)10^{-6}$

$= -0.013 + 0.0093 = 0.0037$ SS < U Interference

Gap 23 $dr = (9.5)(T_2 - T_0)(6.5)10^{-6} - (9.5)(T_3 - T_0)(9.11)10^{-6}$

$= -0.0068 = 0.0095 = +\ 0.0027$ gap

Case 6

$T_1 = T_2 = -40°$ $T_3 = T_4 = 240°$ $T_0 = 70°$

Gap 23 $dr = (9.5)(T_2 - T_0)(6.5)10^{-6} - (9.5)(T_3 - T_0)(9.11)10^{-6}$

$= -0.0068 - 0.0147 = -0.0218$ Interference

2.6.1.6 Analysis of Uranium Shielding in the Inner Closure

Clearances:

The inner closure is made of depleted uranium encased in type 304 stainless steel. Gaps exist between the stainless and the depleted uranium to allow for installation of the uranium during assembly of the closure.

Coefficients of Expansion:

Coefficient of expansion used is 6.5×10^{-6} in./in. °F for uranium. This value is obtained from records of National Lead Company's Albany plant and refer specifically to as-cast 0.2% molybdenum uranium.

Stainless Steel values are from Section III, table N-426 of the Nuclear Code, as follows:

A = instantaneous values at given temperature
B = mean coefficient (from 70°F to indicated temperature)

A	B	Temp. °F
9.11	9.11	70
9.73	9.47	300
10.43	9.82	600
10.90	10.05	800

Temperature Distribution:

The depleted uranium portion of the inner closure is supported by the stainless housng with small gaps (0.030 in. average) between the stainless and the uranium on the top and sides. The stainless and the uranium temperatures are within 25°F of each other during both the steady state conditions and during the transient condition of the hypothetical fire accident.

Dimensional changes:

The stainless steel housing and depleted uranium shielding of the inner closure both expand with increasing temperature. Since the thermal expansion coefficient of the stainless steel is greater than that of the depleted uranium, the stainless housing will expand at a greater rate and the uranium to stainless gap will tend to grow with increasing temperature. There will be no tendency for the uranium to apply thermal expansion stress loads to its stainless steel housing.

The crystal structure of uranium is orthorhombic. This material may exhibit nonuniform crystal lattice growth upon thermal cycling. This growth may result in dimensional growth for hot or cold worked materials with oriented grain structure. The thermal cyclic growth (of uranium) is negligible if peak temperatures of cycling never exceed 299 to 349°C (570 to 660°F). See Ref. 2-26. From Table 3-2 of this document, the maximum temperature of the depleted uranium shielding is 299°F for the normal conditions of transport, and 486°F for the hypothetical accident conditions. Both of these temperatures are well below the critical temperature cycling range of 570 to 660°F.

2.6.2. Vibration

This cask is designed for transport by semitrailer only. Therefore, the only concern is that the fundamental frequency of vibration for the cask as a simply supported beam, loaded by its own weight, be appreciably higher than the repeatable impulse frequencies for the trailer itself.

The cask is considered to have a total moment of inertia (I) equal to the sum of the individual I values of the two shells and the uranium cylinder.

$$I_{outer\ shell} = \pi/4\ (14^4 - 13^4) = 7{,}750\ in.^4$$

$$I_{inner\ shell} = \pi/4\ (9.5^4 - 8.875^4) = 1{,}530$$

$$I_{uranium} = \pi/4\ (13^4 - 9.5^4) = \underline{16{,}041}$$

$$I_{total} = 25{,}321\ in.^4$$

Total weight of cask and contents = 47,600 lb

ℓ = 208 in.

$$\text{Frequency} = \frac{3.55}{\sqrt{\frac{5}{384}\frac{W\ell^3}{EI}}} = \frac{3.55}{\sqrt{\frac{5}{384}\frac{(47{,}600)(208)^3}{29 \times 10^6\ (25{,}321)}}}$$

$= \underline{40.7}$ cycles per second (cps)

Fundamental frequencies developed in trailers are generally in the range of 4 to 16 cps (see "Shock and Vibration Handbook, Vol. 3, Sect. 45).

2.6.3 Internal Pressure 50 psig Roark XIII - Case 1

See section 2.5.2 for inner container description

Hoop Stress

$$S_2 = \frac{PR}{t} = \frac{50(8.62)}{1/2} = 872 \text{ psi} \quad \text{ok, less than 30,000 psi}$$

Meridional Stress

$$S_1 = \frac{PR}{2t} = \frac{862}{2} = 481 \text{ psi}$$

Radial Displacement

$$= \frac{R}{E}(S_2 - \nu S_1)$$

$$= \frac{8.62}{30(10^6)}[862 - 0.3\ (431)z] = \frac{6300}{30(10^6)} = 0.00021 \text{ inches} \quad \text{ok}$$

2.6.4 Free Drop

2.6.4.1 Bottom 1-ft Drop

The integrity of the alternate closure system for a one foot bottom drop was verified through HONDO run No. BOT-11. Details of the HONDO model are presented in 2.7.3. This run is similar to the strain rate sensitive case except for the initial z-velocity v.

$s = 1$ ft = 12 in. for $1/2\ a\ t^2 = 12$

or $t = \frac{2 \times 12}{384} = \underline{0.25 \text{ sec}}$

$v = 0 + (384)(0.25) = \underline{96.0 \text{ in./sec}}$

Initial z-velocity = $\underline{-9.60 \text{ in./sec}}$ for all nodes except nodes 1 - 11. The results are summarized in Table 2-4.

2.6.4.2 Side Drop

This section shows the results of a one-foot side free drop of the cask without the impact limiter onto an unyielding surface and verifies the adequacy of the cask closure bolts' shear and inner closure bearing strengths.

Cask Closure:

Cask closure wt = $\underline{777 \text{ lb}}$

($\pi/4\ (27.12)^2\ 4.75\ (0.283) = 777$ lb)
Load factor n_s = g's

Ref. computer code run 39370 (2-8-79).

$n_s = 302$

Side Load F_s

$$F_s = W\, n_s = 777\ (302) = \underline{234{,}654 \text{ lb}}$$

Cask Closure Bolts

24 1-1/4 - 7 UNC - 2A x 4.5

Bolt Area:

$$24\ A_{root} = 24 \times 0.892 = \underline{21.408 \text{ in.}^2}$$

Bolt Shear:

$$\sigma = F_s/A_B = \frac{234{,}654}{21.408} = \underline{10{,}960 \text{ psi}}$$

If only 50% bolts loaded (no register)

$$60\%\ \sigma_y > \sigma_s = 21{,}920 \text{ psi}$$

Preload 600 lb - $\sigma_x = 6725$ psi

$$\tau_{max} = 1/2\ (\sigma_x^2 + 4\ \tau_{xy}^2)^{1/2} = 1/2 \sqrt{672.5^2 + 4(21{,}920)^2}$$
$$= \underline{22{,}175 \text{ psi}} \text{ max shear}$$

$$\sigma_p = \sigma_x/2 + \tau_{max} = \frac{6725}{2} + 22{,}175 = \underline{25{,}540 \text{ psi}} \text{ principle stress}$$

Inner Closure:

Inner closure wt** 665 lb

All DU assumed to be concentrated at the node.

g's = 602 Ref. computer run 3970 dated March 8, 1979.

F_s Load = W n_s = 665 (602) = 400,330 lb

12 bolts 1/2 13 UNC - 2A

Inner closure bolts not loaded in shear.

Closure side hearing area:

$A_B = D \times \ell = 20.5 \times 6 = 123 \text{ in.}^2$

Bearing Stress:

$$\sigma_p = F_s/A_B = \frac{400,330}{123} = 3255 \text{ psi}$$

**Note: The inner closure extends over two mass stations. The DU of mass two and three were summed and the greater load factor of the node is used for loads analysis.

$Wt = \pi/4 \times 18.5^2 (3 + 1.125) 0.6 = 665$ lb

2.7 HYPOTHETICAL ACCIDENT CONDITIONS

2.7.1 Free Drop

The dynamics of the 30-foot free fall requires that a value be found for the maximum stress at impact in order to use structural analysis methods based on statics.

Literature on the subject of dynamic stresses is largely theoretical and seldom of engineering application value. The complexity can be reduced by limiting the problem to (1) compressive stresses on flat impact (2) at 44 ft/sec and (3) to steel, aluminum and uranium materials.

The most promising engineering formula is that for dynamic compression of rigid-plastic cylinders and is the one used herein. It is well authenticated by:

(1) Goldsmith: Impact - eq. 5.97 page 191

(2) Cristensen: Dynamic plasticity - eq 7.8 page 55

TABLE 2-4
STRESS SUMMARY PER HONDO OUPUT FOR 1 FT BOTTOM DROP
(STRAIN RATE SENSITIVE CASE, RUN. NO. BOT-11)

Component	Element No.	Time (10^{-4} sec.)	Predominant Stress Type(s)	Max. or Min. Principal Stress (psi)	Yield Strength at Temp. (psi)
4340 Stl Bulkhead	232(Bot. CL)	17.0	Radial & Hoop	-11,420	150,000 (300°F)
0.2% Mo-U Alloy Shield, Lid	347 (Top CL) 303 (Bot. CL)	14.0 13.5	Radial & Hoop Radial & Hoop	-12,970 12,270	36,300 (300°F)
Top End of Container	205 (Inner Cyl.)	12.5	Axial Compr.	-28,520	30,300 (250°F)
Top End of Container	468 Cylinder Below Flange	17.5	Axial Tens.	21,580	*29,200 (300°F)
Container Lid Housing	281 (Bot. CL)	13.0	Rad & Hoop	11,650	*29,200 (300°F)

$\rho v_1^2 = \varepsilon_1 (P_1 - P_y)$

$\rho = \frac{lb/in^3}{386}$ $v_1^2 = [44 \text{ ft/sec} \times 12]^2 = 278{,}784 \text{ (in/sec)}^2$

where P_1 = initial, and maximum stress corresponding to moment of impact,

ε_1 = max. strain corresponding to P_1, and

P_y = static compressive yield point (log 0.002 in/in strain method)

Values of ρ and ρv_1^2

Aluminum	ρ = 0.097/386 = 0.000251	ρv_1^2 = 70
Steel (incl SS)	ρ = 0.290/386 = 0.0007512	= 209
Copper	ρ = 0.332/386 = 0.00086	= 240
Lead	ρ = 0.41/306 = 0.001062	= 296
Uranium	ρ = 0.683/386 = 0.001769	= 493

TABLE 2-5
TYPICAL DYNAMIC PROPERTIES

Material	Static Curve	P_y 0.002 offset	P_1	ε_1	P_1-P_y	$\varepsilon_1(R-P_y)$	$\frac{P_1-P_y}{P_y}$
Uranium Cast	NLC (Computed)	73,000	90,000	0.029	17,000	493.	0.233
302 SS	Goldsmith Fig. 250	41,350 F_{cy} = 35,000 (304SS)	53,800	0.01675	12,450	208	0.301

$$P_1 = 40{,}000 + \frac{825{,}000}{\varepsilon}$$

$$\varepsilon_1 = \frac{P_1 - 40{,}000}{825{,}000}$$

Material	Static Curve	P_y 0.002 offset	P_1	ε_1	P_1-P_y	$\varepsilon_1(R-P_y)$	$\frac{P_1-P_y}{P_y}$
0.24 Carbon Stl	Goldsmith Fig. 372	35,000	45,000	0.020	10,000	200	
Ni-Cr Stl	Goldsmith Fig. 118	220,000	228.000	0.024	8,000	192	0.036

2.7.1.1 End Drop

The dynamic analysis required for the cask and its parts, in the flat drop attitude, can be based on the concept of simple cylinders which behave as solid rods impacting squarely upon a rigid surface at the velocity of the specified free fall distance of 30 feet. This velocity is 44 ft/sec.

Values for stress, strain, K-E and G loadings can be derived for the individual masses and for the cask as a whole.

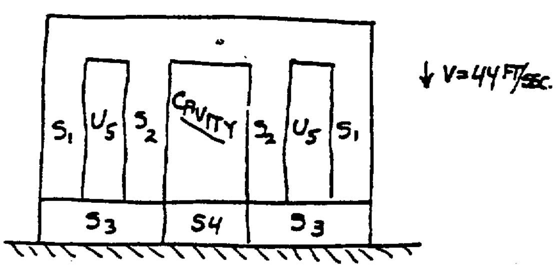

MODEL FOR ANALYSIS

S_1 = Outer S.S. shell

S_2 = Inner S.S. shell

U_5 = Uranium cylinder

These are considered separate cylinders

S_1 and S_2 weights include parts of the head weight

S_3 = SS plate - acting as striking plate under S_1, U_5 and S_2

S_4 = part of S.S. plate stressed by impact from container, etc

	Area	Weight
S_1	86.3 in^2	5125 lb (includes 860 lb-outer closure)
S_2	36.8 in^2	2260 lb (includes 270 lb-inner closure)
U_5	250.9 in.^{2}	32,400 lb
	374 in.^{2}	39,785 lb

S_3	378.5 in.^{2}	990 lb
S_4	248.5 in.^{2}	5,249 lb (1919 container, 1800 contents)
	Total	46,024 lb

Initial and maximum stresses developed by striking a rigid mass are calculated for uranium and steel, derived from

$$\rho v_1^2 = \varepsilon(P_1 - P_y) \text{ as previously shown}$$

P_1 uranium = 90,000 psi

P_1 stainless steel = 53,800 psi

For cylinders S_1, U_5 and S_2, the assumption of striking a rigid mass is conservative. Actually, they strike against an intermediate mass S_3, with some consequential reduction in stress.

S_3, on its under-surface, does strike a rigid mass, and counts S_1 U_5 and S_2 only as added load, considered as an equivalent weight of steel, added to the height of S_3 as a cylinder.

Stress differentials at the interfaces with S_3 are considered localized and quickly find equilibrium, producing a local increase in stress intensity in S_3 to match a reduced stress in U_5.

Total force developed at impacting face F = P_1 (area)

For S_1	F_1 = 86.3 in² x 53,800 psi =	4,640,000 lb
S_2	F_2 = 36.8 in² x 53,800 psi =	1,975,000 lb
U_5	F_5 = 250.9 in² x 90,000 psi =	22,581,000 lb

G's Developed		G = F/wt
S_1	4,640,000/5125 =	905 G
S_2	1,975,000/2260 =	875 G
U_5	22,581,000/32,400 =	697 G
S_3	29,196,000/39,785 =	735 G for bottom of cask

2.7.1.2. Side Drop

Simultaneous impact on the tail and the plywood impact limiter section after release from a 30-ft height induced the side loading of the cask analogous to that of a simply supported beam. This loading, from a bending standpoint, is the most severe loading condition. All the kinetic energy is absorbed by the impact deformation and beam deflection.

The cask model is made up of 69 disk elements with the appropriate section properties. Side drop geometry is described in Figure 2-3.

All extreme yielding was below 35% by a good margin in the case of the stainless steel (Ref. computer code DEC 15-002, side drop 02) and below 8% for uranium (side drop only).

FIG. 2-3

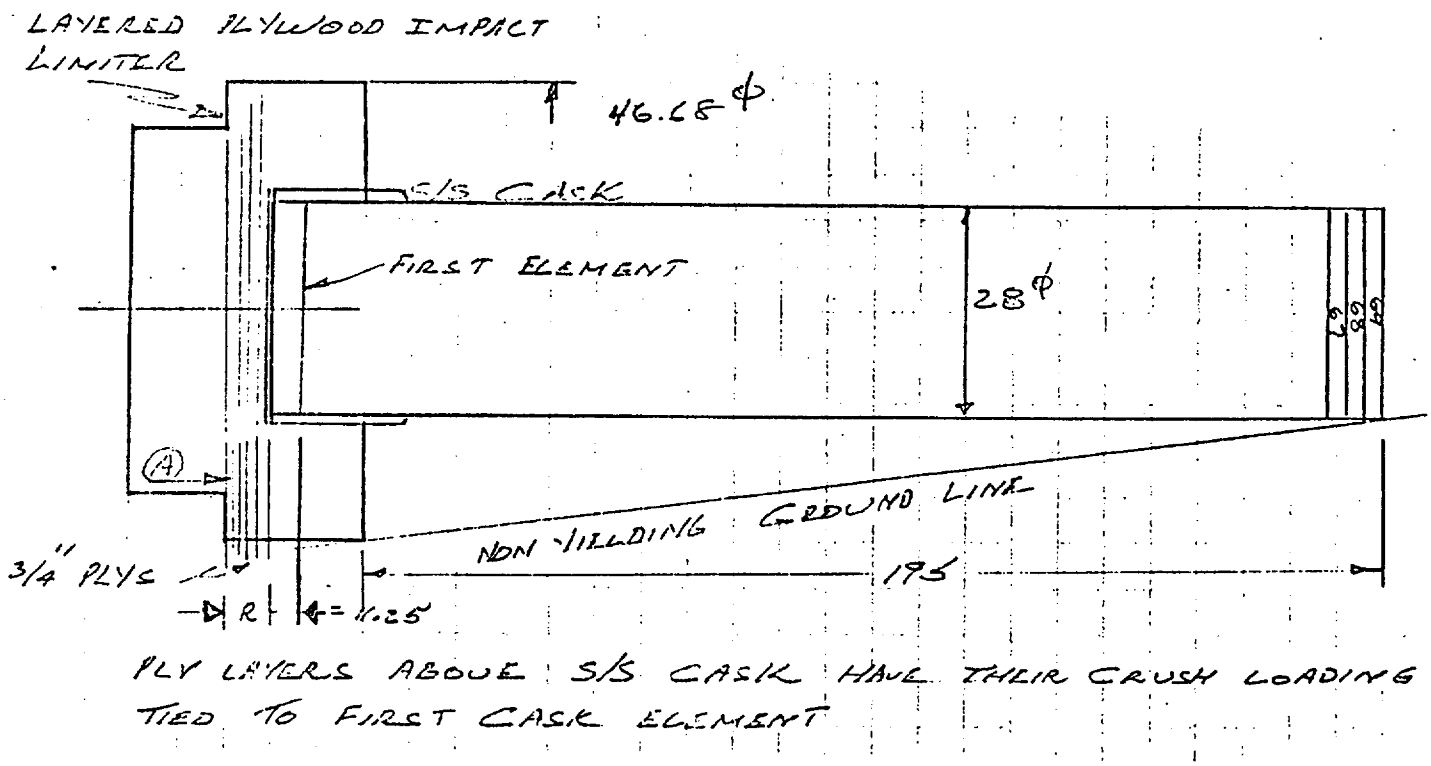
LAYERED PLYWOOD IMPACT LIMITER
46.68 φ
S/S CASK
FIRST ELEMENT
28 φ
(A)
NON YIELDING GROUND LINE
195
3/4" PLYS
R
= 1.25
PLY LAYERS ABOVE S/S CASK HAVE THEIR CRUSH LOADING TIED TO FIRST CASK ELEMENT

Resistance of Cask to Deformation

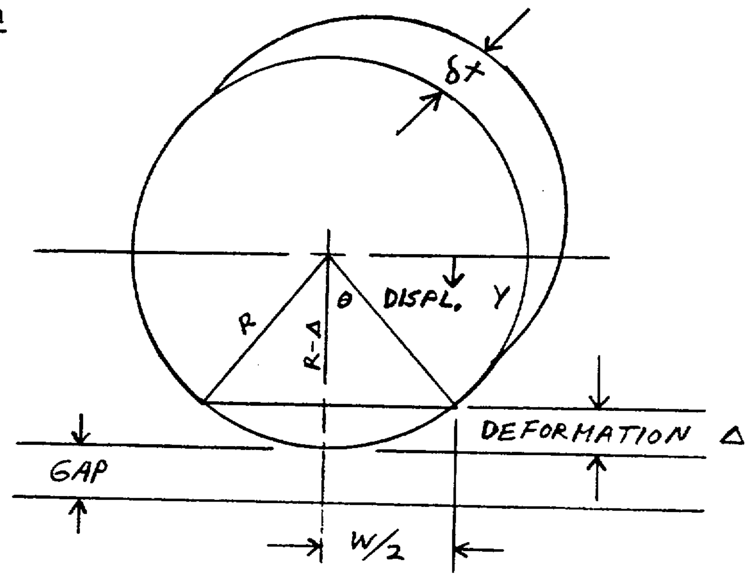

$\delta_F = (W\ \delta_x)\ \sigma_F$

$\theta = \cos^{-1}\{(R - \Delta)/R\}$

$W = 2\ R\ \sin\theta$

$\Delta = y - GAP$ (if positive) otherwise $\Delta = 0$

Resistance Function per Code

Force = 2 * R * sinθ * sigma * Dx

Del = Y-G (if positive)

Theta - A cos ((R - del)/R)

The maximum value of 'del' is saved to be compared to previous value to see if unloading is taking place.

Solid Section

Since type 304 stainless steel lacks a pronounced yield stress, the actual stress-strain curve shown on Figure 2-4 was employed for the moment curvature codes. The standard assumption was made that the strain distribution remains linear.

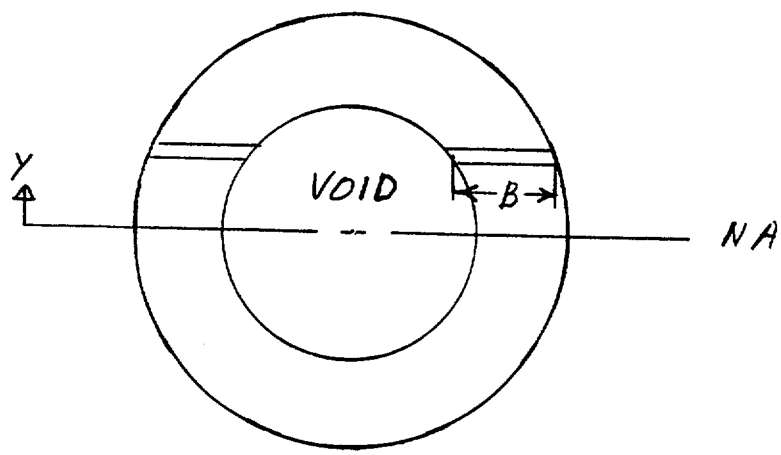

$$\varepsilon(y) = \phi \times y$$

$$F = 2\int_0^R \sigma\, \varepsilon(y) \times B(y)\, dy = 0$$

$$M = \int_0^R y \times \sigma\, (\varepsilon(y) \times B(y)\, dy$$

A computer subroutine was used to evaluate the integral in the above moment expression. The stress-strain curve was approximated by the straight line segments shown on Figure 2-5. Linear interpolation was used between the circled points.

FIG. 2-4

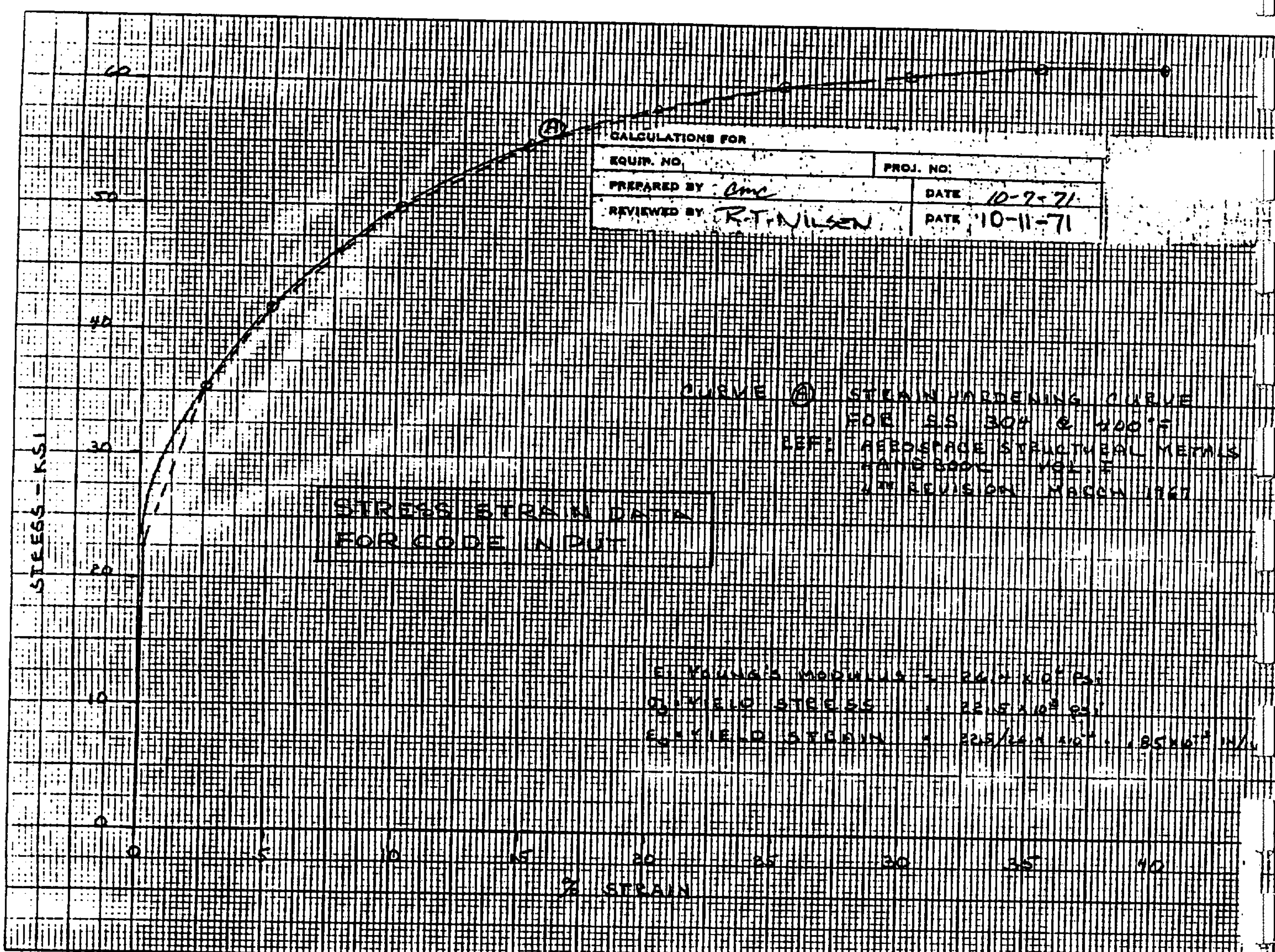
STRESS - KSI
% STRAIN
CALCULATIONS FOR
EQUIP. NO.
PROJ. NO.
PREPARED BY
DATE 10-7-71
REVIEWED BY R. T. NILSEN
DATE 10-11-71
CURVE (A) STRAIN HARDENING CURVE
FOR SS 304 & 400°F
REF: AEROSPACE STRUCTURAL METALS
STRESS STRAIN DATA
FOR CODE INPUT

2.7.1.3 Calculation of Mass Point Properties

Point 1 - Total Impact Plate 4.75 in. + 3 in. ss

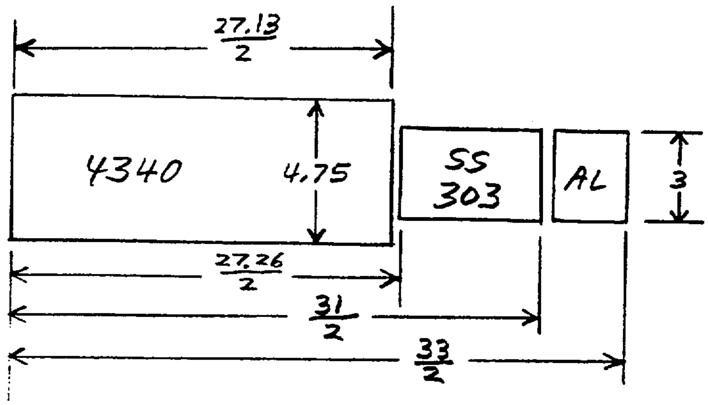

$$W = \pi/4\ (27.13^2 * 4.75 * 2.83 + (31^2 - 27.26\text{-}^2) * 3 * 0.3$$

$$+ (33^3 - 31^2)\ 3 \times 0.1$$

$$\pi/4 \quad 989.4 \quad 196.1 + 38.4) = \underline{961\ \text{lb}}$$

$$M = w/g = 961/384 = \underline{2.50\ \text{lb sec}^2/\text{in.}}$$

I (SS only) $E = 27.7 \times 10^6$ psi

$$\pi/4\ (R_o^4 - R_i^4) = \pi/4\ (15.5^4 - 13.63^4) = \underline{18{,}227\ \text{in.}^4}$$

FIG. 2-5

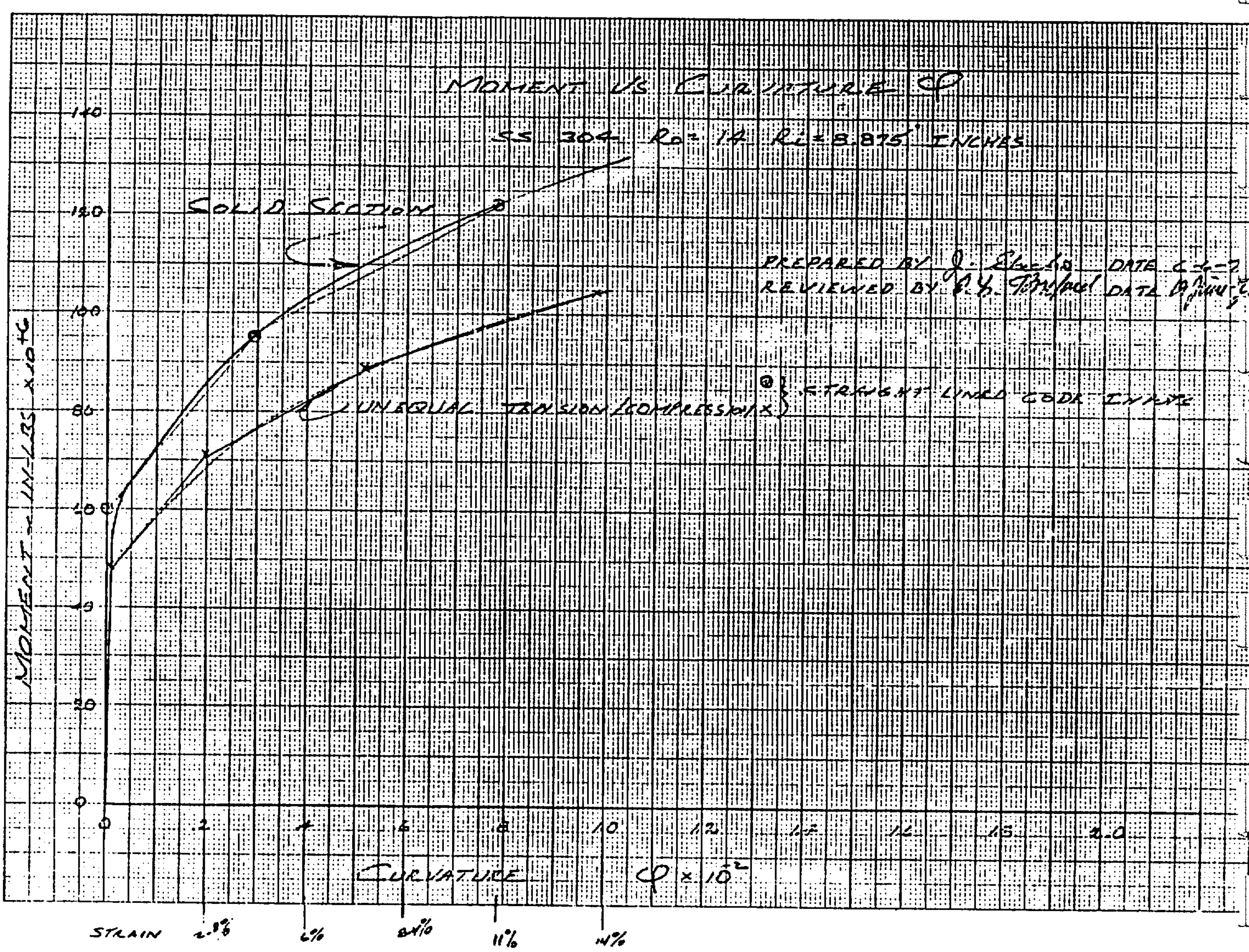
MOMENT VS CURVATURE φ
SS 304 Ro = 14 Ri = 8.875 INCHES
SOLID SECTION
UNEQUAL TENSION/COMPRESSION
STRAIGHT LINED CODE INPUT
PREPARED BY DATE
REVIEWED BY DATE
MOMENT ~ IN-LBS x10+6
140
120
100
80
60
40
20
0
0
.2
.4
.6
.8
1.0
1.2
1.4
1.6
1.8
2.0
CURVATURE φ x 10⁻²
STRAIN
2.8%
6%
8.4%
11%
14%

Point 2

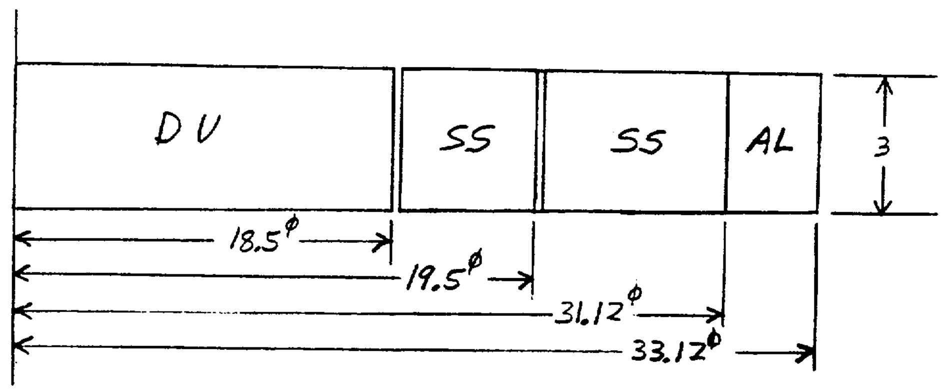

$W = 3\pi/4\ (18.5^2 * 0.6 + 19.5^2 - 18.5^2)\ 0.3 + 31.12^2 - 19.5^2)\ 0.3$

$+ (33.12^2 - 31.16^2)\ 0.1]$

$3\pi/4\ [205.35 + 11.4 + 176.46 + 12.85] = \underline{957\ lb}$

$M = w/g = 957/384 = \underline{2.49\ lb\ sec^2/in.}$

$E = 27.7 \times 10^6$ psi

I - (SS only)

$I = \pi/64\ \{(31.12^4 - 19.5^4) + (19.5^4 - 18.5^4)\} = 40{,}289\ in.^4$

Point 3

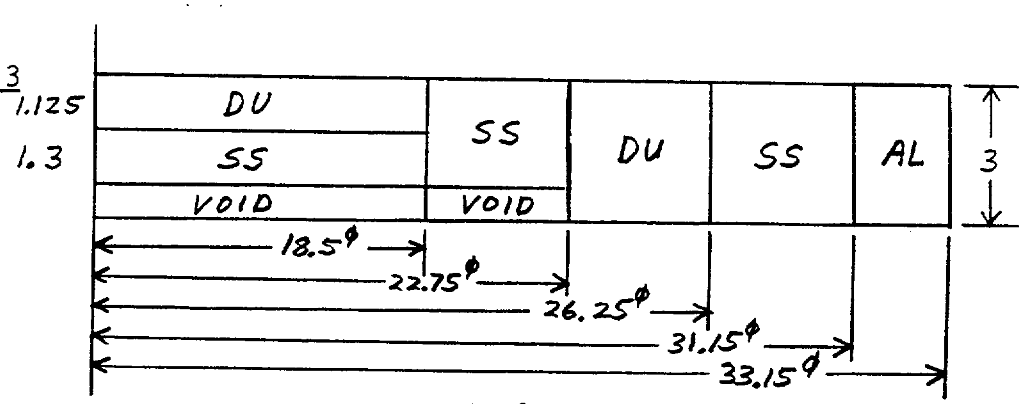

$$w = \pi/4\ (18.5^2 * (1.125 * 0.6 + 1.3 * 0.3) + (22.75\text{-}^2 - 18.5\text{-}^2)\ 2.43 * 0.3 + (26.25\text{-}^2 - 22.75^2) * 3 * 0.6 + (31.15\text{-}^2 - 26.25\text{-}^2) * 3 * 0.3$$

$$(33.15 - 31.15^2) * 3 * 1) = \pi/4\ (1092.7) = 858.2 \text{ lb}$$

$$m = w/g = 838.2/384 = 2.23 \text{ lb sec}^2/\text{in.}$$

$$I = \pi/64\ \{(31.15^4 - 26.25^4) + 26.25^4 - 22.75^4) + (22.75 - 18.5^4)$$

$$\pi/64\ \{824{,}391\} = \underline{40{,}467 \text{ in.}^4}$$

<u>Point 4</u>

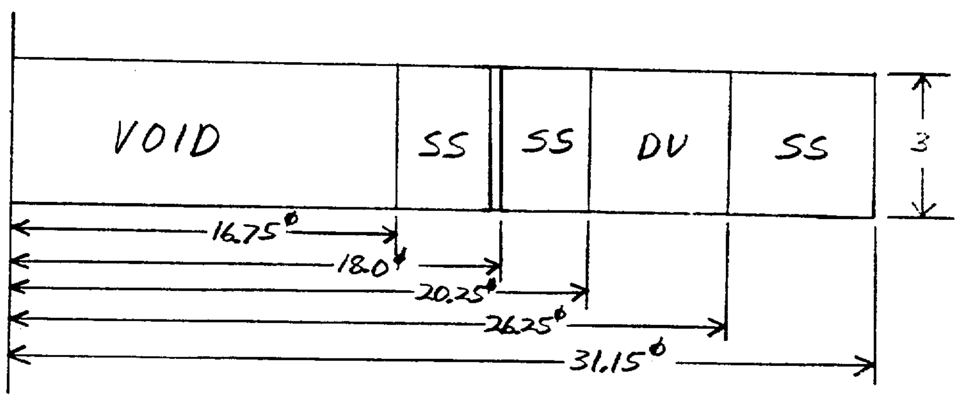

$$w = 3\pi/4\ \{(18^2 - 16.75^2)\ 0.3 + (20.25^2 - 18.0^2)\ 0.3$$

$$+ (26.25^2 - 20.25^2)\ 0.6 + (31.15^2 - 26.25^2)\ 0.3\}$$

$$= 3\pi/4\ (290.628) = \underline{685 \text{ lb}}$$

$$M = w/g = 685/384 = \underline{1.78 \text{ lb sec}^2/\text{in.}}$$

$I = \pi/64\ (31.15^4 - 18.0^4) = \underline{41{,}064\ in.^4}$

Points 5 - 66

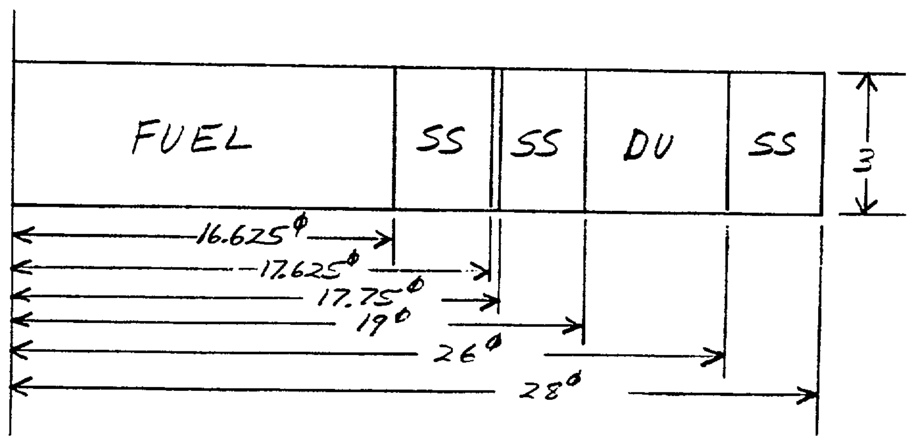

$$W = 3\pi/4\ \{16.625^2 * 0.046 + (17.625^2 - 16.625^2)\ 0.287$$

$$+ (19^2 - 17.75^2)\ 0.287$$

$$+ (26^2 - 19^2)\ 0.683 + (28^2 - 26^2)\ 0.287\} = \underline{664\ lb}$$

$$I = \pi/64\ \{(28^4 - 26^4) + (26^4 - 19^4) + (19^4) - 17.75^4\} = \underline{25{,}999\ in.^4}$$

Points 67-69

$W = 3 * \pi * 14^2 * 0.287 = \underline{530\ lb}$

$M = w/g = 530/384 = \underline{1.38\ lb\ sec^2/in.^2}$

$I = \pi/4\ 14^4 = \underline{30{,}172\ in.^4}$

2.7.1.4 Code Input Plastic Curvature vs. Moment

(Curve Points)

Point 1

$\underline{M = 60.E6}$ $\underline{\phi^P} \underline{= 0}$

Point 2

$M = \underline{95.E6}$

$\phi^P = 0.003 - 95\ EG/27.7E6\ 30/72$

$= \underline{0.00296}$

Point 3

$\underline{M = 122.E6}$

$\phi^P = 0.0079 - 122\ E6/27.7\ E6\ (30{,}172)$

$= \underline{0.0782}$

Point 4

M = 142E6

ϕ^P = 0.0149 - 142E6/27.7 (30,172)

= 0.01479

CASK LAP JOINTS

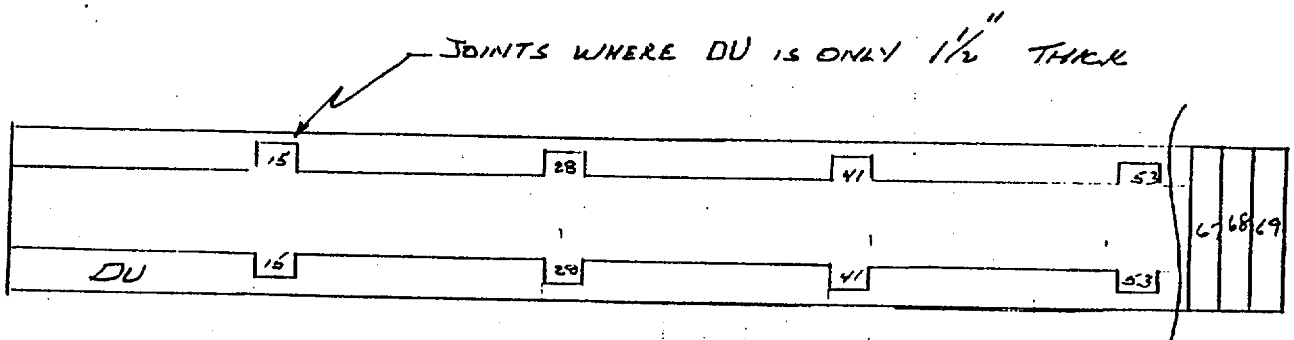

JOINTS 15, 28, 41. AND 53 URANIUM JOINTS

SEE CODE M VS φ UNEQUAL TEN/COMP
FOR: $I_{X_{AV}}$ (21500 LB IN SEC²)
1/3 AIR (≈ 3 IN.)

2.7.1.5 Unequal Sectioned Cask (M vs θ)

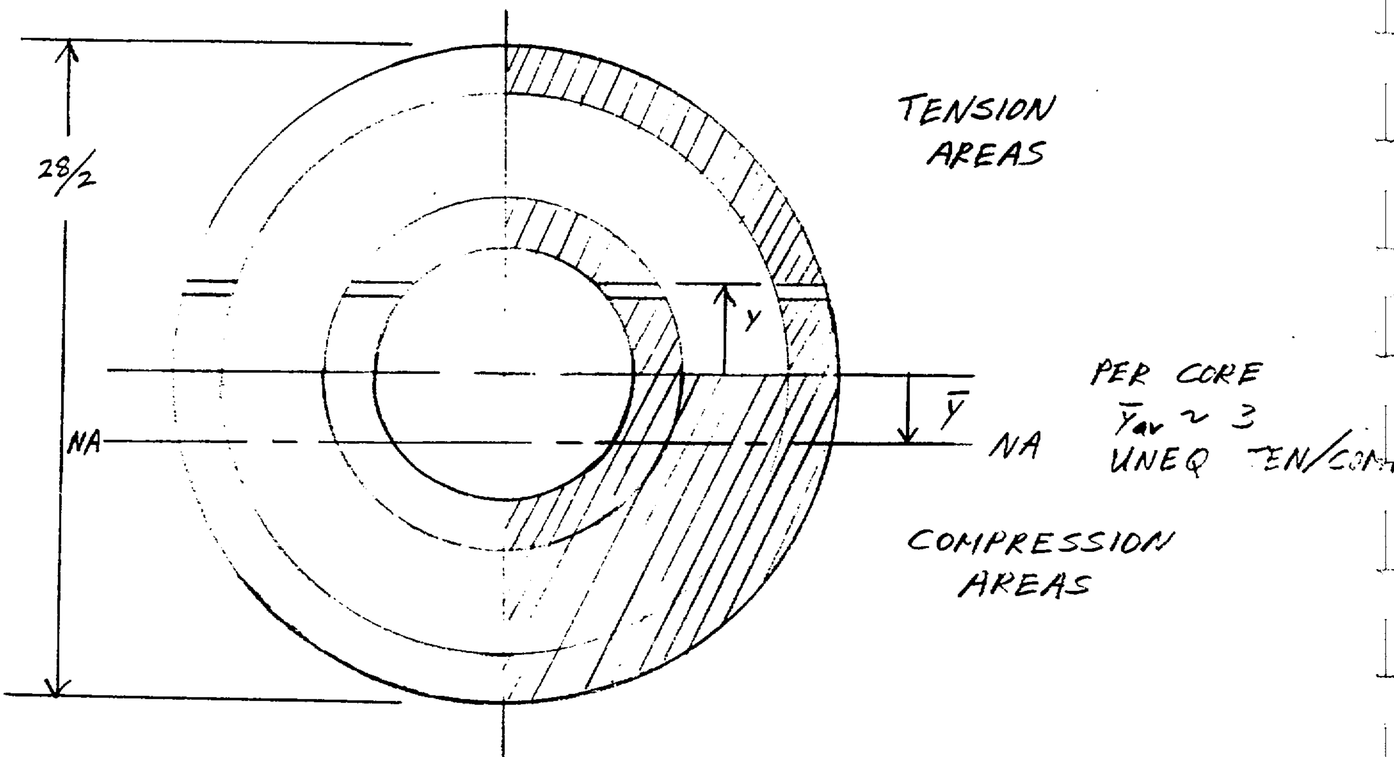

$$M = \int_{-R_o}^{R_o} (y - \bar{y}) \times \sigma (\varepsilon(y) \times B(y) \, dy$$

$$F = \int_{-R_o}^{R} \sigma (\varepsilon(y) \times B(y) \, dy = 0$$

$$\varepsilon(y) = \phi \times (y - \bar{y})$$

Maximum strain: side drop unequal case

$$2.848 \times 10^{-3} * \left[(28/2) + 3\right] = 4.84\% < 8\%$$

Code input plastic curvature vs moment

Point 1

$M = 48.0 \times 10^{6}$ $\phi^{P} = \underline{0.0}$

Point 2

$M = \underline{71.5} \times 10^{6}$

$\phi^{P} = 0.0021 - 71.5 \times 10^{6}/(21{,}500 \times 27.7 \times 10^{6})$

$= \underline{0.00198}$

Point 3

$M = \underline{89.5 \times 10^{6}}$

$\phi^{P} = 0.0053 - 89.5 \times 10^{6}/(21{,}500 \times 27.7 \times 10^{6})$

$= \underline{0.00515}$

Point 4

$M = \underline{105 \times 10^{6}}$

$\phi^{P} = 0.010 - 105 \times 10^{6}/(21{,}500 \times 27.7 \times 10^{6})$

$= \underline{0.00982}$

2.7.1.6 Inner Closure & Cask Bulkhead 30-ft Side Drop (Solid Section)

Results of Computer Analysis

Maximum Load Factors:

Uranium shield, inner closure: 2017 g

4340 alloy steel outer closure: 1133 g

Uranium shield, inner closure:

σ_c = 26,100 psi < S_y = 48,000 psi @ 300°F

4340 alloy steel outer closure: bolts take load

$\sigma_{s_{bolt}}$ = 41,125 psi

Max. strain:

Element 15 plastic curve = 2.032 x 10^{-3}

03A side drop code (solid)

Strain = 2.033 x 10^{-3} x 14 = 2.8% < 8%

$$\phi = \frac{\varepsilon}{R_o}$$

2.7.1.7 Unequal Tension Compression 30-ft Side Drop

Results of Computer Analysis

Max Load Factors

Uranium shield, inner closure = 2094 g

4340 alloy steel outer closure = 1351 g

Max Stress

Uranium shield, inner closure:

$\sigma_c = 27{,}100$ psi < $S_y = 48$ ksi at 300 °F

4340 alloy steel outer closure

Hold down bolts take load in shear:

$\sigma_{s_{bolts}}$ = <u>49,035 psi</u>

Max Strain

Element 15 plastic curvature - 3.925×10^{3}

Strain: 3.925×10^{-3} (28/2 + 3) = 6.7% < 8%

(Neutral axis averages 3 in. below centerline)

$$\phi = \frac{\varepsilon}{R_o}$$

02A side drop code 3.92×10^{-3}

2.7.1.8. Cask Side Drop Equation Derivation

The development of the side drop equations used in the computer code is presented in the following writeup.

The cask is divided into 69 lumped masses joined by a line beam with the appropriate representative section properties, i.e., the initial cask drop velocity is that realized when dropped 30 ft height, making a simultaneous head and tail ground strike. As the cask has a plywood impact limiter of larger diameter than the body proper only the head and tail section make initial ground contact. Then as the beam deflects additional base reactive forces are imparted to the beam as shown in the line element sketched below.

The beam element force and the dynamic equilibrium of each mass element is generated in terms of the bending moment at the mass point. A second central difference is used to approximate the curvature of the beam segments. The bending moment is related to the curvature through a one-dimensional yield criteria and associated flow rule.

GENERAL DEVELOPMENT

DERIVATION OF DYNAMIC RESPONSE OF BEAM

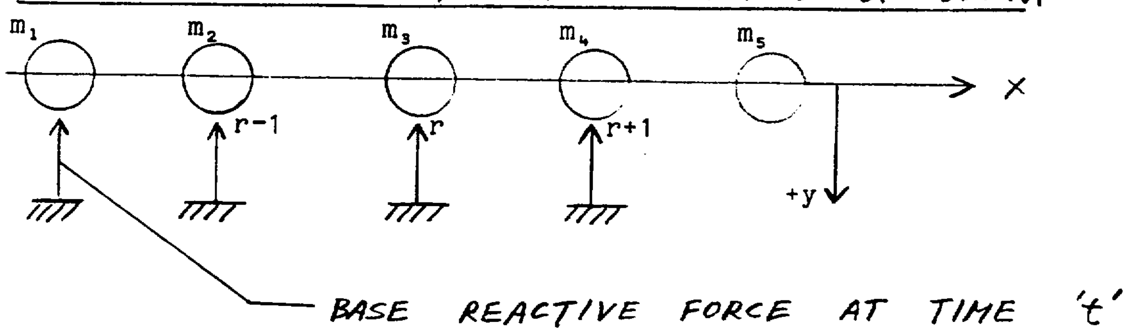

Beam element (between masses) forces

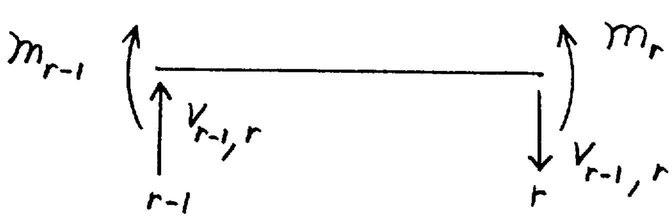

Dynamic Equilibrium of Mass r

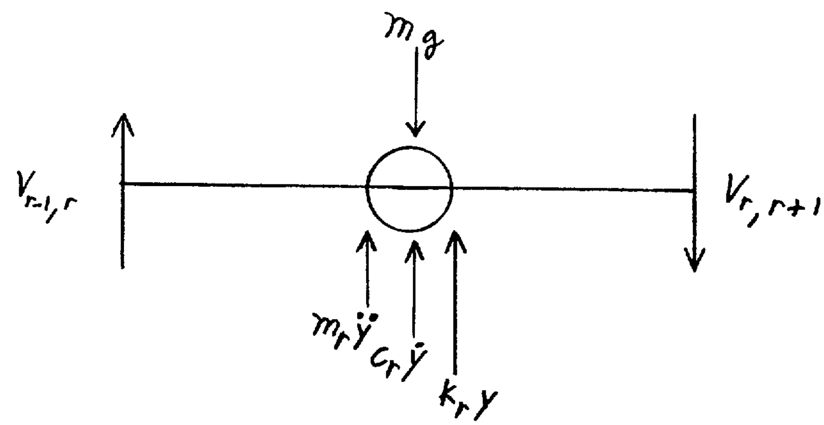

The curvature at point r is approximated by the second central difference for interior points.

$$\left(\frac{d^2y}{dx^2}\right)_r \approx -\frac{1}{\Delta x^2}\left(y_{r+1} - 2y_r + y_{r-1}\right)$$

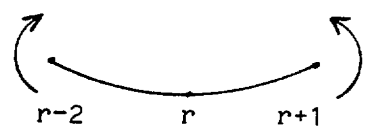

The Moment m is Defined

$$m_r = EI\,\frac{d^2y}{dx^2} \approx -\frac{EI}{\Delta x^2}\left(y_{r+1} - 2y_r + y_{r-1}\right) \qquad (1)$$

Interior Nodes' Dynamic Equilibrium

$$V_{r1,r} = \frac{m_r - m_{r-1}}{\Delta x} \qquad (2)$$

$$m_r \ddot{y} + V_{r-1,r} - V_{r,r+1} + C \dot{y}_r + K y_r = m_r g$$

Substituting the shear expression in the above yields:

$$m_r \ddot{y}_r - \frac{\left(m_{r-1} - 2 m_r + m_{r+1}\right)}{\Delta x} + C \dot{y}_r + K y_r = m_r g$$

<u>At the first node</u>

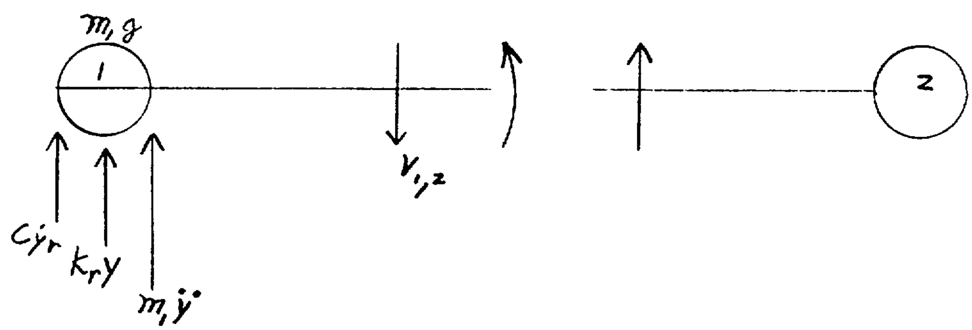

<u>Then for Node 1</u>

$$m_1 \ddot{y} - V_{1,2} + C_1 \dot{y} + k_1 y = m_1 g \qquad (3)$$

Substituting as before but with the moment on one side only of the mass.

$$m_1 \ddot{y} - \frac{m_2}{\Delta x} + C_1 \dot{y}_1 + k_1 y = m_1 g$$

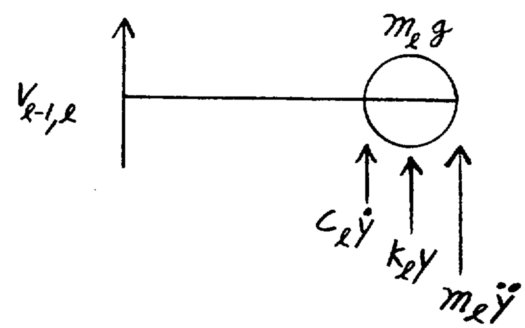

and in similar fashion, the last mass

equation is defined:

$$m_\ell \ddot{y}_\ell - \frac{m_{\ell-1}}{\Delta x} + c \dot{y}_\ell + k y_\ell = m_\ell g \quad (4)$$

The second difference scheme and predicting algorithm are indicated below (see Ref. 2-14) for the Δt time stations:

$$y^{(s+1)} = 2y^{(s)} - y^{(s-1)} + \ddot{y}^{(s)} \Delta t^2 \quad (5)$$

and

$$\dot{y}^{(s)} = \frac{y^{(s)} - y^{(s-1)}}{\Delta t} + \ddot{y}^{(s)} \frac{\Delta t}{2} \quad (6)$$

Substituting Eq. (6) into Eq. (2) gives the following:

$$\ddot{y}^{(s)} = \frac{m_r g - k\, y^{(s)} - c\, (y^{(s)} - y^{(s-1)})/\Delta t + \frac{m_{r-1} - 2\, m_r + m_{r+1}}{\Delta t}}{(m_r + c\, \Delta t/2)} \quad (7)$$

To start assume (Ref. 2-14, p. 6)

$$y^{(2)} = \frac{1}{6} \left[2\, \ddot{y}^{(1)} + \ddot{y}^{(2)}\right] \Delta t^2 + \dot{y}^{(1)} \Delta t \quad (8)$$

As $\ddot{y}^{(2)}$ is not known the first value is assumed and then Eq. (7) may be solved for a corrected $\ddot{y}^{(2)}$. This process is repeated until no change is noted in $\ddot{y}^{(2)}$.

2.7.1.9 Determination of Stress During Elasto-Plastic Straining

Considering the elastic strain

$$d\varepsilon_e = D^{-1}\, d\sigma \qquad D = \text{elastic constant matrix}$$

If yield is reached

$$F(\sigma, \varepsilon_p, k) = 0$$

where σ = relevant stress comp,
ε_p = accumulated plastic strain, and
k = strain hardening parameter.

Plastic straining may occur and the total strain changes are given as:

$$\underline{d\varepsilon = d\varepsilon_e + d\varepsilon_p}$$

For added generality the plastic potential to which the normally principles is applicable,

$$Q(\sigma, \varepsilon_p, k_o) = 0$$

where $F \equiv Q$

During plastic deformation by the normality rule:

$$d\,\varepsilon_p = d\lambda \frac{\partial Q}{\partial \sigma} = d\lambda\, \bar{a} \; ; \; \bar{a} = \begin{Bmatrix} \partial Q/\partial x \\ \vdots \\ \vdots \end{Bmatrix} = \frac{|M|}{M}$$

and is a vector defined at any stress state. During plastic deformation $F = 0$ and

$$dF = (\partial F/\partial \sigma)^T d\sigma + \partial F/\partial k \, dk + \{\partial F/\partial \varepsilon_p\}^T d\varepsilon_p = 0$$

If $a = \left\{ \begin{matrix} \partial F/\partial F \\ \vdots \end{matrix} \right\}$ and $A = \frac{-1}{d\lambda} \left[\frac{\partial F}{\partial k} dk + (\partial F/\partial \varepsilon_p)^T d\varepsilon_p \right]$

dF may be defined: $dF = a^T d\sigma - A \, d\lambda = 0$ so that

$$\underline{d\varepsilon = D^{-1} d\sigma + d\lambda \, \bar{a}}$$

Premultiplying the aforementioned $d\varepsilon$ expression by $a^T D$ and eliminating $d\sigma$ by $dF = 0$, the following is obtained

$$d^T d\varepsilon = A \, d\lambda + d\lambda \, \bar{\beta}$$

where $d = Da$, $\bar{\beta} = A^T \bar{d}$ $\bar{d} = D \, \bar{a}$, now the plastic multiplier is:

$$d\lambda = \frac{1}{A + \bar{\beta}} d^T d\varepsilon$$

substituting $d\lambda$ in the $d\varepsilon$ expression and rearranging

$$d\sigma = (D - D_p) \, d\varepsilon = D\varepsilon_p \, d\varepsilon$$

where

$$D = \frac{1}{A + \bar{\beta}} \bar{d} \, d^T \qquad (D \, d\varepsilon = d\lambda \, \bar{d})$$

In the $d\sigma$ expression above, the stresses are uniquely determined during any iteration in which known finite changes or strain are imposed.

Isotropic hardening assumes a uniform expansion of the initial yield surface, assuming $\partial F/\partial \varepsilon_p = 0$ with k defined $dk_p = d\bar{\varepsilon}$. Then for the isotropic work hardening $A = \frac{1}{d\lambda} M' \frac{d\varepsilon_u^P}{dk} dk = H'$ where H' is the scope of the curve relating the uniaxial stress and the corresponding plastic strain.

$$d\lambda = \frac{1}{A + \bar{\beta}} d^T dk = \frac{1}{H' + \bar{\beta}} d^T dk$$

a = ABS(M)/M

with $d^T = Da$, D = H = EI

$\beta = \bar{a}^T d, \; \bar{d}^T = D\bar{a}$

$$d\lambda = \frac{H \; ABS(M)/M}{H' + H} dk$$

d = H ABS(M)/M

$$H' = \frac{H^*H}{H - H^*} = \frac{H^*}{1 - H^*/H}$$

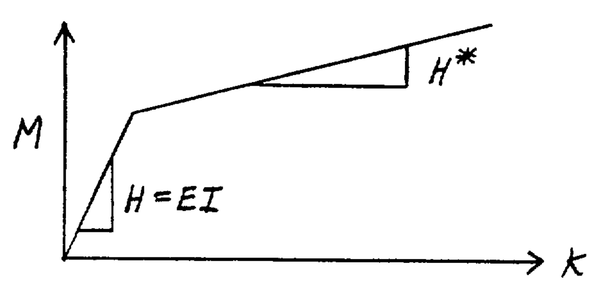

2.7.1.10 Corner Drop-Bottom Corner

In the corner drop calculations the assumption is made that the ungula developed at the impact position represents the total compressive effects at a focal point, rather than the actual nonlinear distribution of strain throughout the whole impacting mass, both elastic and plastic. It allows calculation of maximum stress values, etc., without regard for actual distribution of stress and strain at noncritical values.

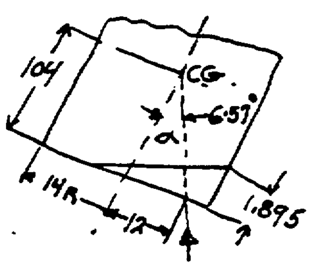

$\alpha = \arctan \frac{12}{104} = .1152$

$= 6.57°$

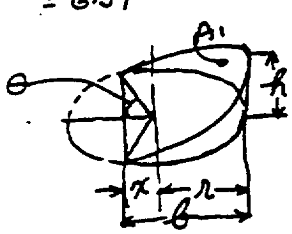

The calculated ungula is a greater volume than will actually result from impact, for this reason.

$$V_{(ungula)} = \frac{h}{b} r^3 \left[\sin\theta - \frac{\sin^3\theta}{3} - \theta\cos\theta\right]$$

$$\frac{h}{b} = 0.1152 \qquad r^3 = 14^3 = 2744$$

$\therefore\ = (0.1152)2744[\ ] = 317[\ ]$

Assume center of impact 2 in. from edge, at R = 12 in.

Total weight impacting on SS bottom plate = 46024 lb

KE = (46024)(360 in.) = 16,600,000 in. lb

Mean flow stress for SS. (Approximately)

P = 53,800 psi

$$\frac{KE}{P} = \frac{16{,}600{,}000}{53{,}800} = 308 \text{ in.}^3$$

This is the calculated ungula volume

$\therefore$ Vol = 317 [ ] = 308 $\qquad [\ ] = \frac{308}{317} = 0.972$

Let $\theta = 100°$, then $[0.9848^3 - \frac{0.9848^3}{3} - (1.745)(-0.1736)] = 0.970$

and $\theta = 1.745$ radians

$x = r \cos\theta = 14(0.1736) = \underline{2.43 \text{ in.}}$

$b = r + x = 14 + 2.43 = \underline{16.43 \text{ in.}}$

$h = b\ (0.1153) = 1.895$ in.

Contact area A_1 = approx. $\frac{\pi r^2}{2} + 2rx = \frac{615.75}{2} + 28\ (2.43)$

$A_1 = 307.9 + 68 = \underline{375.9 \text{ in.}^2}$

$F_{max} = A_1 P_1 = (375.9)(53{,}800) = \underline{20{,}200{,}000 \text{ lb}}$

$F/wt = \frac{20{,}200{,}000}{46{,}024} = \underline{438\ G}$ vertically,

Component along axis:

$(438\ G)(\cos 6.57°) = 438\ (0.99343) = \underline{435\ G}$

Bottom Plug Bolt Stresses:

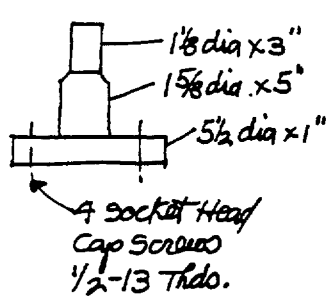

$\pi/4\ (1.125)^2 \times 3 = 3.0 \text{ in}^3$

$\pi/4\ (1.625)^2 \times 5 = 10.4$

$\pi/4\ (5.5)^2 \times 1 = 23.8$

$37.2 \text{ in}^3 \times .284 = \underline{10.57 \text{ LBS}}$

Component of deceleration along axis of cask in corner drop is 435G.

Impact force on bottom plug is:

$F = W \cdot G = (10.57)\ (435) = \underline{4600\ \text{lb}}$

Each socket head cap screw has a tensile yield strength of:

20,400 lb (high strength steel - 130,000 psi yield)
4,700 lb (stainless steel - 30,000 psi yield)
Minimum strength: $4 \times 4{,}700 = \underline{18{,}800\ \text{lb}}$
Margin: $\dfrac{18{,}800}{4{,}600} - 1 = 3.08$

2.7.2 Puncture

This cask has uranium as shielding between the inner and outer shells. Therefore, piercing of the outer shell with potential loss of shielding in the fire case cannot occur.

Instead, a shallow indent appears on the stainless steel outer shell where the edge of the 6-in. diameter pin partly cuts into it. This is clearly shown in report KY-546 by Clifford, Ref. 2-15. Actually, the pin is more damaged than the cask.

Energy is, however, absorbed in the three concentric shells of the cask in bending, with the possible formation of a plastic hinge.

The approximate distribution of moments among the shells can be made, assuming elastic deflections and an extreme fiber stress of 30,000 psi for both uranium and stainless steel inner and outer shells, with the same deflections, of course. Relative values follow:

34.2%	25,300 in. lb	1 in. SS outer shell
59%	43,500 in. lb	3-1/2 in. uranium
6.8%	5,030 in. lb	5/8-in. inner shell
100%	73,830 in. lb	

Reference 2-16 in the Handbook of the Engineering Sciences - Vol. I - "The Basic Sciences" (pg. 1302-1307) gives the plastic region diagram in a beam when the midsection is just completely plastic.

For the uranium cylinder

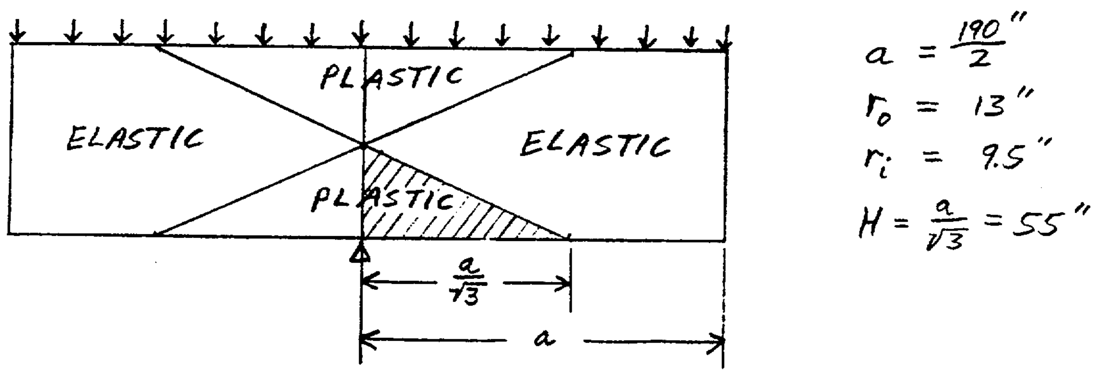

The plastic volume = 4 x volume of shaded ungula

$$= 4 \left(\frac{2}{3}\right)(r_o^2 - r_i^2)\, H = 4\left(\frac{2}{3}\right)(13^2 - 9.5^2)\, 55$$

$$= 11{,}520 \text{ in.}^3$$

Each plastic cubic inch has been elongated 0.2% to reach a terminal stress of 30,000 psi (yield point for uranium).

The energy absorbed is

$$U = \frac{30{,}000}{2} (11{,}520)\ (0.002) = \underline{345{,}600 \text{ in. lb}}$$

The total energy of the 40-in. fall is

$$U_{tot} = (46,500 \text{ lb})\ 40 \text{ in.} = 1,860,000 \text{ in. lb}$$

The difference must be absorbed in bending of the "plastic hinge."

$$U_B = 1,860,000 - 345,600 = \underline{1,514,400 \text{ in. lb}}$$

Determination of plastic section modulus

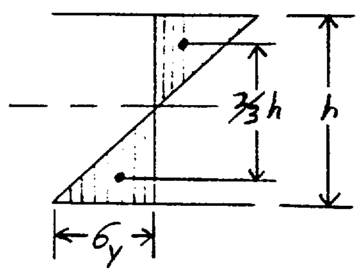

b = WIDTH
RECTANGULAR
SECTION

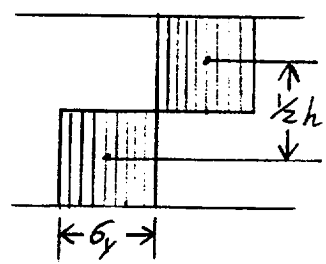

Elastic

$$M_E = \frac{\sigma_y}{2} \times \frac{h}{2}\left(\frac{2}{3}h\right) b$$

$$= \sigma_y \frac{bh^2}{6}$$

Plastic

$$M_p = \sigma_y x \frac{h}{2}\left(\frac{h}{2} b\right) \qquad \therefore M_p = \frac{3}{2} M_E$$

$$= \sigma_y \frac{bh^2}{4}$$

For the circular section of the uranium cylinder

$$I = \frac{\pi}{4}(r_o^4 - r_i^4) \qquad Z_E = \frac{\pi}{4}\frac{(r_o^4 - r_i^4)}{r_o}$$

and

$$Z_p = \frac{3}{2}\,\frac{\pi}{4}\,\frac{(r_o^4 - r_i^4)}{r_o}$$

$$= \frac{3\pi}{8}\,\frac{(13^4 - 9.5^4)}{13} = 1860$$

The plastic moment at the midplane is

$$M_p = \sigma_p Z_p$$

$$= (30,000)(1860) = 55,800,000 \text{ in. lb}$$

But $U_B = M\theta$

or $1,574,400 = 55,800,000\ (\theta)$

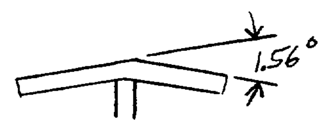

$$\theta = \frac{1,514,400}{55,800,000} = 0.0271 \text{ radians} = \underline{1.56°}$$

Estimated Actual Angle of Bend and Elongation

We are now justified in assuming that the actual conditions, showing loadings on all three shells, would reduce their common angle of bend to

$$(0.59\ (1.56°) = 0.925°\ \theta$$

For the outer fibers of the outer shell this gives

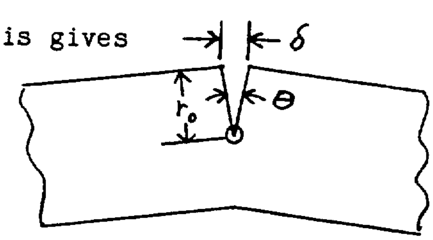

$r_o = 14 \quad \delta = r_o\theta = (14)(0.925)\ (0.01745) = 0.226$ in.

Consider this to be the measured elongation over a 2-in. gage length tension test piece.

$$\frac{0.226}{2} = 11.3\% \text{ elongation}$$

Stainless steel has 40% elongation o.k. No Rupture

Uranium elongation 13/14 in. (11.3) = 10.5% elong. at R = 13 in.

10.5/14 in. (11.3) = 8.5% elong. at R = 10.5 in.

9.5/14 in. (11.3) = 7.7% elong. at R = 9.5

2.7.3. Summary of Damage - 30 ft Bottom Drop

The HONDO runs simulate a cask bottom impact on immovable ground by assigning the 30-ft free fall z-velocity to all nodes, except nodes 1 through 11 on the bottom surface, which are given zero velocity from time point 0 and on. (HONDO model geometry described in Section 2.7.5). From these initial velocity conditions the dyamic response of the cask is determined by the code, and selected displacements, velocities, accelerations, and stresses printed out at specified time intervals.

The computed answers are based on idealized material properties that conservatively substitute the actual material properties within strain and strain-rate ranges experienced in all regions of the cask.

$$V = V_o + a\ t$$

$$S = S_o + V\ t + \frac{1}{2}\ a\ t^2$$

$a = 32\ ft/sec^2 = 384\ in./sec^2 \quad V_o = 0 \quad S_o = 0$

$S = 30\ ft = 360\ in.$ for $1/2\ a\ t^2 = 360$

or

$$t = \frac{2 \times 350}{384} = \underline{1.3693\ sec}$$

$$V = 0\ (384)\ (1.3693) = \underline{525.8\ in./sec}$$

Initial z-velocity = -525.8 in./sec for all nodes except nodes 1 - 11.

2.7.4 Materials Data for HONDO Input

The following material characteristics at applicable temperatures are required input:

1. Mass density.

2. Stress as a function of strain up to a permanent set of approximately 0.5% (which correspond to approx. one inch compression of the cask.

3. Yield strength as a function of strain rate.

The stress-strain function is idealized into straight lines and expressed by parameters E, ν, t_o, E_t , and β. A stress-strain curve for the 0.2% Mo-uranium alloy lid shield material was not available from the supplier until after the analysis was made. The idealized curve used in the HONDO input was therefore based on estimates derived from several available sources of information regarding pure uranium and uranium alloys with varying amounts of molybdenum. The idealized curve is conservative in that $\sigma'_y < \sigma_y$. All HONDO runs made produced stresses in the lid shield that were lower than σ'_y (σ'_y = 30,700 psi for 300°F and $\dot{\varepsilon} = 10^{-3}$.

The strain rate sensitivity for the cast 304 stainless steel is based on a 3571 lb/in.^{2} increase in yield strength per decade increase in strain rate (Ref. 2-27). The cask steel temp. is 250°F → 300°F which corresponds to 121°C → 149°C. The actual strain rate sensitivities at these temperatures are probably lower than at room temperature. (Ref. 2-22). The strain rate ($\dot{\varepsilon}$) for a normal tensile test is ~10^{-3}. For strain rates below 10^{-5}

the 304 steel yield strength is assumed constant and equal to the value at $\dot{\varepsilon} = 10^{-5}$.

For the uranium-moly alloys the strain rate sensitivity was assumed similar to the one depicted on Fig. 17, Ref. 2-23 for purge α-uranium-extrapolated downward to $\dot{\varepsilon} = 10^{-6}$. In the range above $\dot{\varepsilon}$ the yield strength is assumed governed by the power equation: (Ref. 2-24, p. 18)

$$t_y = t_o \left[1 + \left(\frac{|\dot{\varepsilon}|}{D} \right)^{1/P} \right]$$

where t_o = the yield strength at $\dot{\varepsilon} = 10^{-6}$ (~zero rate. $\dot{\varepsilon} = 10^{-6}$ in./in./sec corresponds to a doubling of length in 10^6 sec = 278 h, which is a very low rate of strain.)

The "t_o" value read from the idealized stress-strain curve is based on $\dot{\varepsilon} = 10^{-3}$.

Because of uncertainty regarding the validity or the strain rate sensitivity data, the HONDO run will be repeated with strain rate parameters p and D input as zero (gives strain rate insensitive behavior per Ref. 2-24, pg. 71). The model which produces the highest stresses in the lid will be used for analysis of the lid.

The required materials input data are tabulated in Section 2.7.4.

To clarify the results obtained in the HONDO analysis a further discussion of materials data and procedures is provided in Section 2.7.4.

2.7.4.1 Material Identification Nos. 1 & 5

(Cask shells, container shell, inner closure, top member).

304 Stainless Steel --------→ at 250°F / 350°F

ASTM A 351 SR CF-8, ASME Code Sect. III Designation: SA-351, CF-8

ρ = 0.290 lb/in.^{3}

g = 980.665 cm/sec.^{2} ~980.665 (0.3937 in./cm) = 386.0.88 in./sec

$$\text{Mass density} = \frac{\rho}{g} = \frac{0.290}{368.088} = \underline{0.0007511 \text{ lb/sec}^2\text{/in.}^4}$$

E = 27.4 x 10^6 psi @ 250°F
27.1 x 10^6 psi @ 300°F

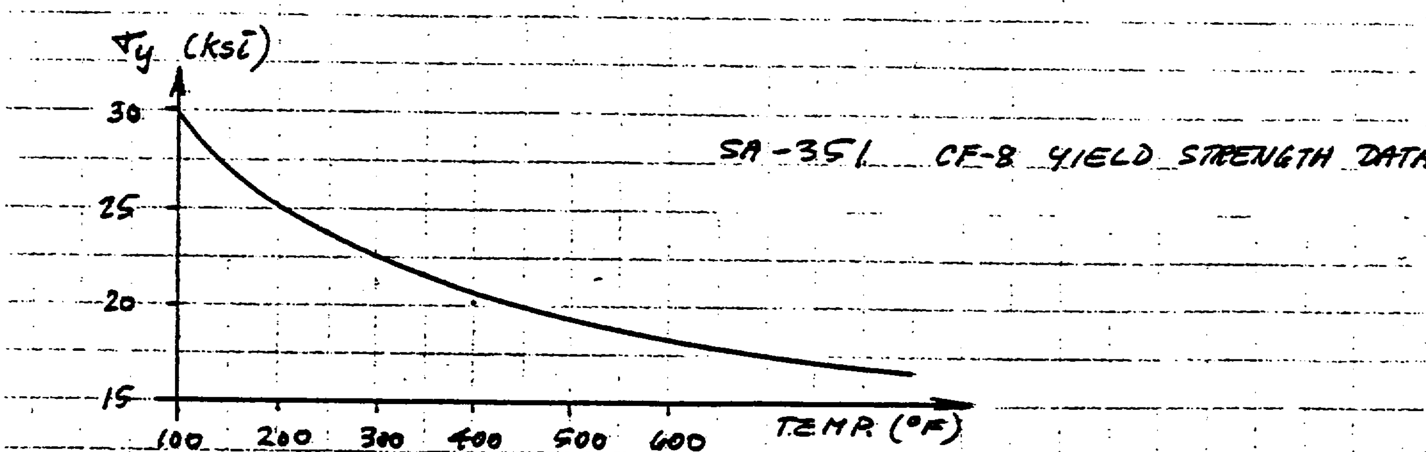

σ_y 250°C = 23.7 ksi

σ_y 300°F = 22.5 ksi

σ_y 400°F = 20.7 ksi

$$\frac{\sigma_y\ 250°F}{\sigma_y\ 400°F} = \frac{23.7}{20.7} = \underline{1.145}$$

$$\frac{\sigma_y\ 250°F}{\sigma_y\ 400°F} = \frac{22.5}{20.7} = \underline{1.087}$$

Idealized stress-strain curves are drawn upon Fig. 3.03112 (from Ref. 2-7) below, using E-values and σ_y-ratios from preceding page.

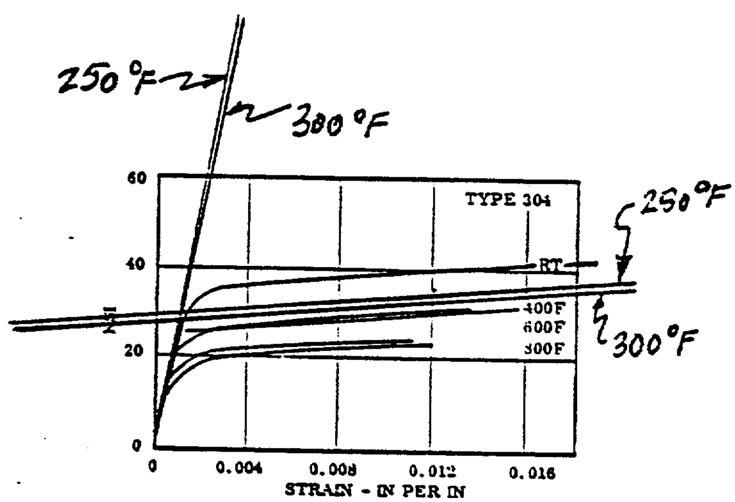

FIG 3.03112 STRESS - STRAIN CURVES AT ROOM AND ELEVATED TEMPERATURES (23)

By scaling graph:

For 250°F (E = 27.4 x 10^6 psi): t_o = <u>29,500 psi</u>

For 300°F (E = 27.1 x 10^6 psi): t_o = <u>28,400 psi</u>

Hardening modulus in both cases:

$$E_t = \frac{\Delta\sigma}{\Delta E} = \frac{7368}{0.018} = \underline{409{,}300 \text{ psi}}$$

Strain rate sensitivity: $\Delta\sigma$ = 3571 lb/in.^{2} per decade increase in $\dot{\varepsilon}$ for $\dot{\varepsilon} \geq 10^{-5}$. (Ref. 2-27)

$$t_y = t_o = \begin{matrix} \underline{29{,}500 \text{ psi}} \text{ @ } 250°F \\ \underline{28{,}400 \text{ psi}} \text{ @ } 300°F \end{matrix} \qquad \text{for } \dot{\varepsilon} = 10^{-3}$$

$$t_y = \underline{t_o + [3571]\,[\log_{10}\,(10^3\,\dot{\varepsilon})]} \qquad \text{for } \dot{\varepsilon} \geq 10^{-5}$$

2.7.4.2 Material Identification No. 2 (Uranium Shield, Lid)

0.2% Mo Uranium Alloy (Cast) @ 300°F

Density per supplier's data:

$$\rho = \underline{18.81 \text{ g/cm}^3}$$

$$\rho = 18.81 \text{ g/cm}^3 \sim (18.81)\,(0.03613) = \underline{0.67961 \text{ lb/in.}^3}$$

$$\text{Mass density} = \frac{0.67961}{386.088} = \underline{0.0017602 \text{ lb sec}^2/\text{in.}^4}$$

ν = 0.21 compared with ν = 0.25 for pure uranium.

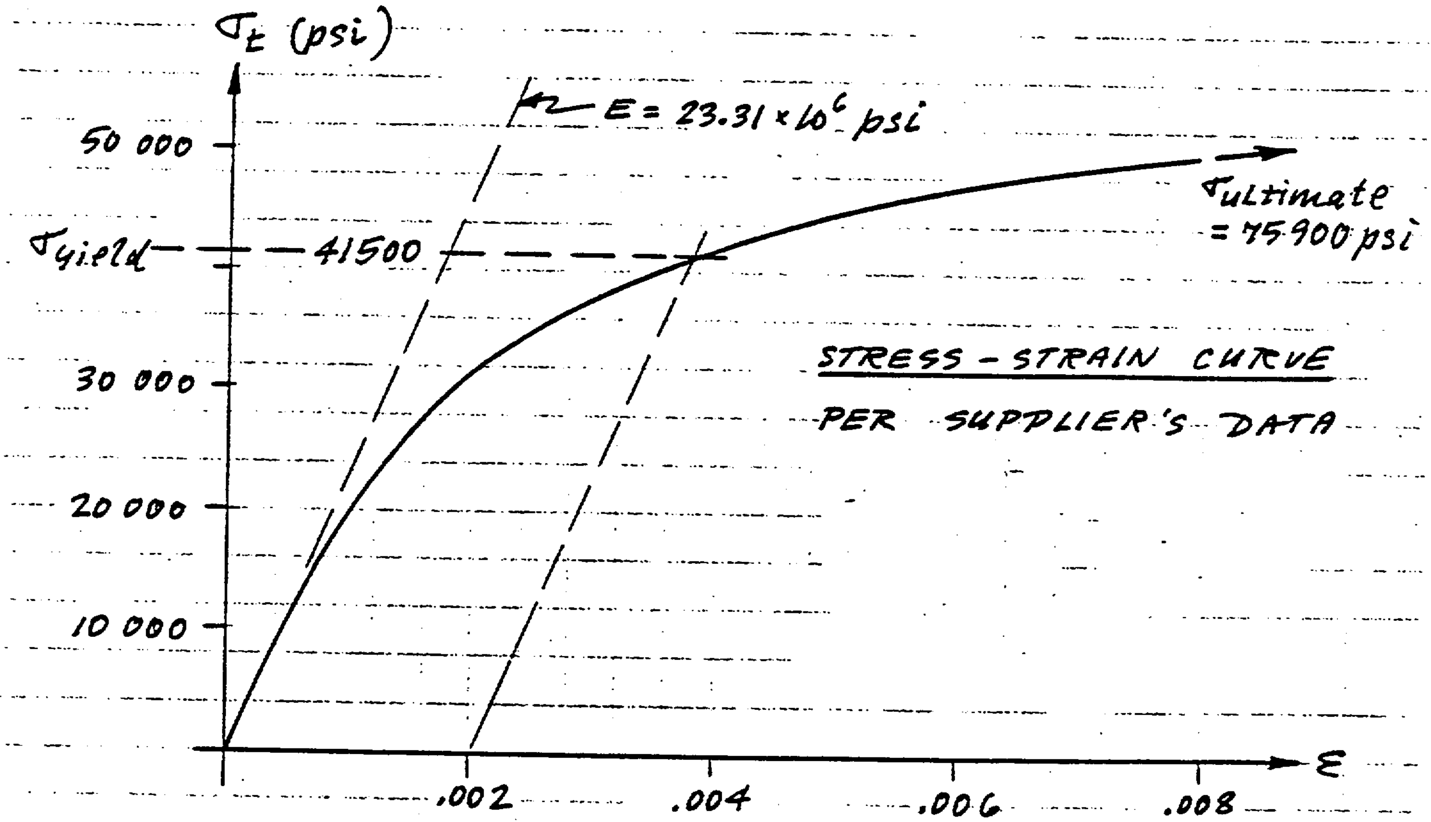

0.2% Mo-uranium alloy (cast) lid shield material @ 70°F in tension.

Strain rate $\dot{\varepsilon} = 10^{-3}$.

Adjustment for 300°F Temperature

Ref. 2-23 — 70°F ~21°C ~294 K. Read: $E_{70} = 29.0 \times 10^6$ psi
300°F ~149°C = 422 K. Read: $E_{300} = 26.2 \times 10^6$ psi

Ref. 2-23 — 70°F ~21°C. Read: $\sigma_{yield} = 48$ ksi.
$\sigma_{ult} = 100$ ksi
300°F ~21°C. Read: $\sigma_{yield} = 48$ ksi.
$\sigma_{ult} = 78$ ksi

Adjusted Data:

$$\sigma_y = (41{,}500)\ \frac{42}{48} = \underline{36{,}300\ \text{psi}}$$

$$\sigma_u = (75{,}900)\ \frac{78}{100} = \underline{59{,}200\ \text{psi}}$$

$$E = (23.31 \times 10^6)\ \frac{26.2}{29.0} = \underline{21.1 \times 10^6\ \text{psi}}$$

The stress-strain curve below was constructed on the basis of the adjusted values of σ_y, σ_u, and E.

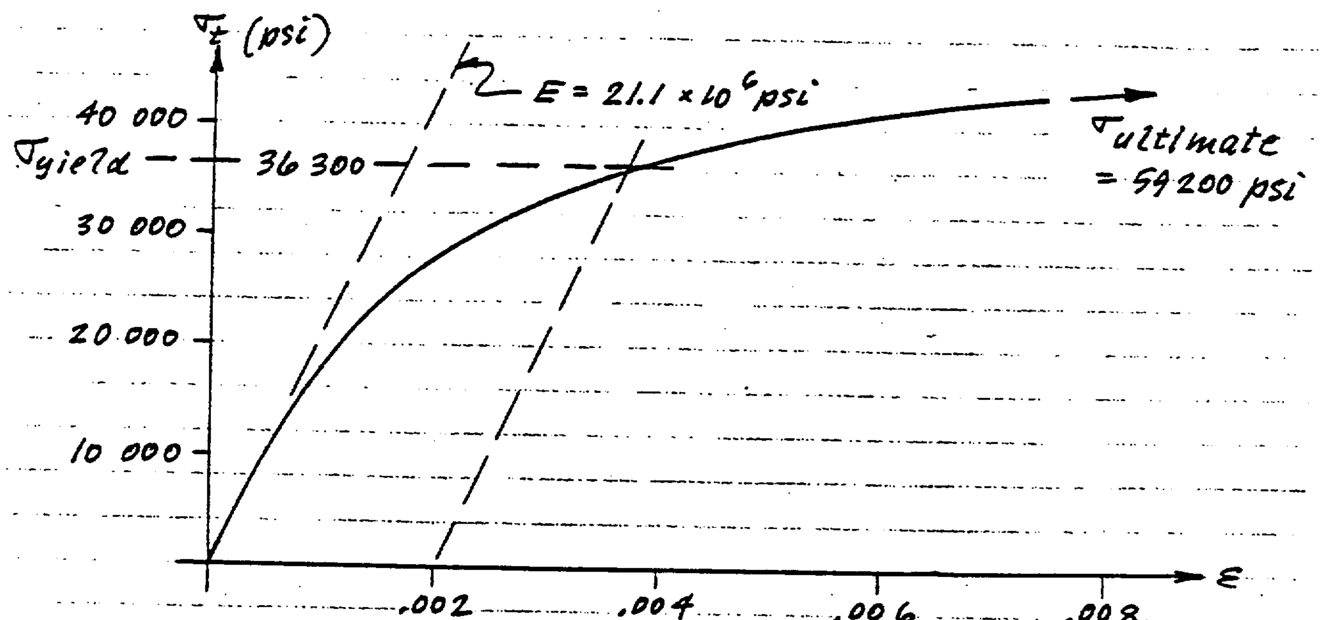

Supplier's Stress-Strain Curve Adjusted for 300°F Temperature

$\dot{\varepsilon} = 10^{-3}$.

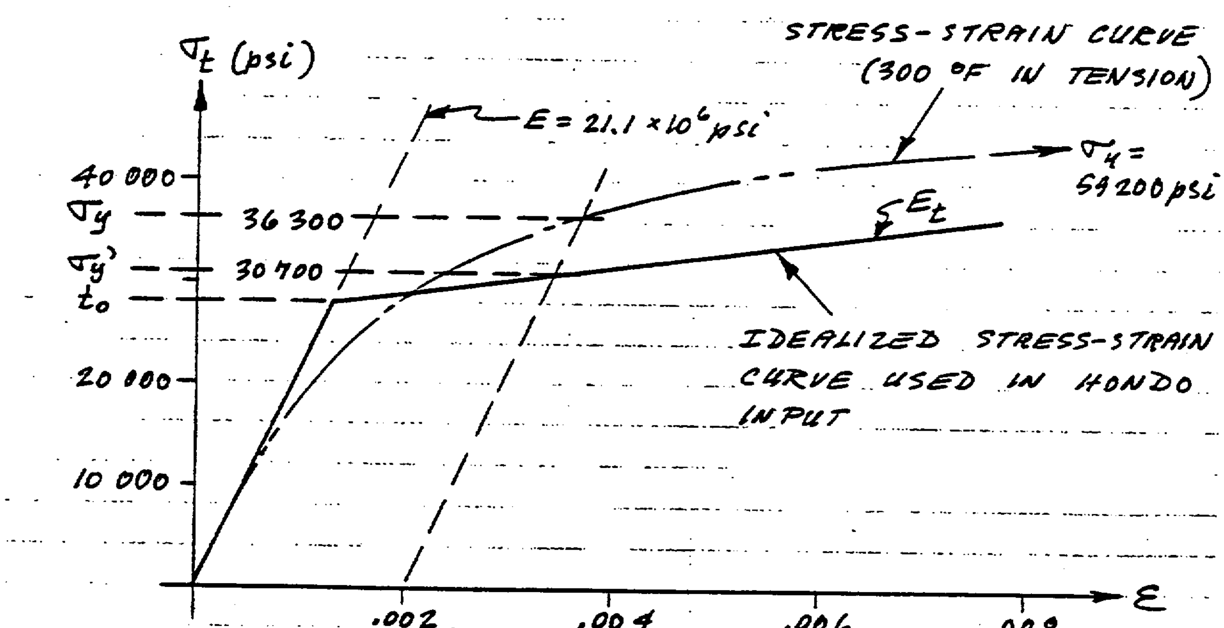

0.2% Mo-uranium Alloy (Cast) @ 300°F in Tension

Strain Rate $\dot{\varepsilon} = 10^{-3}$.

$E_t = \underline{1.35 \times 10^6 \text{ psi}}$

$t_o = \underline{28{,}000 \text{ psi}}$

$\sigma'_y = t_o + (E_t)(\varepsilon) = 28{,}000\ (1{,}350{,}000)\ (0.002)$

$= 28{,}000 + 2700 = \underline{30{,}700 \text{ psi}}$

σ'_y = 30,700 psi exceeds stresses experienced in lid.

Slope of E_t line is acceptable for the 30-ft drop analysis since stresses in the lid never reach the idealized static ($\dot{\varepsilon} = 10^{-3}$) yield strength σ'_y.

Strain Rate Sensitivity Constants P&D

Refer to Ref. 2-23 and use $t_o = \sigma$ at $\dot{\varepsilon} = 10^{-6}$ (by extrapolation).

extrapolation).

Analysis of Fig. 17, Ref. 2-23:

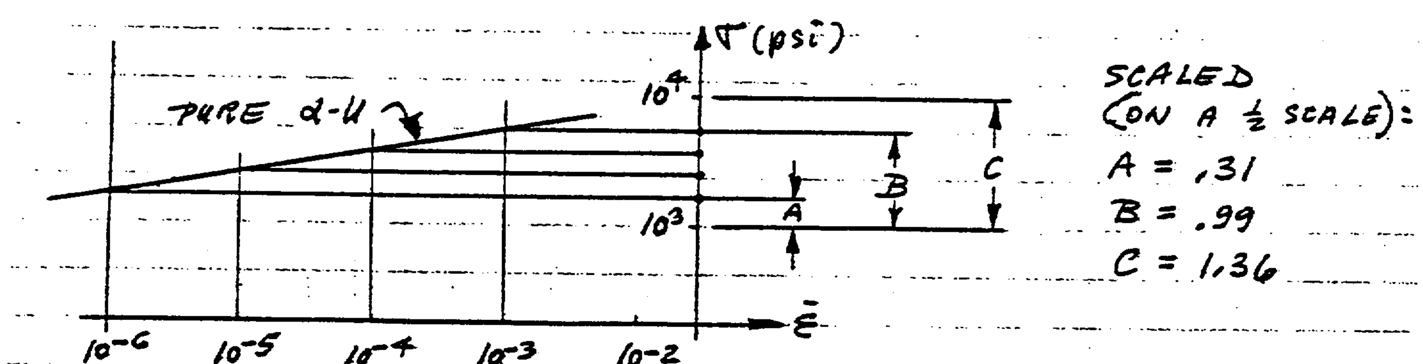

$1/3\ (B-A) = 1/3\ (0.99 - 0.31) = \underline{0.22667}$

$A + 1/3\ (B-A) = 0.31 + 0.22667 = \underline{0.53667}$

$A + 2/3\ (B-A) = 0.31 + 0.45334 = \underline{0.76334}$

$\text{Log } 1.6881 = 0.2274 - (0.2274)\ (1.36) = 0.31 = A$

$\sigma_{10^{-6}} = \underline{1688 \text{ psi}}$

$\text{Log } 2.481 = 0.3946 - (0.3946)(1.36) = 0.53667 = A + 1/3\ (B-A)$

$\sigma_{10^{-5}} = \underline{2481 \text{ psi}}$

$\text{Log } 3.6415 = 0.56128 - (0.56128)(1.36) = 0.76334 = A + 2/3\ (B-A)$

$\sigma_{10^{-4}} = \underline{3642 \text{ psi}}$

$\text{Log } 5.345 = 0.72794 - (0.72794)\ (1.36) = 0.99 = B$

$\sigma_{10^{-3}} = \underline{5345 \text{ psi}}$

Power law (Ref. 2-24):

$$t_y = t_o\left[1 + \left(\frac{|\dot{\varepsilon}|}{D}\right)^{1/p}\right] \text{ or } |\dot{\varepsilon}| = D\left(\frac{t_y}{t_o} - 1\right)^p$$

$$\text{for } |\dot{\varepsilon}| > 10^{-6}$$

Taking $t_o = t_y$ for $\dot{\varepsilon} = 10^{-6}$: $t_o = 1688$ psi

$$(1):\quad 10^{-5} = D\left(\frac{2481}{1688} - 1\right)^{p}$$

$$(2):\quad 10^{-4} = D\left(\frac{3642}{1688} - 1\right)^{p}$$

$$(3):\quad 10^{-3} = D\left(\frac{5345}{1688} - 1\right)^{p}$$

$$\frac{(1)}{(2)}\quad 10^{-1} = \left(\frac{\frac{2481}{1688} - 1}{\frac{3642}{1688} - 1}\right)^{p} = \left(\frac{0.4698}{1.1576}\right)^{p} = (0.4058)^{p}$$

$$-1 = p \log (0.4058)$$

$$p = \frac{-1}{-0.3917} = \underline{2.553}$$

$$(1):\quad 10^{-5} = D\left(\frac{2481}{1688} - 1\right)^{2.553}$$

$$\frac{10^{-5}}{D} = (0.4698)^{2.553} = 0.1453$$

$$D = \frac{10^{-5}}{0.1453} = \underline{6.882 \times 10^{-5}}$$

$$\frac{(2)}{(3)} \quad 10^{-1} = \left(\frac{\frac{3642}{1688} - 1}{\frac{5345}{1688} - 1} \right)^p = \left(\frac{1.1576}{2.1665} \right)^p = (0.5343)^p$$

$$-1 = p \log (0.5343)$$

$$p = \frac{-1}{-0.2722} = \underline{3.6738}$$

$$(2): \quad 10^{-4} = D\,(1.576)^{3.6738}$$

$$\frac{10^{-4}}{D} = (1.576)^{3.6738} = 1.7110$$

$$D = \frac{10^{-4}}{1.7110} = \underline{5.8412 \times 10^{-5}}$$

For HONDO analysis use average values:

$$p = 1/2\,[2.553 + 3.6738] = \underline{3.113}$$

$$D = 1/2\,[6.882 + 5.8412]\,10^{-5} = \underline{6.362 \times 10^{-5}}$$

For 0.2% Mo-uranium alloy @300°F: idealized

t_y = 28,000 psi for $\dot{\varepsilon} = 10^{-3}$

$$|\dot{\varepsilon}| = D \left[\frac{t_y}{t_o} - 1 \right]^p$$

$$10^{-3}\ [6.362 \times 10^{-5}] \left[\frac{23{,}000}{t_o} - 1\right]^{3.113}$$

$$15.718 = \left[\frac{28{,}000}{t_o} - 1\right]^{3.113} = x^{3.113}$$

$$\text{Log } 15.718 = 3.113 \text{ Log } x = 1.1964$$

$$\text{Log } x = \frac{1.1964}{3.113} = 0.3843$$

$$x = \frac{28{,}000}{t_o} - 1 = 2.4228$$

$$\frac{28{,}000}{t_o} = 3.4228 \qquad t_o = \frac{28{,}000}{3.4228} = \underline{8180 \text{ ksi}}$$

$$t_y = t_o \left[1 + \left(\frac{\dot{\varepsilon}}{D}\right)^{1/p}\right]$$

$$\dot{\varepsilon} = 10^{-5} : t_y = (8180) \left[1 + \left(\frac{10^{-5}}{6.362 \times 10^{-5}}\right)^{1/3.11}\right] = (8180)\ [1.552]$$

$$= \underline{12{,}695 \text{ psi}}$$

$$\dot{\varepsilon} = 10^{-4} : t_y = (8180) \left[1 + \left(\frac{10^{-4}}{6.362 \times 10^{-5}}\right)^{1/3.113}\right] = (8180)\ [2.156]$$

$$= \underline{17.640 \text{ psi}}$$

$$\dot{\varepsilon} = 10^{-3} : t_y = (8180)\left[1 + \left(\frac{10^{-3}}{6.362 \times 10^{-5}}\right)^{1/3.113}\right] = (8180)\,[3.423]$$

$$= \underline{27{,}800 \text{ psi}}$$

$$\dot{\varepsilon} = 10^{-2} : t_y = (8180)\left[1 + \left(\frac{10^{-2}}{6.362 \times 10^{-5}}\right)^{1/3.113}\right] = (8180)\,[3.423]$$

$$= \underline{49{,}707 \text{ psi}}$$

2.7.4.3 Material Identification No. 3 (Uranium Shield, Cylinder)

0.2% Mo Uranium Alloy (Cast) @250°F

Densities per Ref. 2-25,

Pure Cast Uranium : $\rho = 18.9$ g/cm³

2% Mo-Uranium Alloy: $\rho = 18.4$ g/cm³

0.2% Mo-Uranium Alloy: $\rho = 18.9 - 1/10\ (18.9 - 18.4) = \underline{18.85 \text{ g/cm}^3}$

$\rho = 18.85 \text{ g/cm}^3 \sim (18.85)(0.3613) = \underline{0.68105 \text{ lb/in.}^3}$

$$\text{Mass density} = \frac{0.68105}{386.088} = \underline{0.0017640 \text{ lb.sec}^2 \text{ in.}^4}$$

For Poisson's ratio use: $\nu = 0.21$

Stress-Strain Data

The cask items of this material are primarily subject to compression loading. The stress-strain constants will therefore be based on the compression curve in Fig. 2-6. The average curve from Ref. 2-23, which is for pure uranium at room temperature, has been adjusted for 0.2% Mo addition and 250°F temperature and shown together with E and E_t lines for strain range of up to 0.5% permanent set.

Ref. 2-25 $E = [25 - 1/10\ (25 - 21)] \times 10^6$

s 2 $= 24.6 \times 10^6$ psi

For 0.2% Mo-uranium alloy at room temperature.

Reduction of E for 250°F temperature:

For 70°F ~21°C ~294 K. Read: $E_{70} = 29.0 \times 10^6$ psi

For 250°F ~121°C ~394 K. Read: $E_{250} = 26.8 \times 10^6$ psi

$$E = [24.6 \times 10^6] \frac{26.8}{29.0} = \underline{22.73 \times 10^6 \text{ psi}}$$

Reduction of σ_{yield} for 250°F temperature:

70°F ~21°C. Read: $\sigma_{yield} = 48$ ksi

250°F ~121°C. Read: $\sigma_{yield} = 43$ ksi

$$\text{Factor} = \frac{43}{48} = \underline{0.8958}$$

Increase of σ_{yield} for 0.2% Mo addition:

Pure uranium: $\sigma_{yield} = 25$ ksi

0.2% Mo-uranium alloy: $\sigma_{yield} = 55$ ksi

0.2% Mo-uraniium alloy: $\sigma_{yield} = 25 + 1/10\ (55-25)$ =28 ksi

$$\text{Factor} = \frac{28}{25} = 1.12$$

Total Adadjustment factor = (0.8958)(1.12) = 1.0033

By scaling and adjusting points on the curve in Section 2.7.4.2, the following points are arrived at:

$$\varepsilon = 0.002 \text{ permanent set} = \sigma = \sigma_{yield} = (73{,}000)\ (1.0033)$$
$$= \underline{73{,}241 \text{ psi}}$$

$$\varepsilon = 0.005 \text{ permanent set} = \sigma = (82{,}105)\ (1.0033)$$
$$= \underline{82{,}376 \text{ psi}}$$

Using E = 22.73 x 10^6 psi together with the two stress values above, the stress-strain curve detail in Section 2.7.4.3 was drawn.

HONDO input values are scaled from this graph:

t_o = 64,200 psi

E_t = 3.15 x 10^6 psi

t_o for the strain rate sensitive case is determined from equation;

$$t_y = t_o \left[1 + \left(\frac{|\dot{\varepsilon}|}{D} \right)^{1/p} \right]$$

$$64{,}000 = t_o \left[1 + \left(\frac{10^{-3}}{6.362 \times 10^{-5}} \right)^{1/3.113} \right]$$

$= t_o\,[1 + 2.4228]$

t_o = <u>18,756 psi</u>

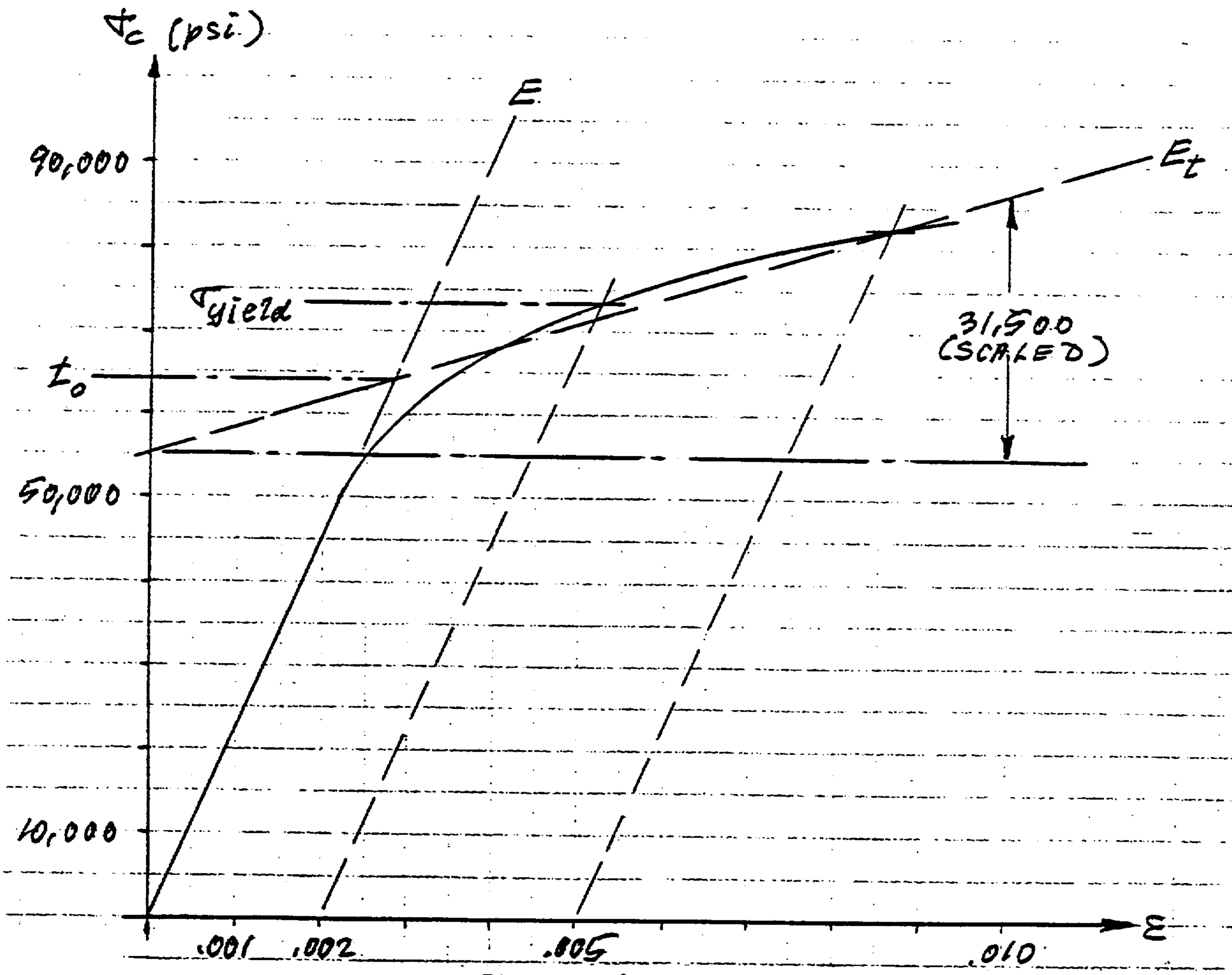

Figure 2-6

Detail of Stress-Strain Curve for 0.2% Mo-Uranium Alloy (Cast) @250°F in compression.

$E = 22.73 \times 10^6$ psi

$\sigma_{yield} = 73{,}241$ psi

By scaling graph:

$t_o = \underline{64{,}200 \text{ psi}}$

$$E_t = \frac{\sigma}{\varepsilon} = \frac{31{,}500}{0.01} = \underline{3.15 \times 10^6 \text{ psi}}$$

2.7.4.4 Material Identification No. 4 (Inner Closure Top Membrane)

Identical to material identification No. 5 except for the use of an arbitrary small E value. This was done in order to simulate the weight effect of the lid membrane without taking advantage of any stiffness that in the solution could unrealistically benefit the uranium shield.

Material Identification No. 6 (Top Head of Cask)

4340 Low Alloy Steel. Heat treated to minimum 150,000 psi yield @300°F. Composition = 0.4C, 1.8 Ni, 0.8 Cr, 0.25 Mo.

150 ksi yield @300°F requires an F_{tu} = approximately 175 psi at room temperature (Ref. 2-7).

$\rho = 0.285 \text{ lb/in.}^3$

$$\text{Mass density} = \frac{\rho}{g} = \frac{0.285}{386.088} = \underline{0.0007382 \text{ lb/sec}^2\text{/in.}^4}$$

$E = 29.0 \times 10^6$ psi @300°F.

Stress-Strain Data

The 0.002 yield point for 175 ksi material will be ~165 ksi.

By comparison with low alloy steel SA-533 (1/2 Mo):

$$\sigma_{yield} = \begin{array}{l} 82.5 \text{ ksi @100°F} \\ 76.0 \text{ ksi @300°F} \end{array}$$

$$\text{4340 yield point @300°F} = \frac{76.0}{82.5}(165)$$

$$= 152 \text{ ksi} \sim 150 \quad \text{o.k.}$$

Although the curve is flat at room temperature, there will be some slope at 300°F.

$$E = \frac{1}{2} \; \frac{54{,}000}{0.01221} = \underline{2.22 \times 10^6 \text{ psi}}$$

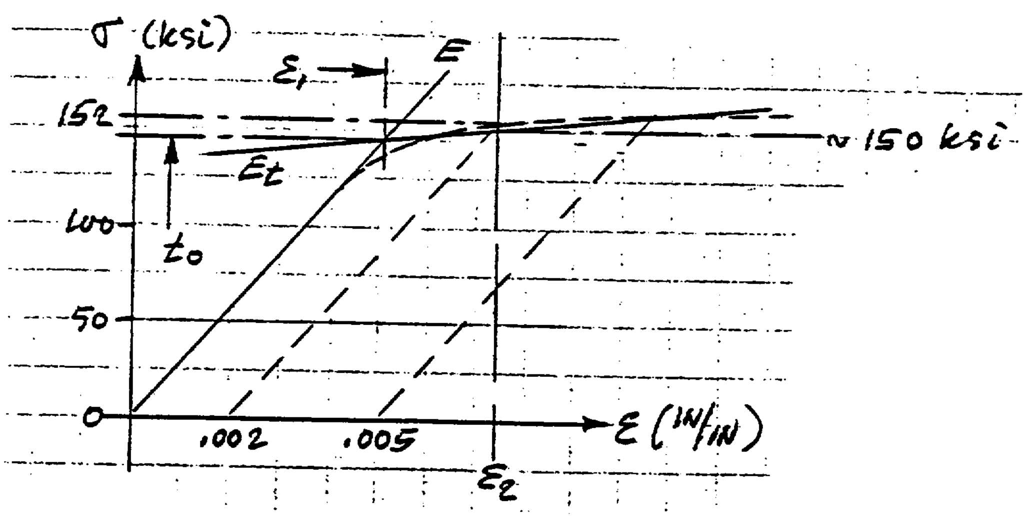

* Stresses in the bulkhead never reached t_o in any of the HONDO runs. Consequently, the E_t value had no effect on the computer answers.

$$\varepsilon_2 = 0.002 + \frac{\sigma}{E} = 0.002 + \frac{152{,}000}{29.0 \times 10^6}$$

$$= 0.002 + 0.00524 = \underline{0.00724}$$

$$t_o = E\,\varepsilon_1 = \underline{29.0 \times 10^6\ \varepsilon_1}$$

$$150{,}000 = t\ \ + (\varepsilon_\tau - \varepsilon_r)\,E_t = t_o + (0.00724 - \varepsilon_1)\ (2.22 \times 10^6)$$

or

$$150{,}000 = t_o + \left(0.00724 - \frac{t_o}{29.0 \times 10^6}\right)(2.22 \times 10^6)$$

$$150{,}000 = t_o + 16{,}076 - 0.07655\ t_o$$

$$t_o = \underline{145{,}000\ \text{psi}}$$

4340 Low Alloy Steel

Strain Rate Sensitivity is minimal for 4340 material @300°F (Ref. 2-22).

Materials Data from Ref. 2-7:

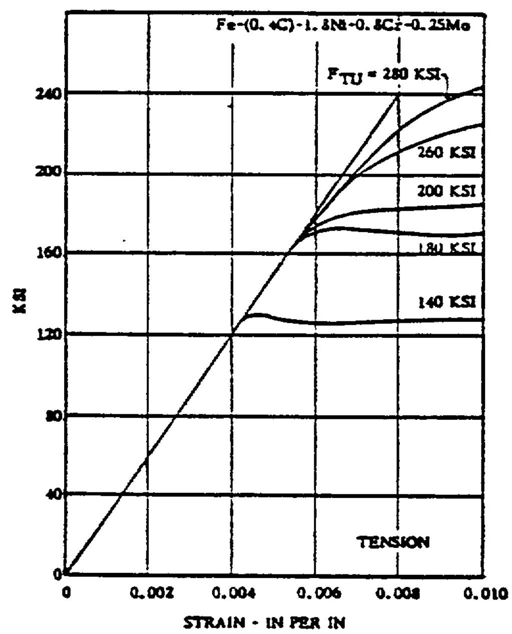

FIG. 3.02111 TYPICAL STRESS-STRAIN CURVES FOR VARIOUS STRENGTH LEVELS (31) (35)

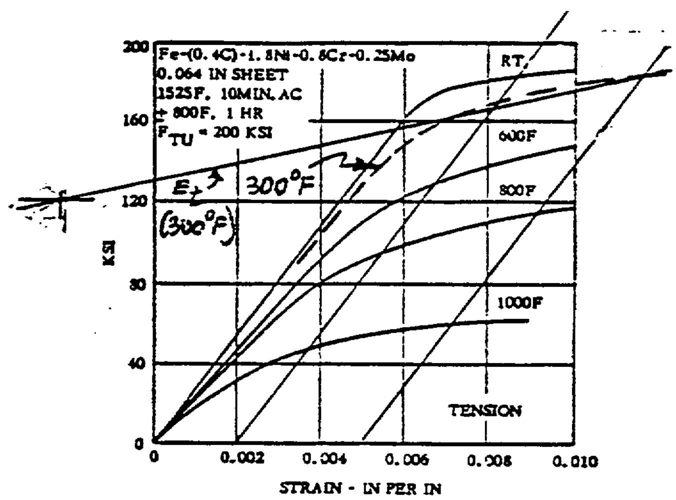

FIG. 3.03111 STRESS-STRAIN CURVES AT ROOM AND ELEVATED TEMPERATURES FOR SHEET HEAT TREATED TO F_{TU} = 200 KSI (20, p. 15)

CODE	1206
PAGE	13

CODE	1206
PAGE	6

	Fe
0.4	C
1.8	Ni
0.8	Cr
0.25	Mo

43404337

FIG. 3.03111: 300 °F DATA & .002 & .005 ELASTIC LINES ADDED.

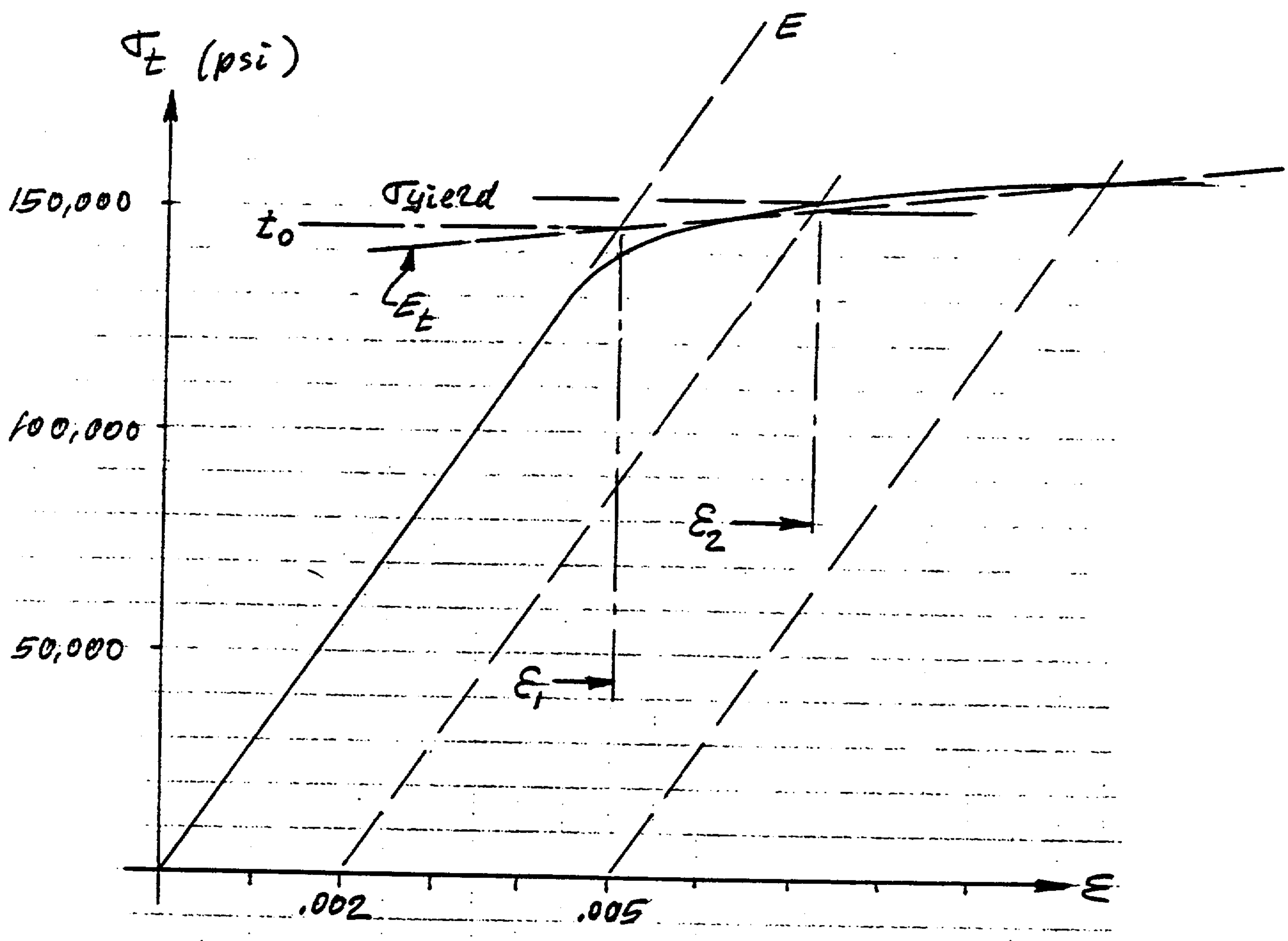

DETAIL OF STRESS-STRAIN CURVE FOR 4340 LOW ALLOY STEEL (F_{tu} = 175 ksi) @ 300 °F

t_0 = 145 000 psi

E_t = 2.22×10^6 psi

TABLE 2-6

SUMMARY OF MATERIALS DATA FOR HONDO INPUT

Item	Mat'l Ident. No.	Mat'l	Temp. (°F)	Mass Density $\left(\frac{lb\ sec^2}{in.^4}\right)$	E (10^6 psi)	ν	t_o (psi) Strain Rate Sensitive Case ($\dot{\varepsilon} = 10^{-6}$)	t_o (psi) Strain Rate In-Sensitive Case ($\dot{\varepsilon} = 10^{-3}$)	E_t (10^6 psi)	p	D x 10^5	Notes
Cask shells container shell	1	304 SS cast	250	0.0007511	27.4	0.3	29,500	29,500	0.4093	←--Note 3--→		9
Uranium shield, lid	2	0.2% Mo-U alloy cast	300	0.0017602	21.1	0.21	8,180	28,000	1.35	3.113	6.362	4 5 6
Uranium shield, cylinder	3	0.2% Mo-U alloy cast	250	0.0017640	22.73	0.21	18,756	64,200	3.15	3.113	6.362	4 7
Primary closure, top membrane	4	304 SS (low E)	300	0.0007511	Aribtrary	0.3	28,400	28,400	0.4093	←--Note 3--→		5 9
Prim. closure plate, top end of cask shells	5	304 SS	300	0.0007511	27.1	0.3	28,400	28,400	0.4093	←--Note 3--→		5 9
Top head of cask	6	4340 low alloy steel F_{tW} = 175 ksi	300	0.0007382	29.0	0.3	Note 8	145,000	2.22	←--Note 8--→		5 6 9

NOTES:
1. Symbols per Ref. 2-24.
2. β = 1.0 for all materials.
3. 304 SS = $t_y = t_o + [3571][\log_{10}]\ (10^3\ \dot{\varepsilon})]$ for $\dot{\varepsilon} \geq 10^{-5}$ in strain rate sensitive case.
4. Strain rate sensitivity governed by power law (Ref. 2-24 for materials No. 2 and 3.
5. Top end of cask is insulated by plywood. Design temp. = 300°F.
6. Stress-strain constraints bsaed on tensile data.
7. Stress-strain constants based on compression data.
8. Strain rate sensitivity is negligible for material No. 6 @ 300°F (Ref. 2-22).
9. Stress-strain functions for this material are similar for tension and compression within range considered (permanent set ≤ 0.5%).

910013 NC

2.7.5 Cask Model for HONDO Analysis. Figure 2-7 on the following pages describes the computer model with node and element numbers which were produced by a mesh generation program.

TABLE 2-7

HONDO MODEL. TOP BULKHEAD

4340 LOW ALLOY STEEL (F_{tu} = 175 ksi)

SCALE : 1/2 DIMENSIONS IN INCHES

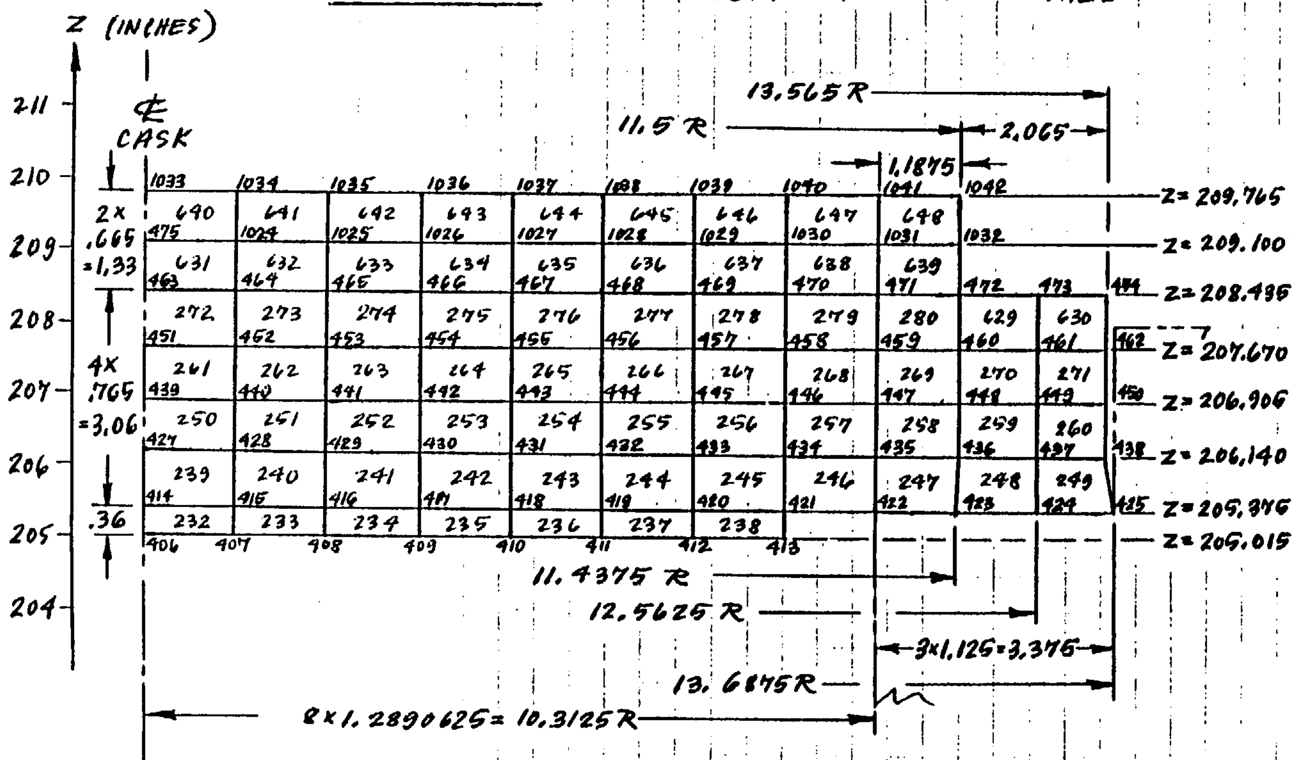

TABLE 2-8
BOTTOM 30-FT DROP HONDO MODEL
ELEMENT MATERIALS SUMMARY

Element From	Element To	Item	Material	Type (Identification)
1	206	Cask shells	304 SS @250°F	1
207	231	Top end of cask shells	304 SS @300°F	5
232	280	Bulkhead top end	4340 low alloy steel	6
281	302	Primary closure plate	304SS @300°F	5
303	358	Uranium shield, lid	0.2% Mo-U alloy	2
359	370	Primary closure, top membrane	304 SS (Low E)	4
371	464	Container shell	304 SS @250°F	1
465	474	Container shell, top end	304 SS @300°F	5
475	628	Uranium shield, cylinder	0.2% Mo-U alloy	3
629	648	Bulkhead top end	4340 low alloy steel	6

Figure 2-7.

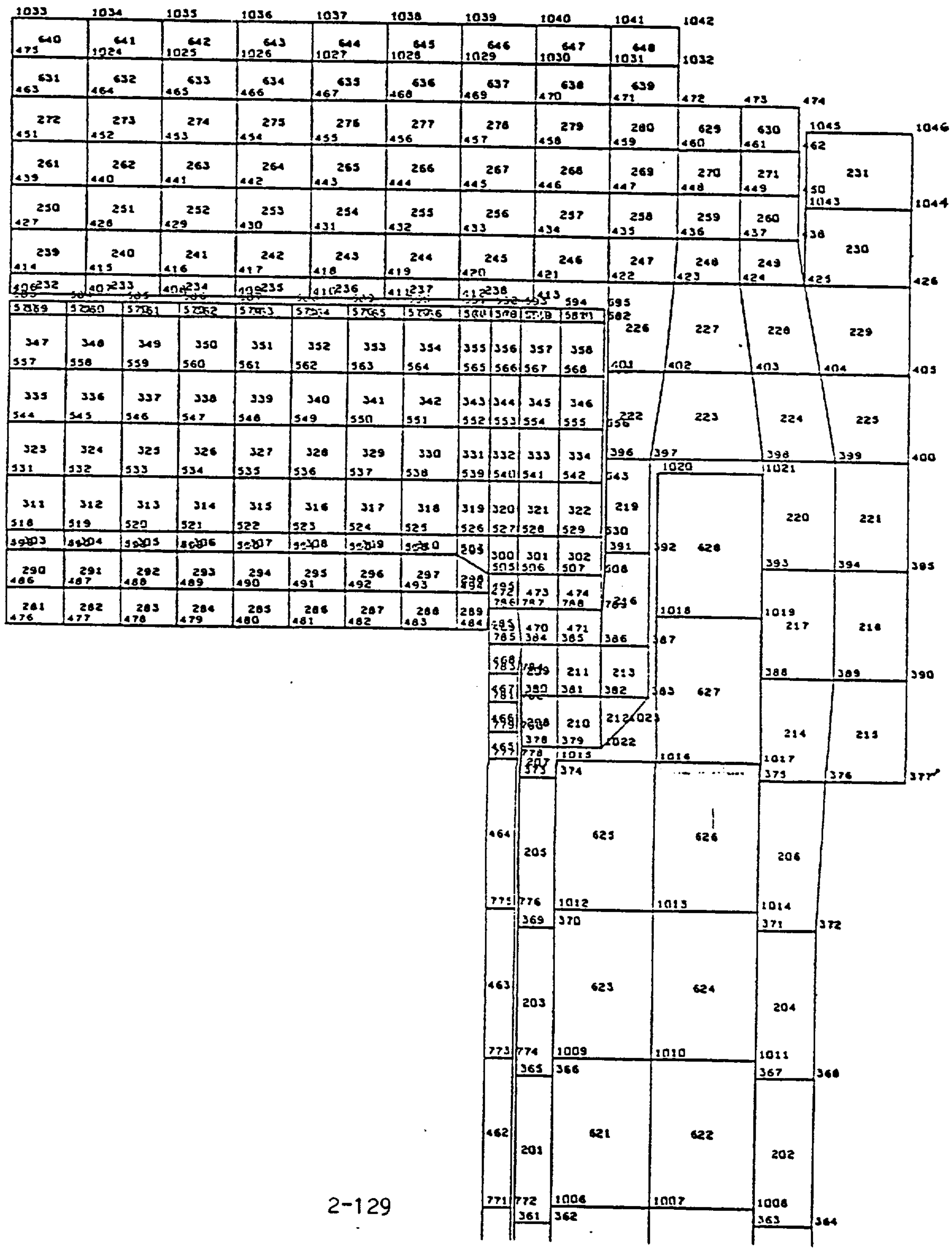

Figure 2-7 cont.

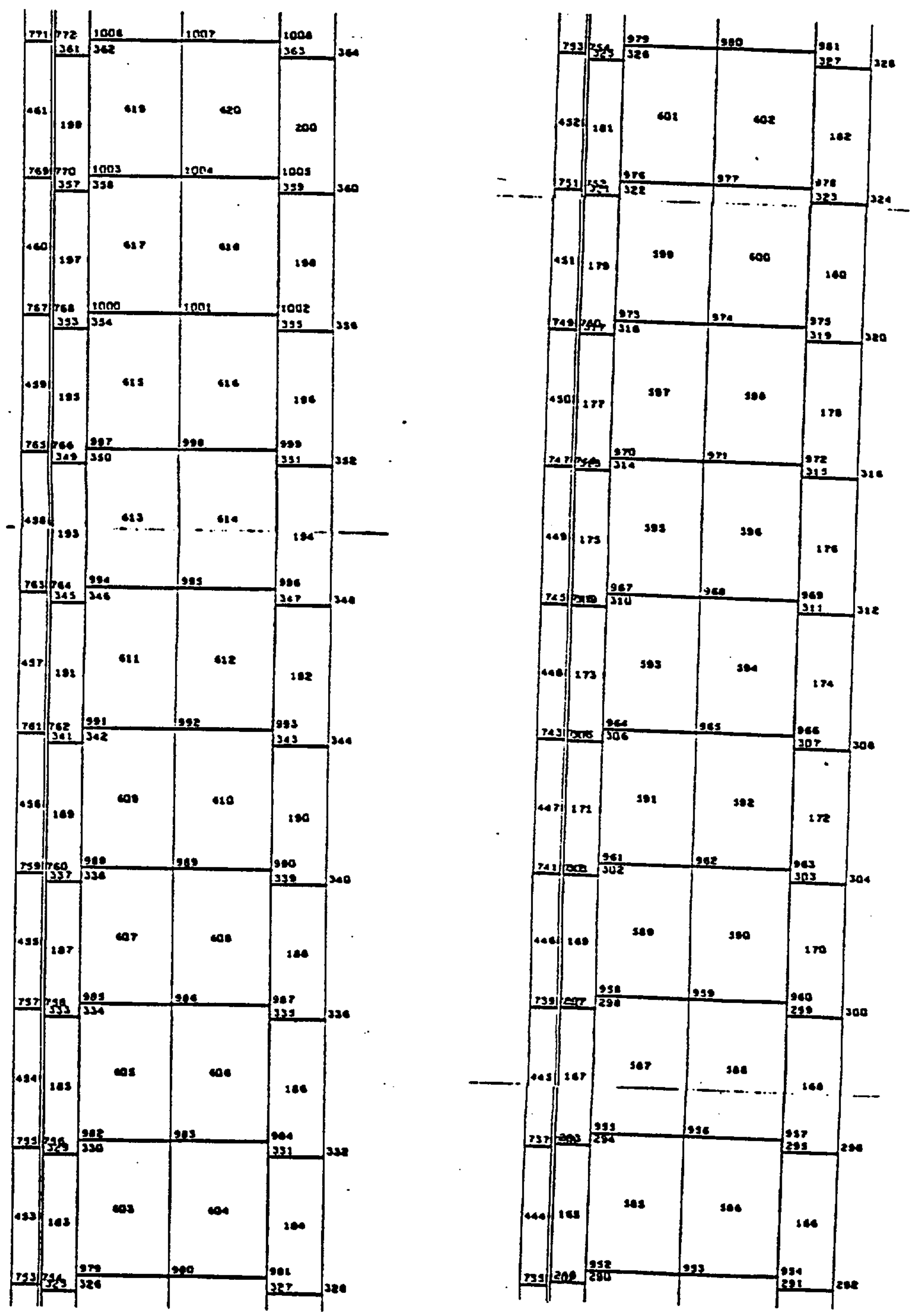

Figure 2-7 cont.

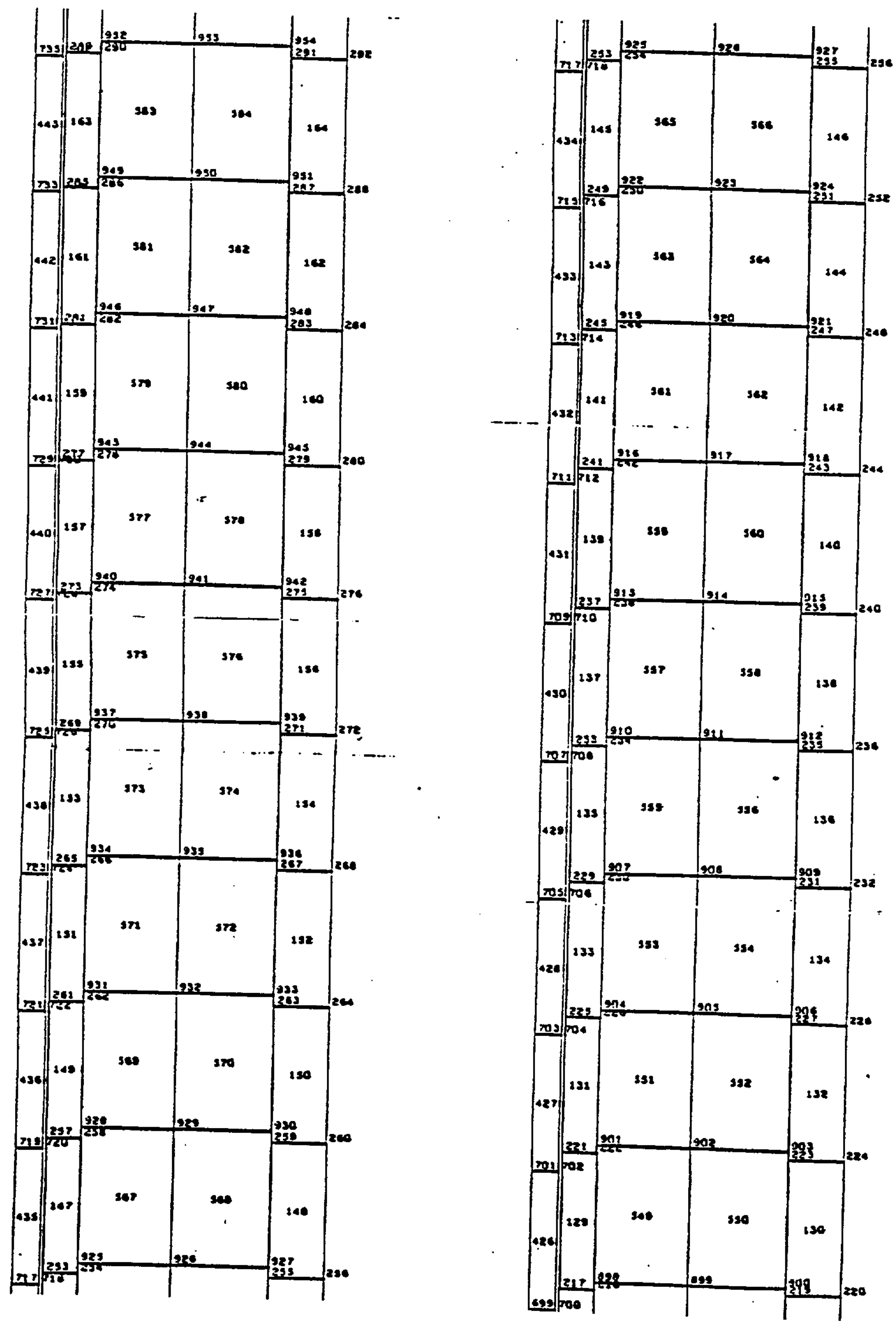

Figure 2-7 cont.

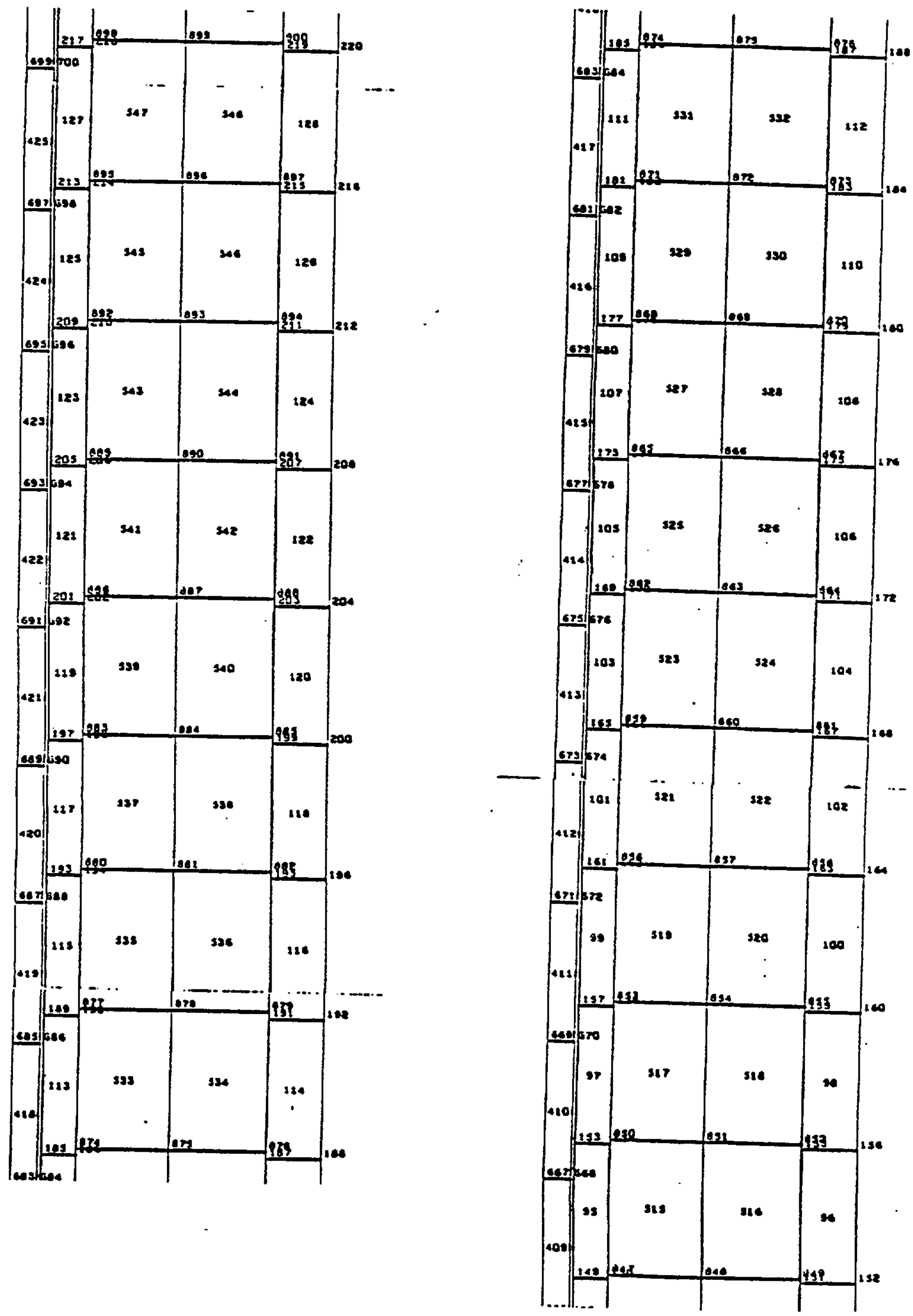

Figure 2-7 cont.

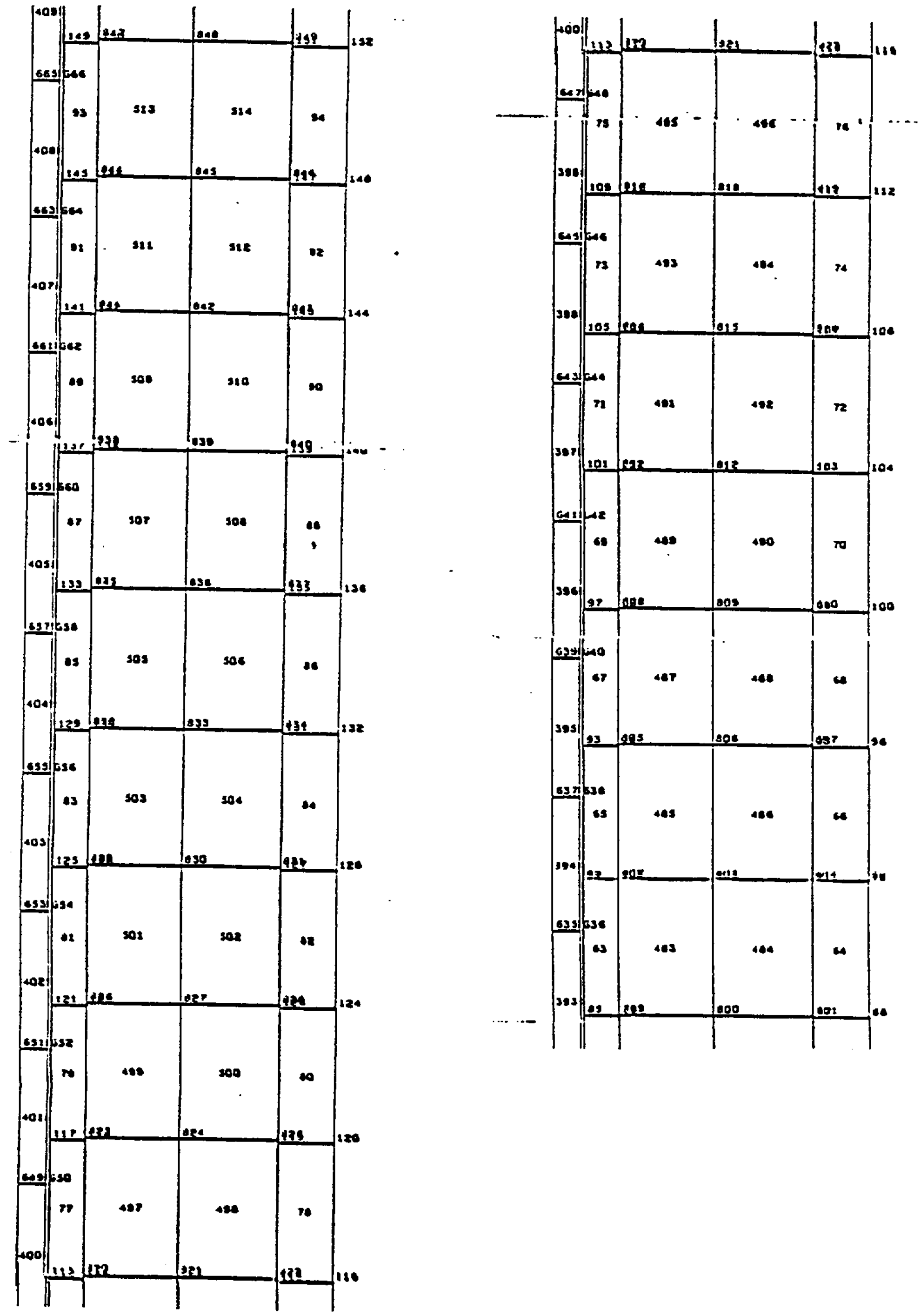

Figure 2-7 cont.

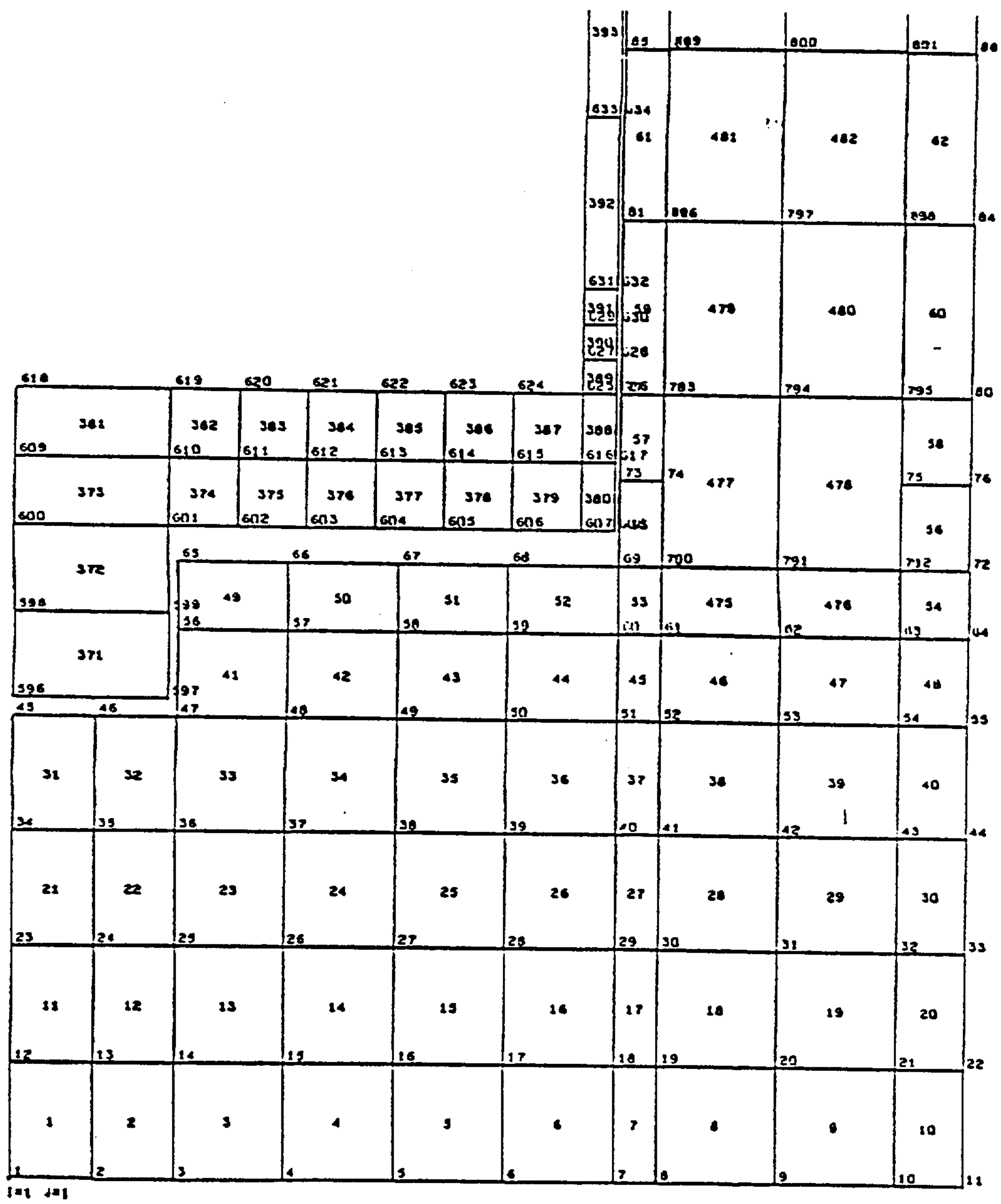

2.7.6 Conclusions of HONDO Analysis

2.7.6.1. Summary of HONDO Analysis

The two HONDO runs made (for strain rate sensitive and strain rate insensitive material behavior) were based on an assumed perfectly vertical bottom impact after a 30-ft drop.

Any impact at an angle with the vertical sufficiently small to prevent the cask from falling on its side after the initial contact (that is with the projected C.G. being within the bottom support circle) will be very similar to the perfectly vertical case. In fact, an impact at a slight angle will probably result in more energy absorption through plastic flow [in compression with no tendency to cracking] of the impacted corner and consequently a lower G-loading of the container lid structure. The perfectly vertical case analyzed should therefore conservatively cover all impacts with the projected C.G. within the bottom support circle.

A drop at a larger angle with the vertical will be less severe on the initial impact because part of the fall energy is being converted into rotation of the cask. The eventual side impact of the cask would be less severe than a perfect side impact after a 30-ft drop. In conclusion the perfectly vertical impact and the perfectly horizontal impact cases will conservatively cover any case in between.

The following computer generated plots are presented on the following pages:

1. Computer model with node and element numbers (result of a mesh generation program).

2. Plots from time of impact of selected stresses, displacements, and displacement gradients ($L + \Delta L/L$) vs. time for the strain rate sensitive and strain rate insensitive case (HONDO plot).

It is evident from the plots that absolute values of all critical stresses are maximum for the strain rate sensitive case. Absolute values of all critical displacements are maximum for the strain rate insensitive case.

Vertical displacements of top bulkhead lower surface and container lid upper surface vs. time are virtually identical. Similarly, the bottom surface of the uranium shield in the container lid and the top surface of the lid itself are moving at the same rate. Thus, there appears to be no problem of interference among these parts by closing of the initial gaps between them.

The maximum absolute principal stresses in the top end of the cask have been extracted from the HONDO output and listed below. As expected some yielding will take place in the cylindrical stainless steel portion of the cask and container shells. However, stresses in the container lid and bulkhead are below the yield strengths of the materials at 300°F. Distortion of the structure supporting the seals should therefore be negligible, assuring that no leakage past the seals develops as a result of the drop.

TABLE 2-9
MAXIMUM ABSOLUTE STRESS SUMMARY PER C.P.O.
(STRAIN RATE SENSITIVE CASE) (RUN NO. BOT-12)

Component	Element No.	Time (10^{-4} sec)	Predominant Stress Type(s)	Max. or Min. Principal Stress (psi)	Yield Strength at Temp. (psi)
4340 Stl Bulkhead	232(Bot. CL)	12.0	Radial & Hoop	38,970	150,000 (300°F)
0.2% Mo-U Alloy Shield, Lid	347 (Top CL) 303 (Bot. CL)	13.5 13.5	Radial & Hoop Radial & Hoop	-29,030 28,850	36,300 (300°F)
Top End of Container	205 (Inner Cyl.)	12.0	Axial Compr.	-53,140	*30,300 (250°F)
Top End of Container	468 Cylinder Below Flange	19.0	Axial Tens.	**50,990	*29,200 (300°F)
Container Lid Housing	281 (Bot. CL)	13.0	Rad & Hoop	27,860	*29,200 (300°F)

$*\sigma_y \sim t_o + E_t\ (0.002) = 29,500 + (409,300)(0.002) = \underline{30,300\ \text{psi}}$ @250°F

$\sigma_y \sim t_o + E_t\ (0.002) = 28,400 + (409,300)(0.002) = \underline{29,200\ \text{psi}}$ @300°F

**Ultimate tensile strength = 64,300 psi at 300°F
(0.90 (UTS) = (0.90) (64,300) = 57,870 psi

Bolts

The 1/2-in. bolts for the container lid and the 1-1/4 in. bolts for the cask cover head are designed for side and drop cases, and are not critical for the bottom drop conditions, where the lids are being forced by inertia downward toward the seals.

blank page

Drop Conditions at Low Temperature (-40°F)

Protection against brittle fracture at temperatures down to -40°F is provided through the selection of proper materials for the structural parts of the alternate closure system.

The container lid housing (304 stainless steel SA-240) with its bolts (high alloy steel per ATM 5735), and the outer lid bolts (SA-453, Grade 660) are all of austenitic stainless steel material for which no impact testing is required (see Ref. 2-2).

For the outer lid HY-140(T) material typical data from Ref. 2-7 indicate an energy absorption of at least 15 ft lb at -40°F.

The 0.2% Mo-uranium alloy lid shield material has been impact tested and found to exhibit acceptable toughness at -40°F. Documentation of the charpy V-notch testing of this and other alloys of depleted uranium is provided in Ref. 2-21.

Figure 2-8

AXIAL STRESS IN ELEMENT 205. STRAIN RATE SENSITIVE CASE

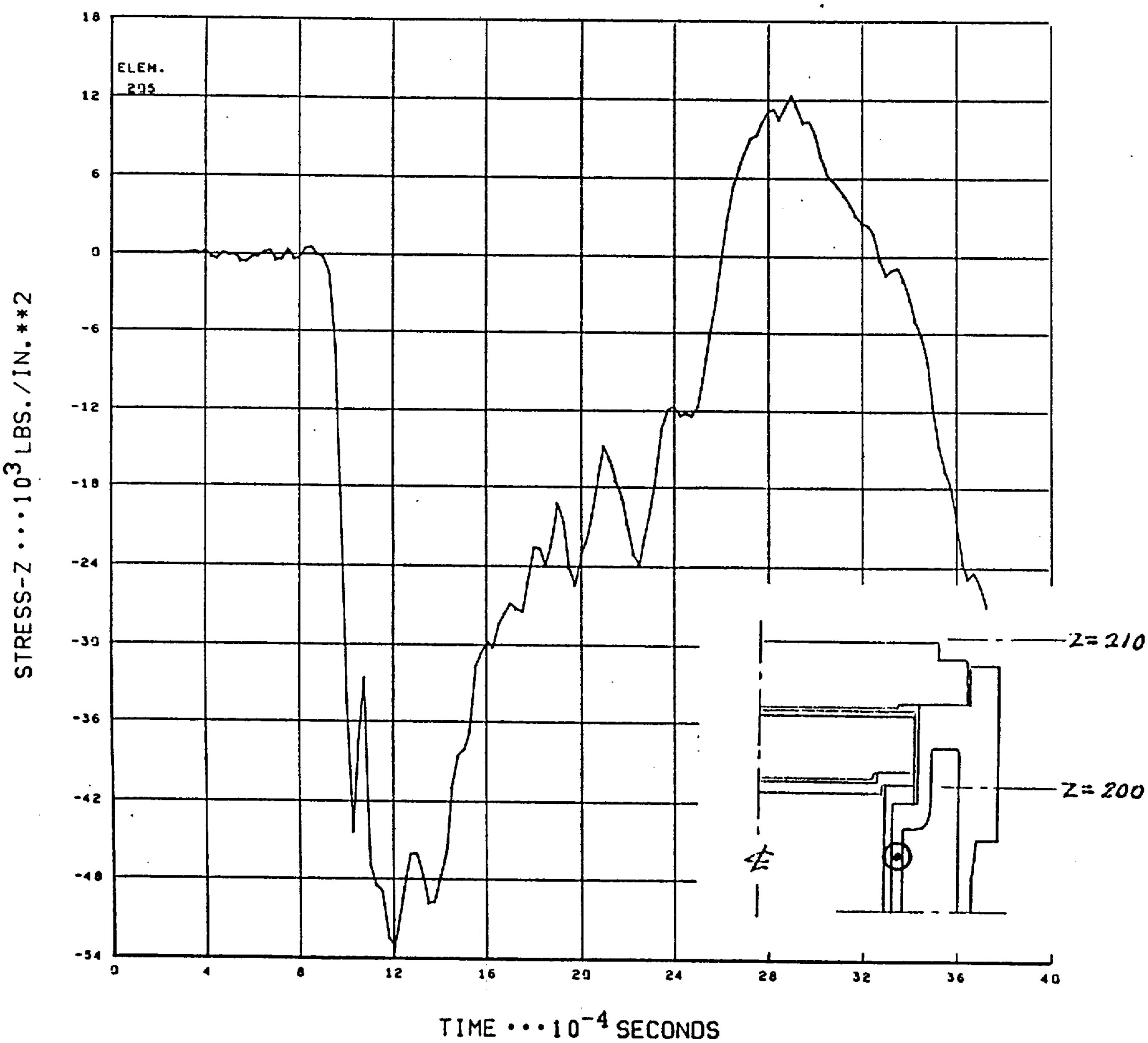

REF. HONDO RUN NO. 30T-12.

Figure 2-9

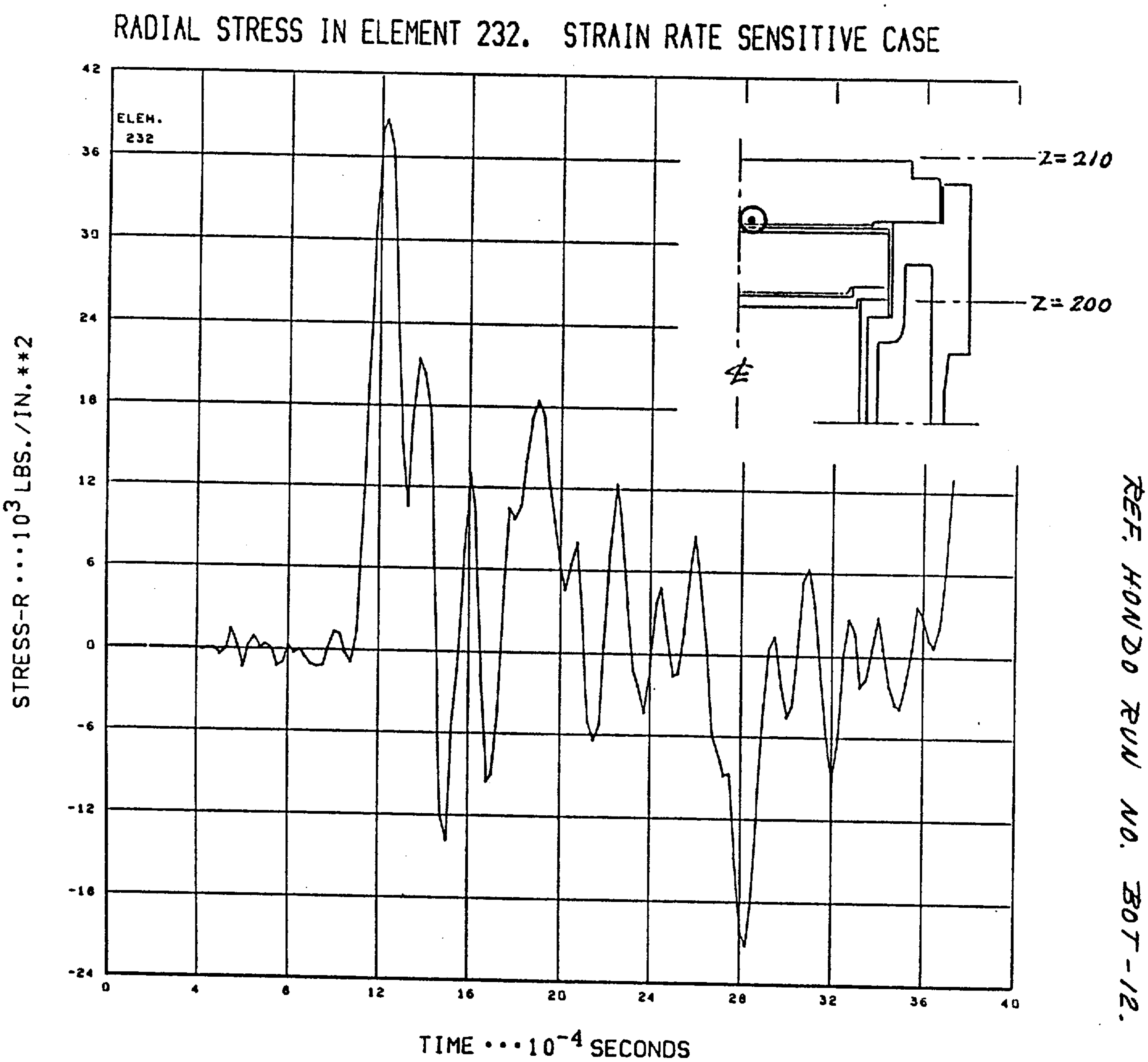
RADIAL STRESS IN ELEMENT 232. STRAIN RATE SENSITIVE CASE
ELEM. 232
Z= 210
Z= 200
STRESS-R ···10³ LBS./IN.**2
42
36
30
24
18
12
6
0
-6
-12
-18
-24
0
4
8
12
16
20
24
28
32
36
40
TIME ···10⁻⁴ SECONDS
REF. HONDO RUN NO. BOT-12.

Figure 2-10

HOOP STRESS IN ELEMENT 303. STRAIN RATE SENSITIVE CASE

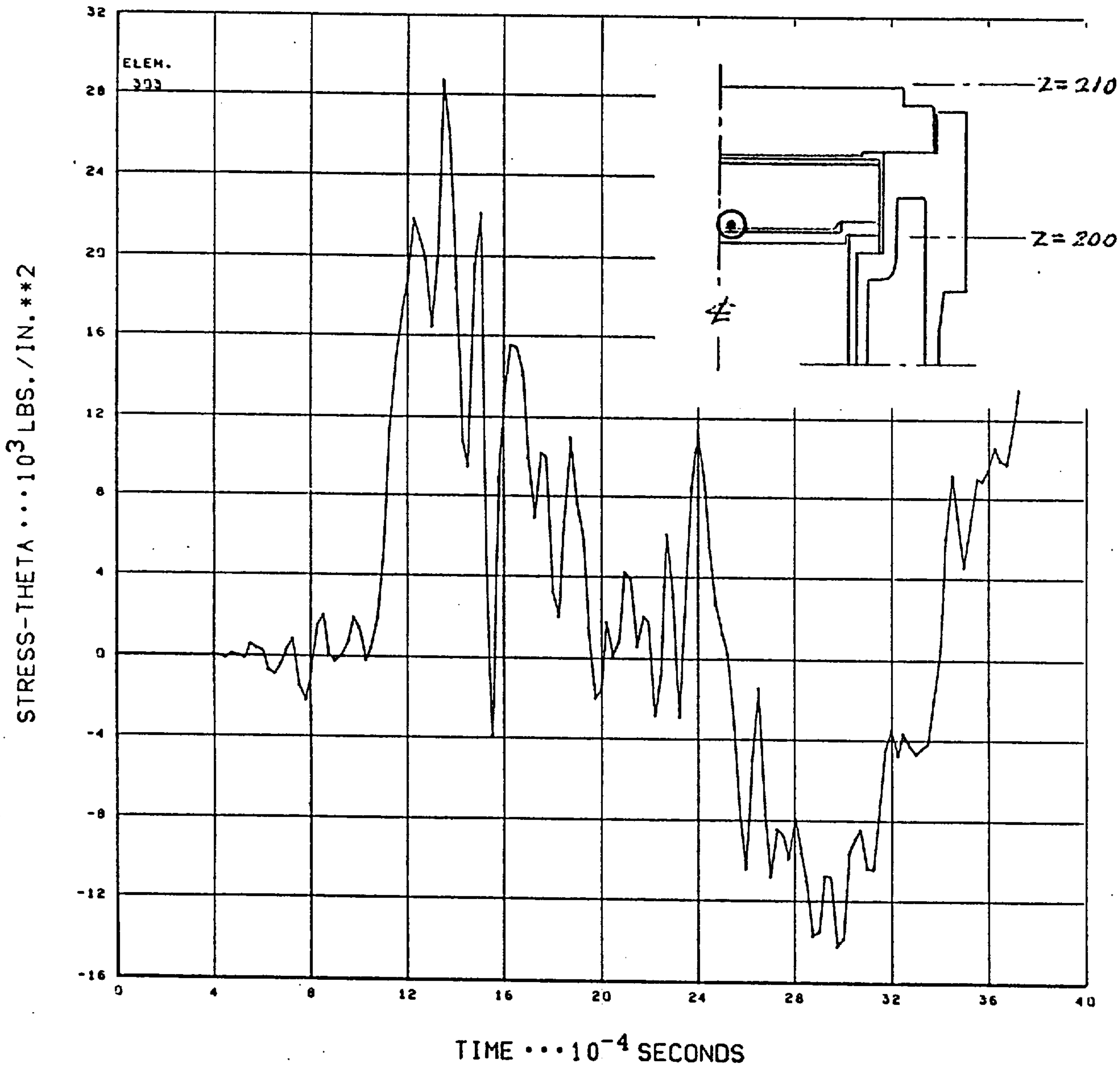

REF. HONDO RUN NO. BOT-12.

Figure 2-11

SHEAR STRESS IN ELEMENT 318. STRAIN RATE SENSITIVE CASE

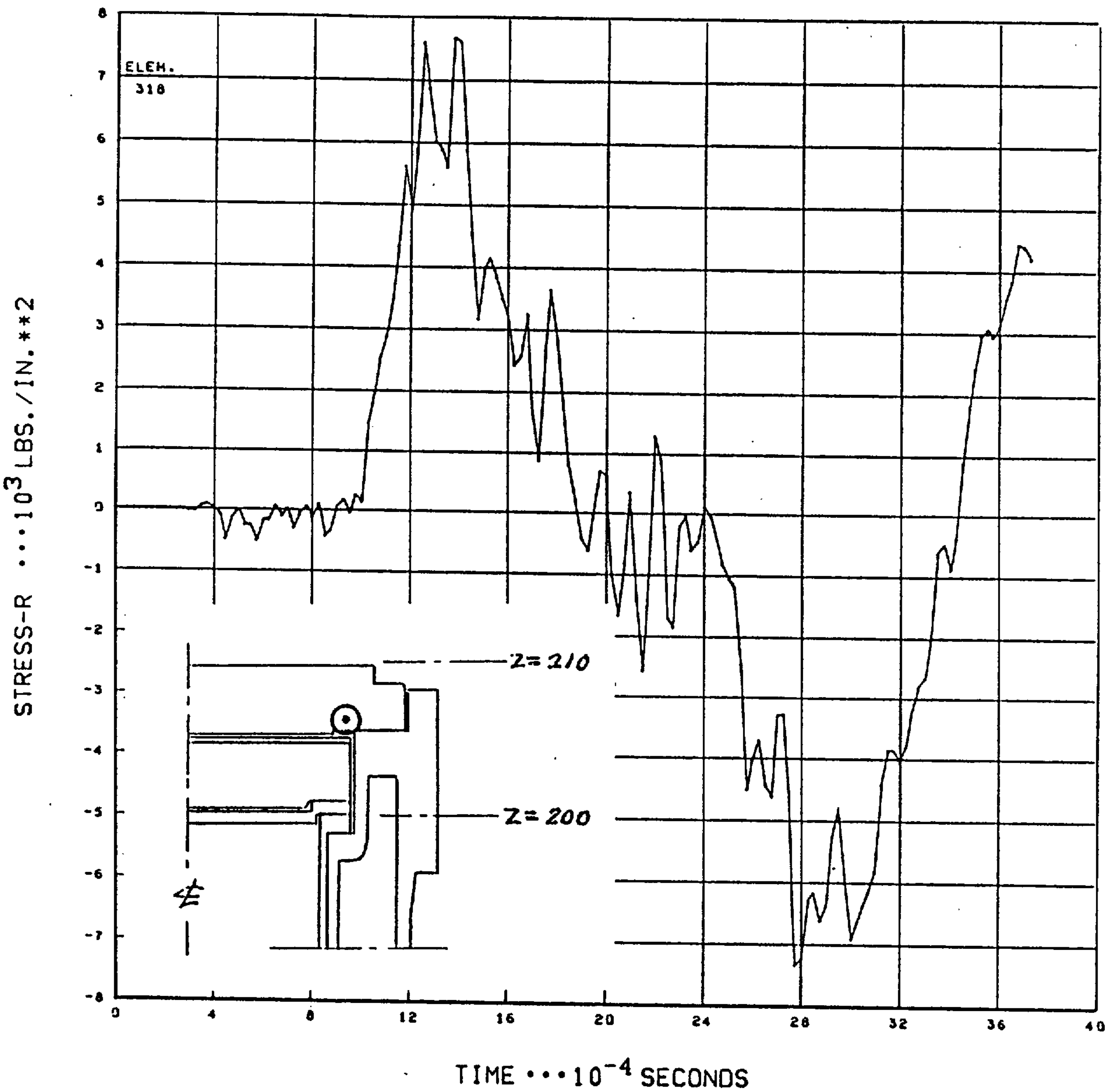

REF. HONDO RUN NO. BOT-12.

Figure 2-12

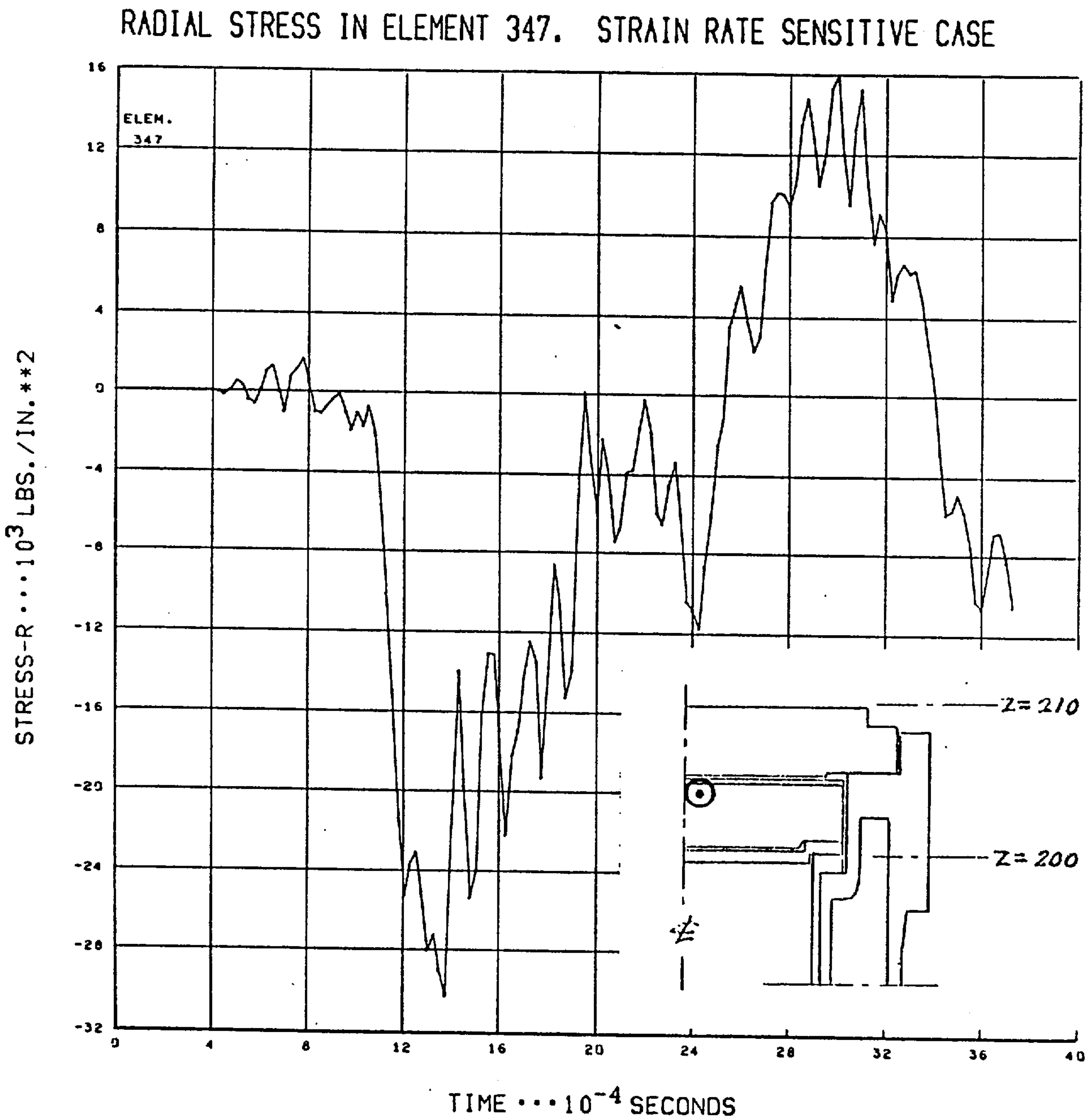

REF. HONDO RUN NO. BOT-12.

Figure 2-13

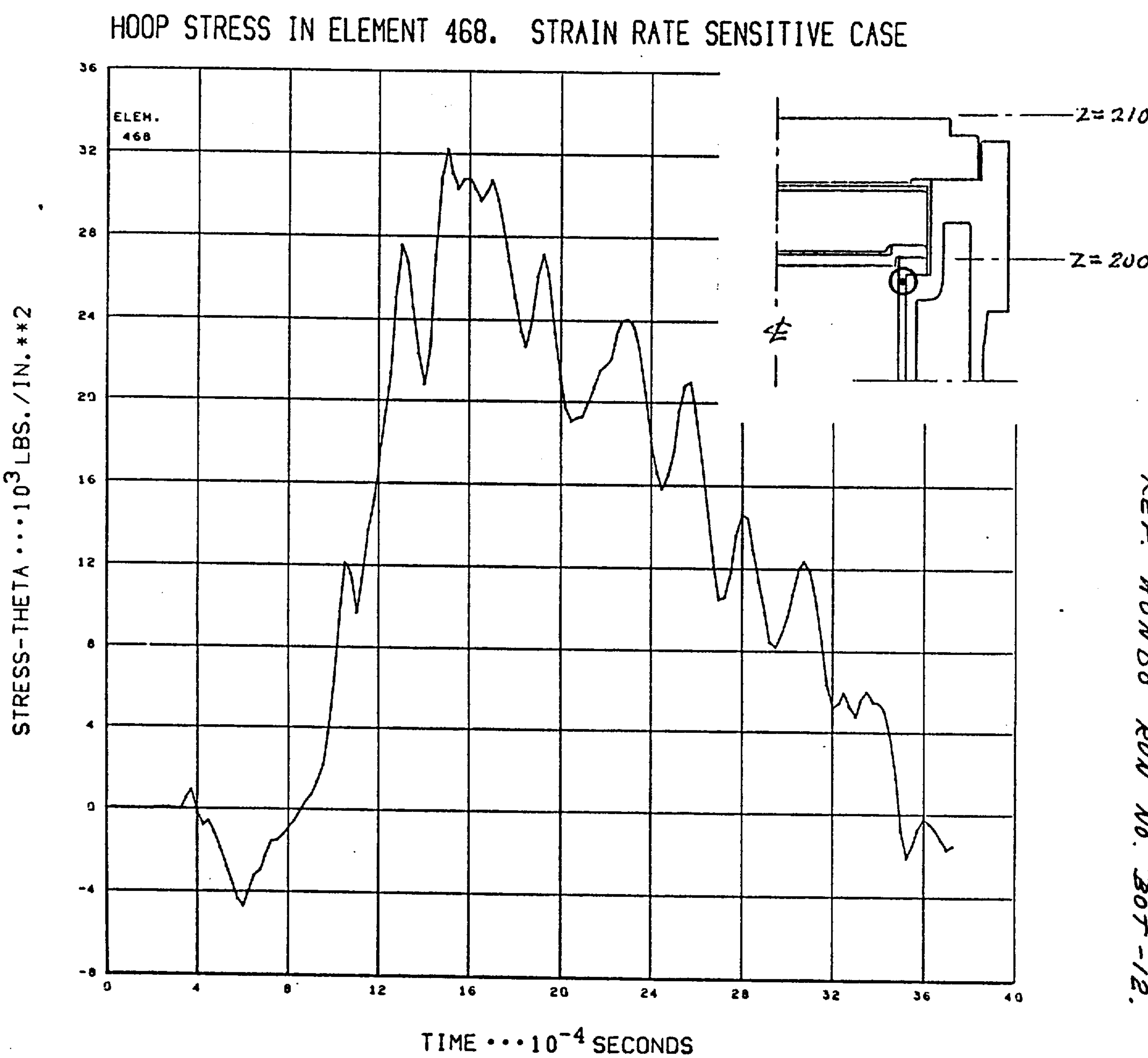
HOOP STRESS IN ELEMENT 468. STRAIN RATE SENSITIVE CASE
ELEM. 468
STRESS-THETA ···10^3 LBS./IN.**2
TIME ···10^-4 SECONDS
36
32
28
24
20
16
12
8
4
0
-4
-8
0
4
8
12
16
20
24
28
32
36
40
Z=210
Z=200
REF. HONDO RUN NO. BOT-12.

Figure 2-14

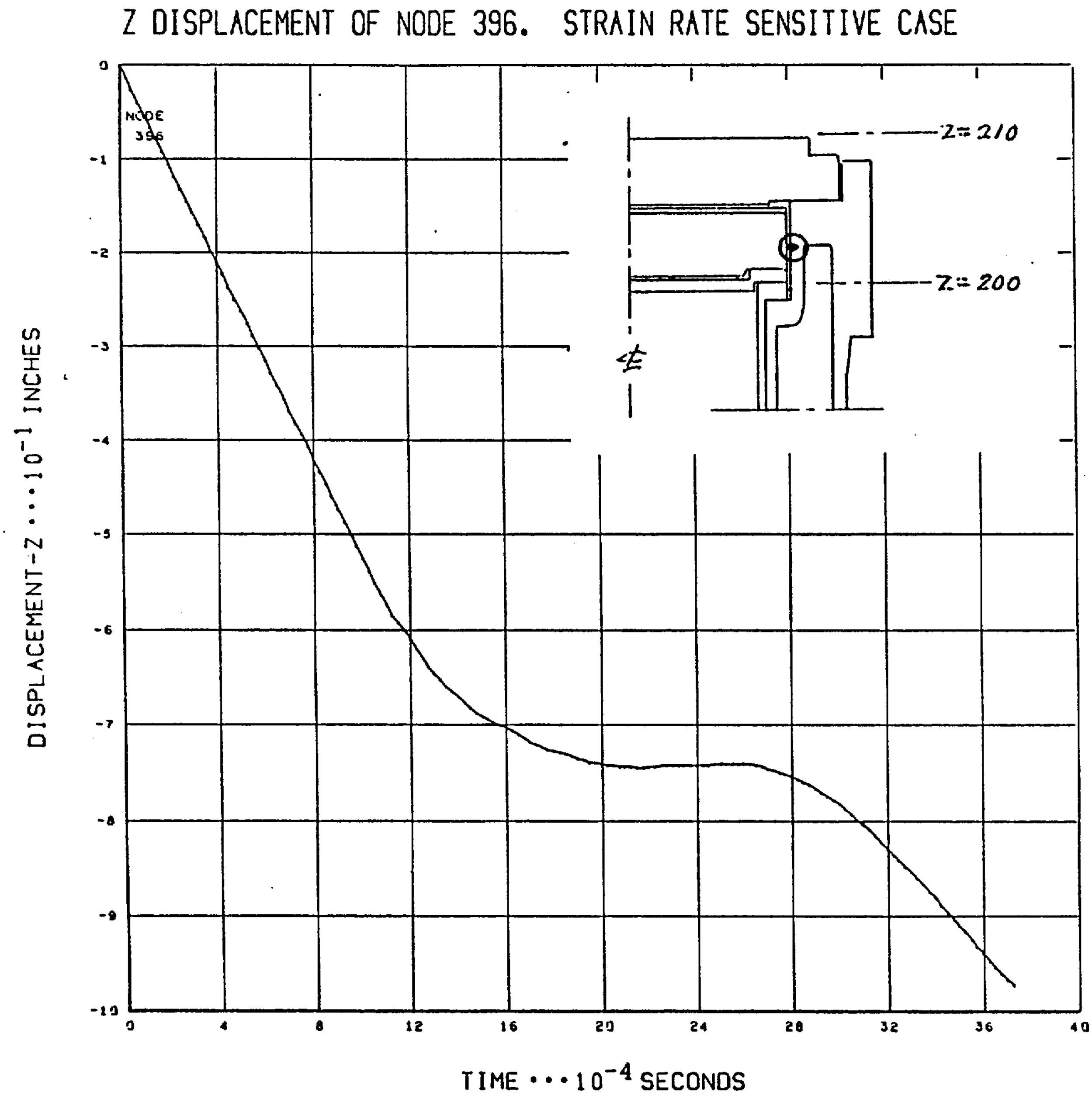

REF. HONDO RUN NO. BOT-12.

910013 hc

Figure 2-15

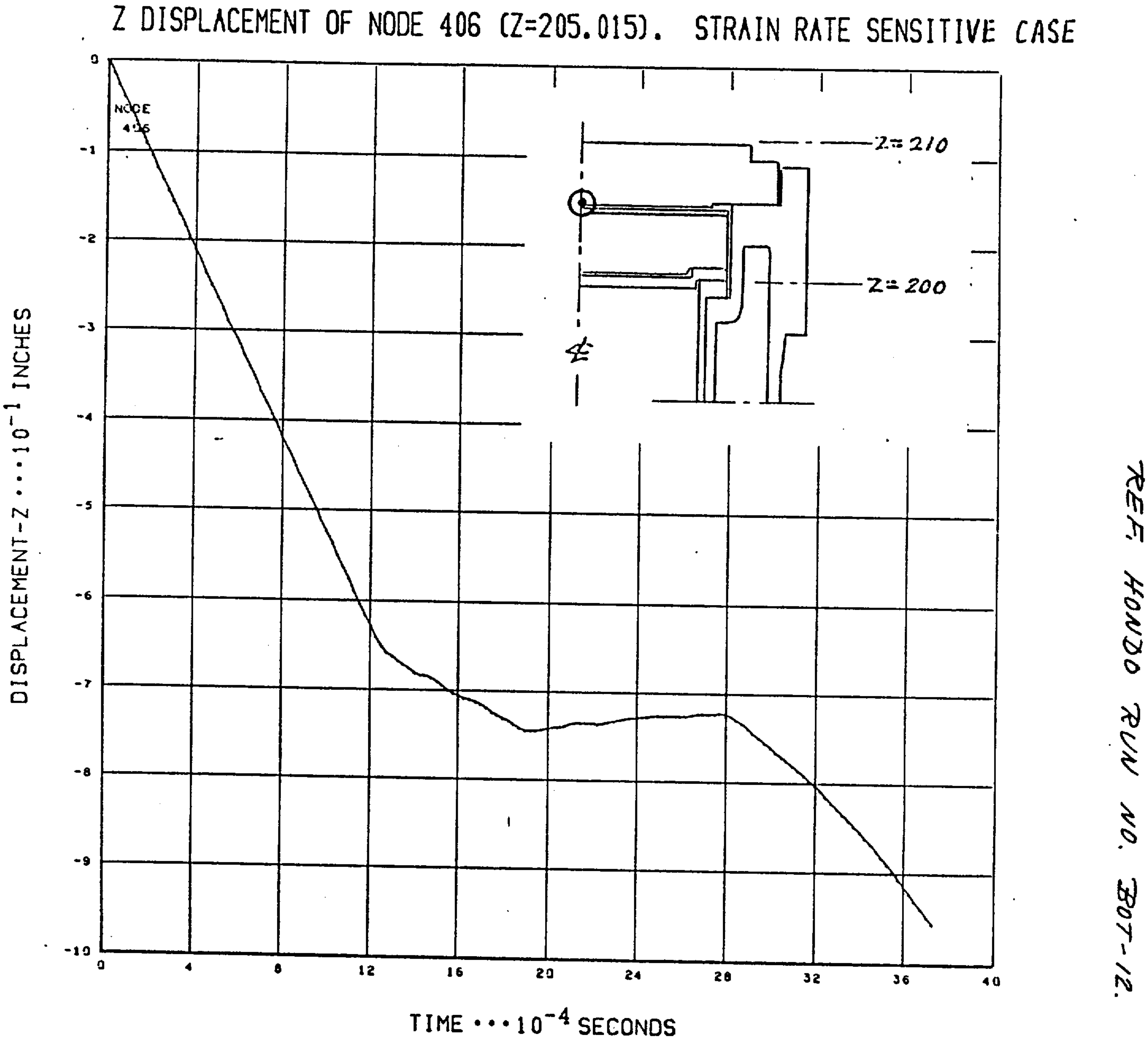

Figure 2-16

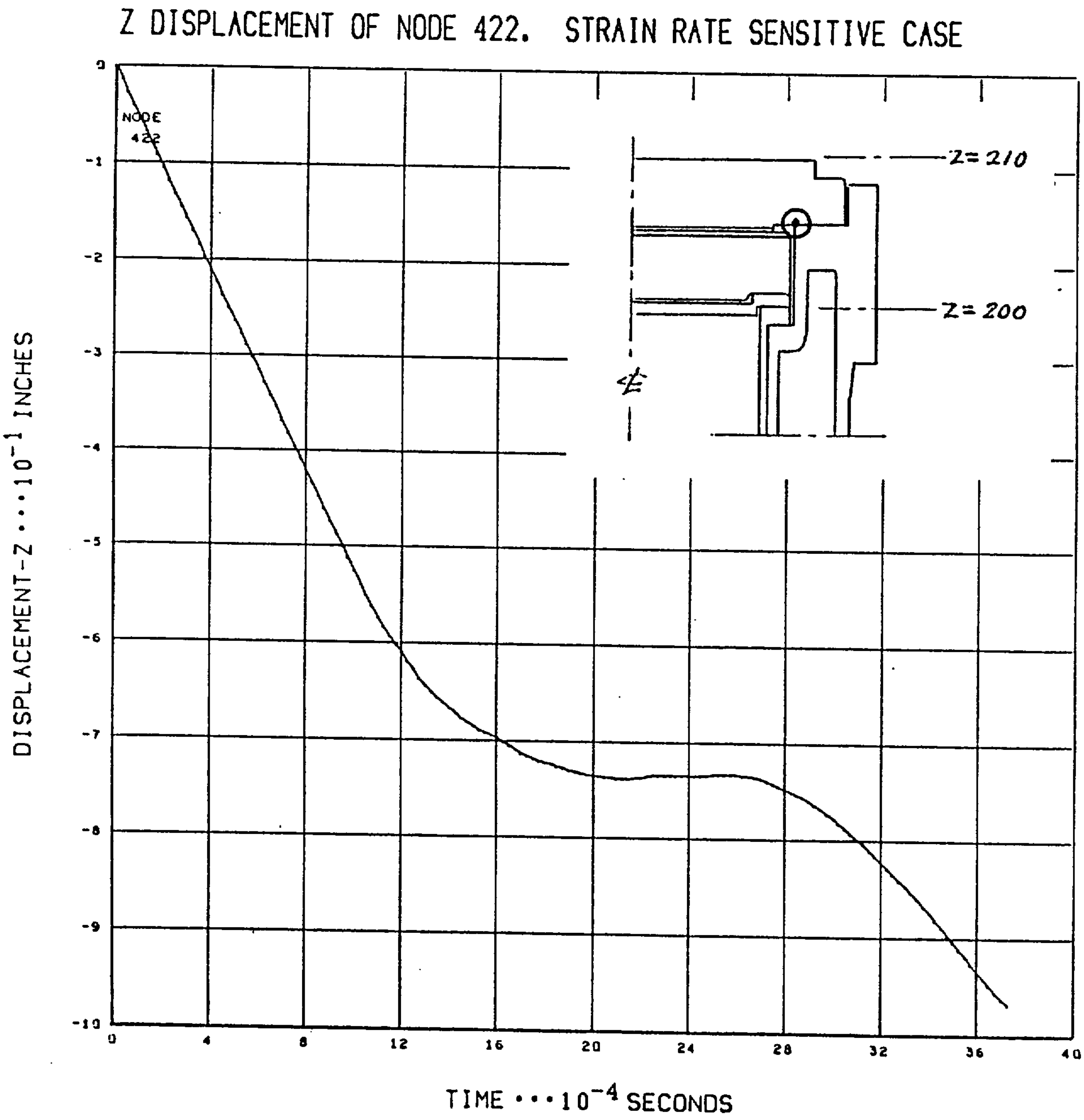

REF. HONDO RUN NO. B0T-12.

Figure 2-17

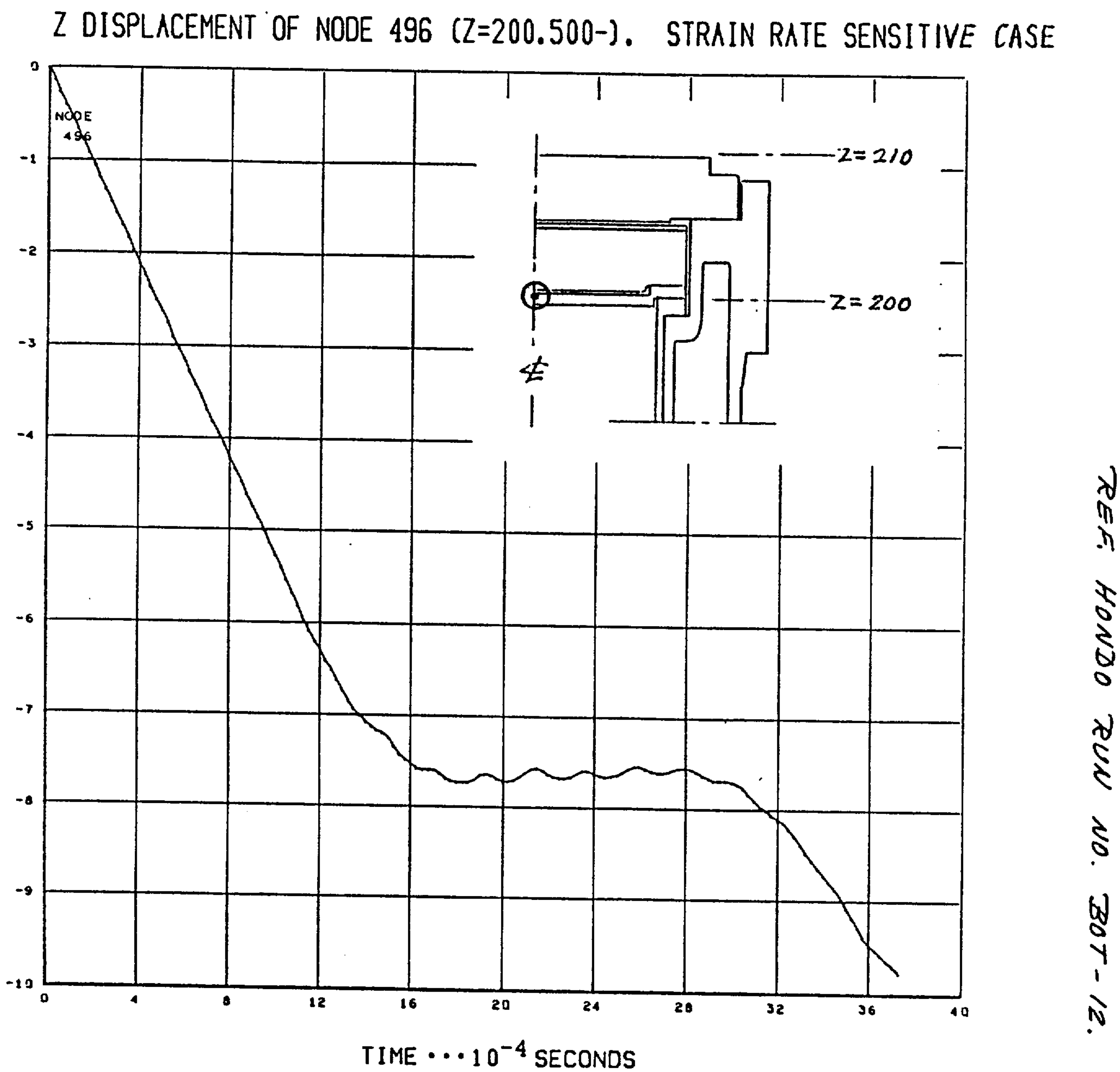
Z DISPLACEMENT OF NODE 496 (Z=200.500-). STRAIN RATE SENSITIVE CASE
NODE
496
Z=210
Z=200
DISPLACEMENT-Z ···10^-1 INCHES
TIME ···10^-4 SECONDS
0
-1
-2
-3
-4
-5
-6
-7
-8
-9
-10
0
4
8
12
16
20
24
28
32
36
40
REF. HONDO RUN NO. BOT-12.

Figure 2-18

Z DISPLACEMENT OF NODE 509 (Z=200.500+). STRAIN RATE SENSITIVE CASE

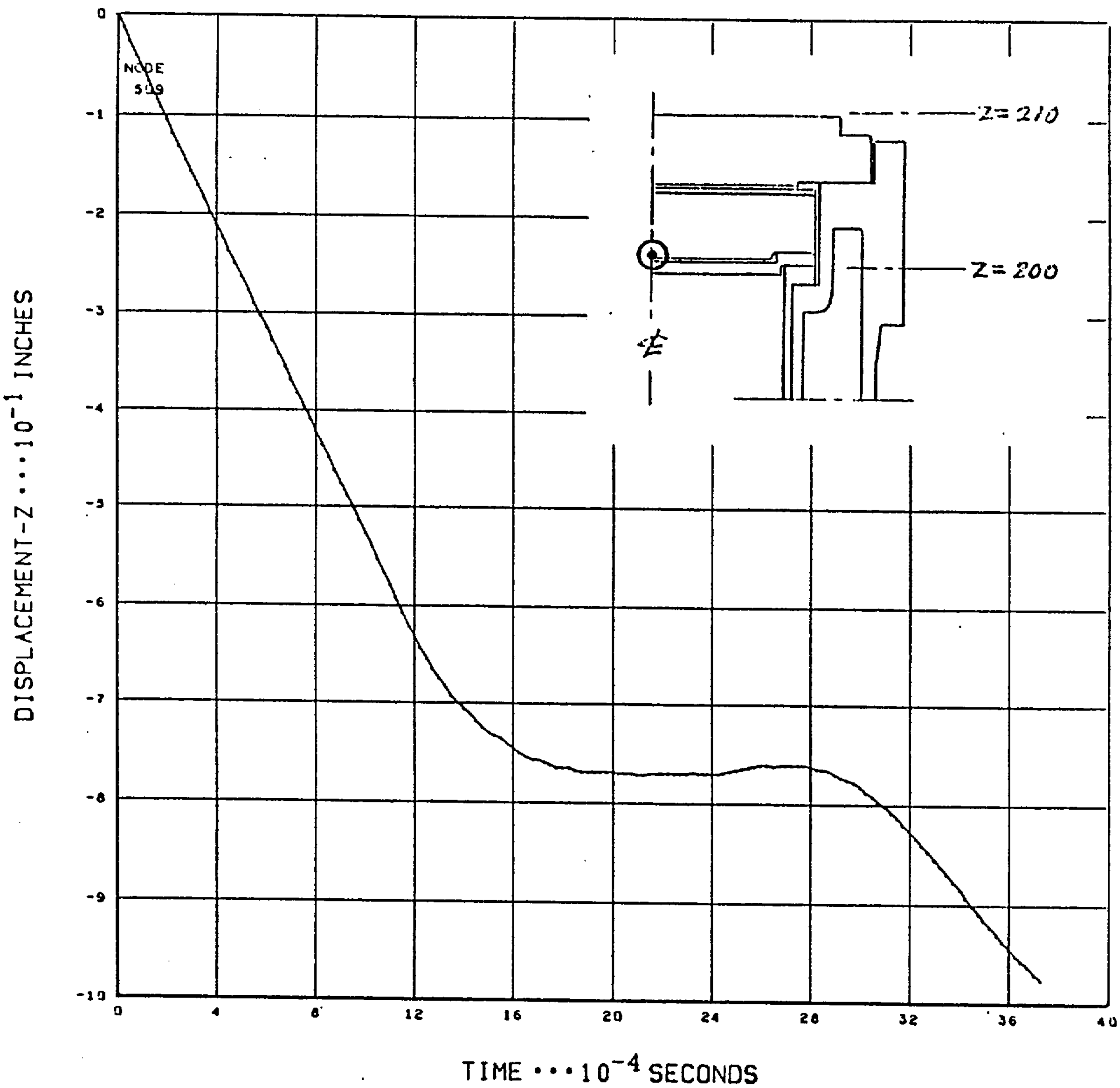

REF. HONDO RUN NO. BOT-12.

Figure 2-19

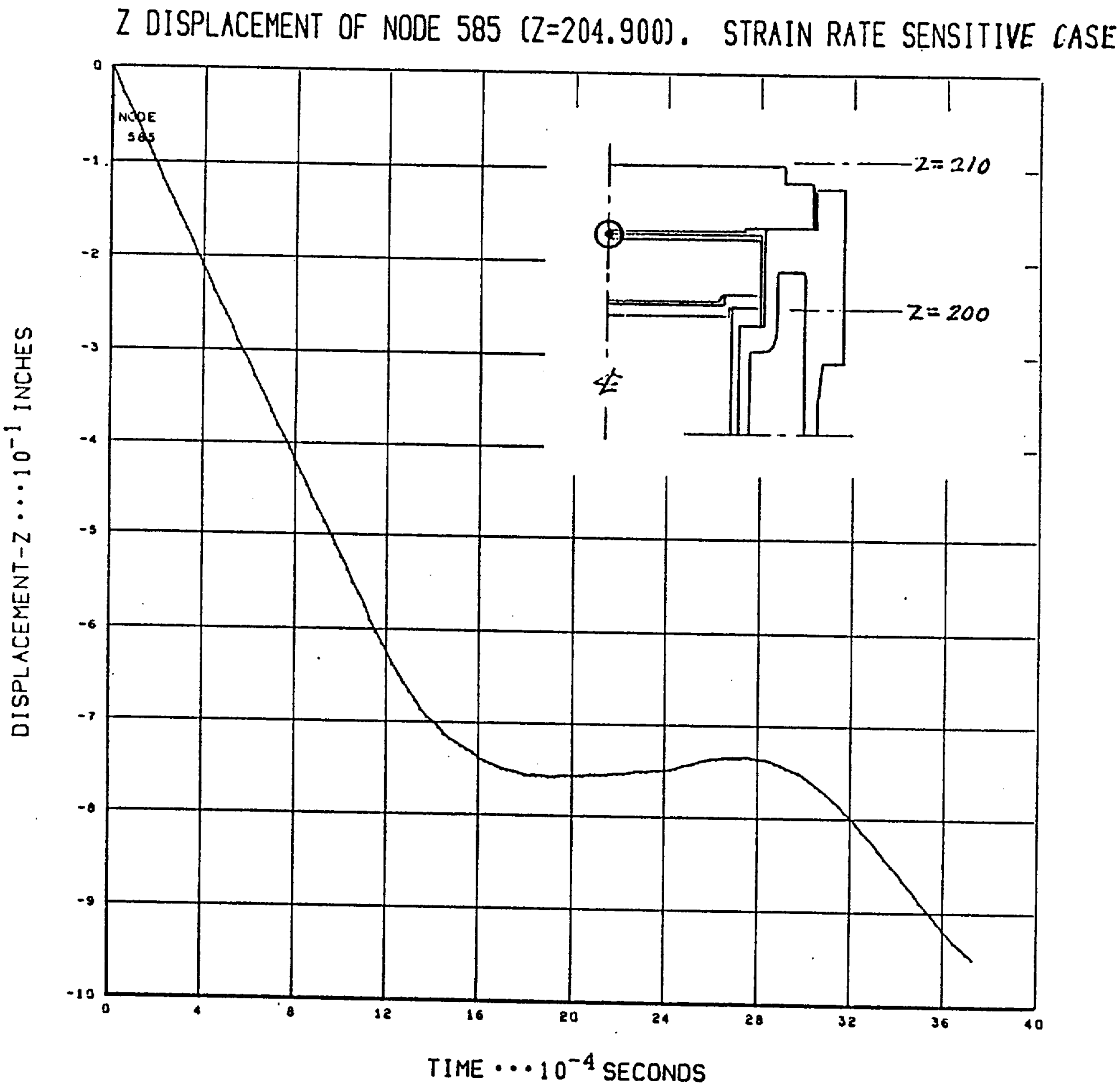

REF. HONDO RUN NO. BOT-12.

Figure 2-20

Z DISPLACEMENT AT TOP CENTER OF UPPER BULKHEAD. STRAIN RATE SENSITIVE CASE

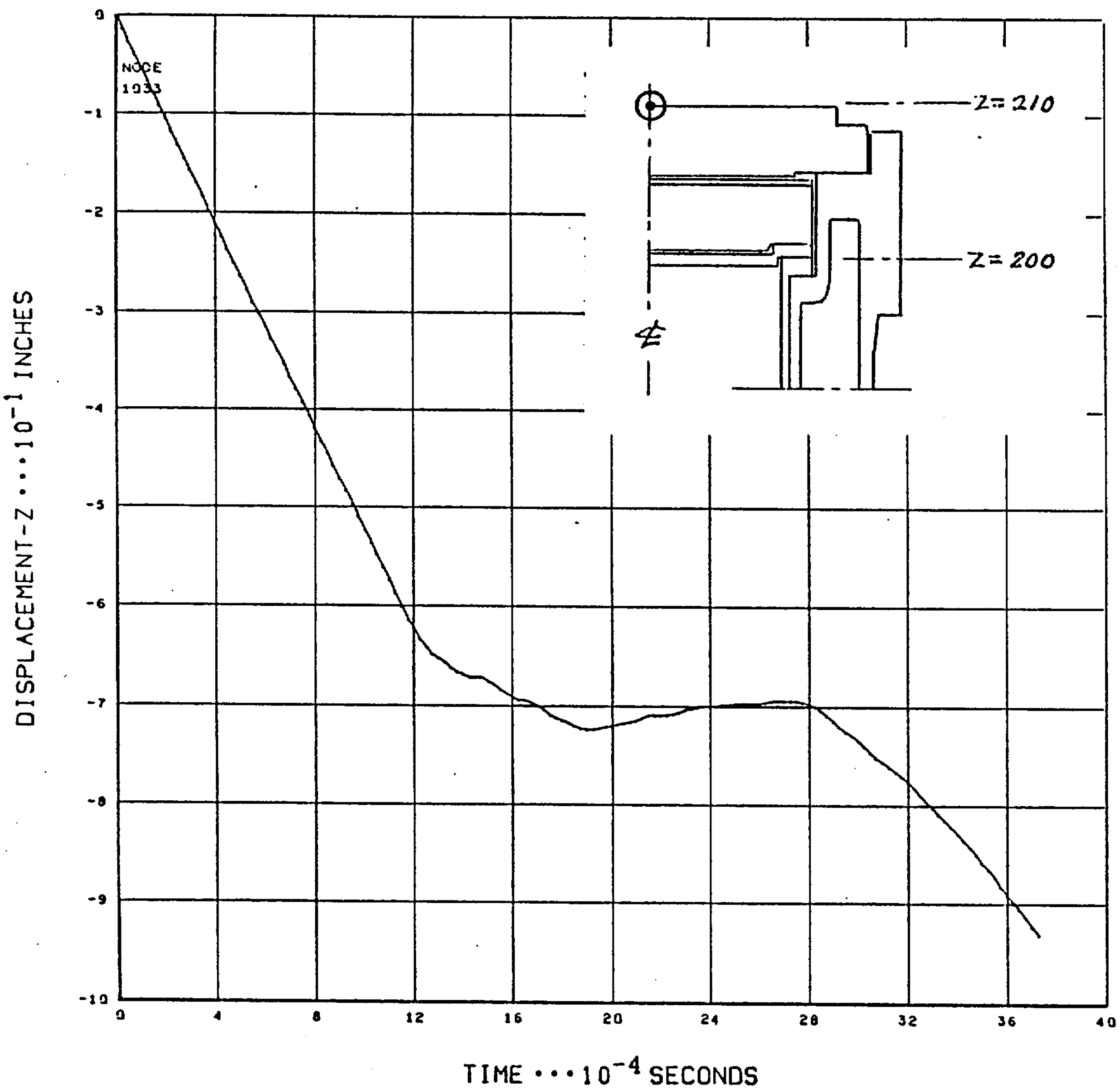

REF. HONDO RUN NO. BOT-12.

Figure 2-21

AXIAL DISPLACEMENT GRADIENT IN ELEMENT 205. STRAIN RATE SENSITIVE CASE

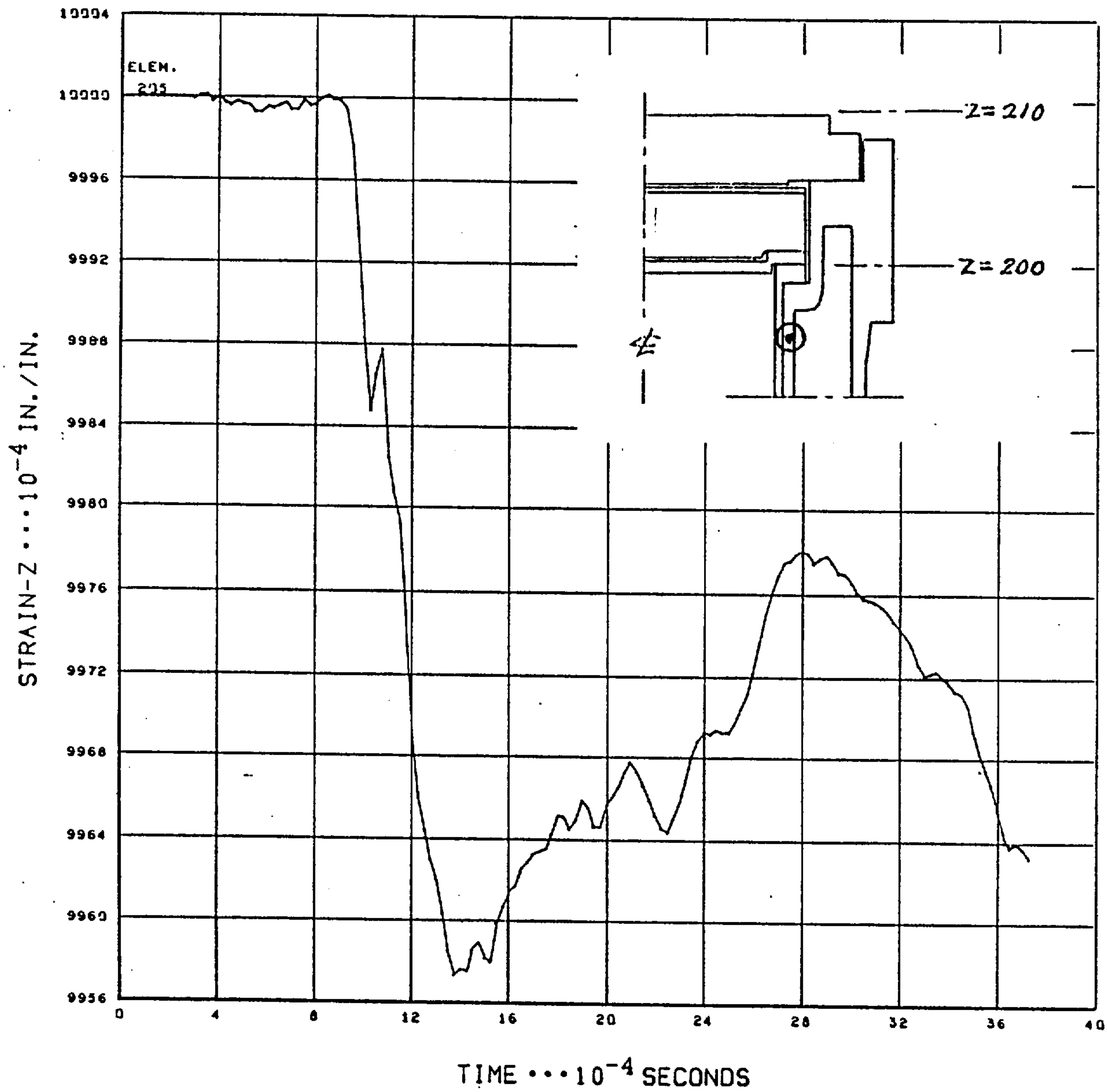

REF. HONDO RUN NO. BOT-12.

F 2-22

AXIAL STRESS IN ELEMENT 205. STRAIN RATE INSENSITIVE CASE

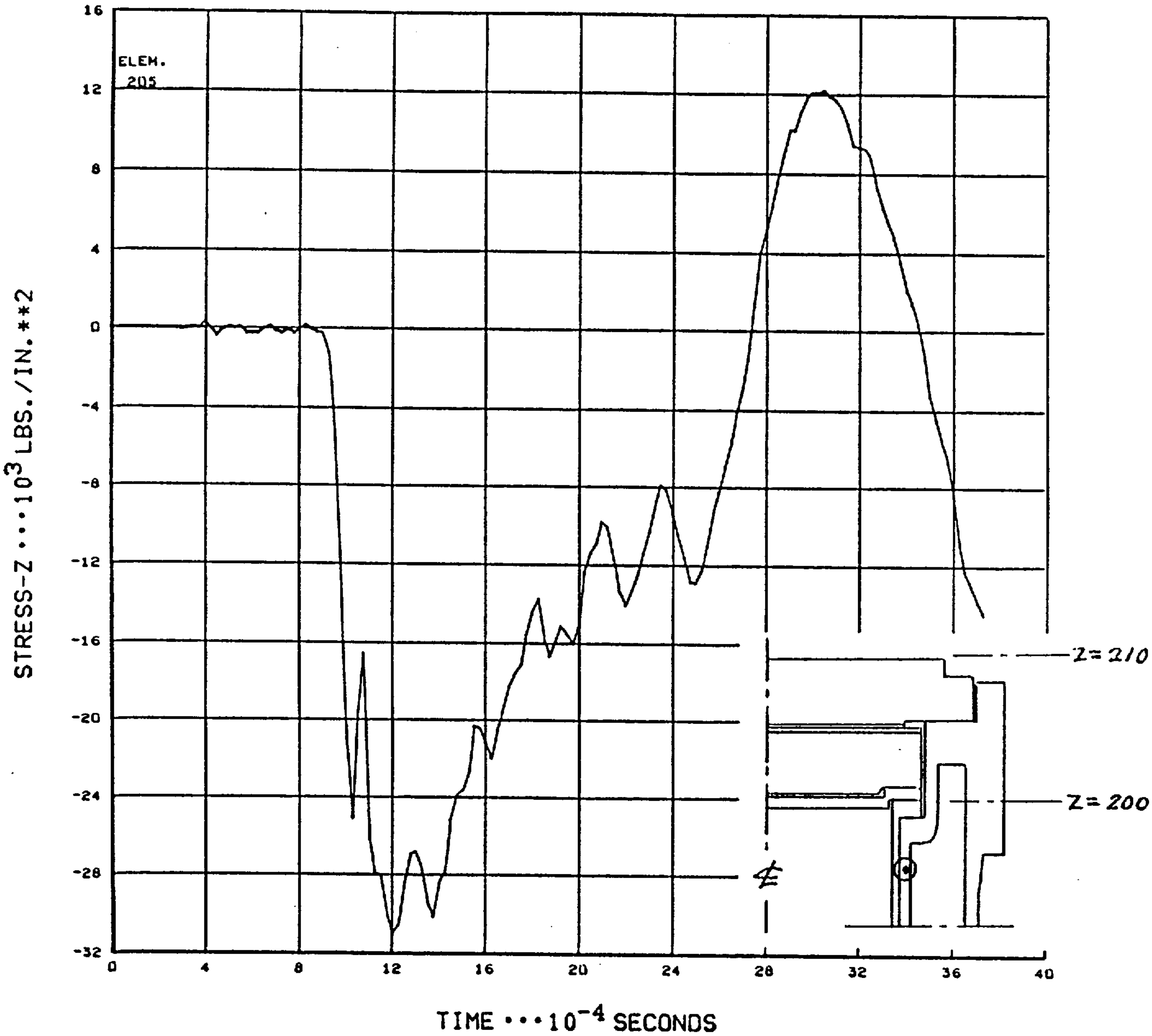

Figure 2-23

RADIAL STRESS IN ELEMENT 232. STRAIN RATE INSENSITIVE CASE

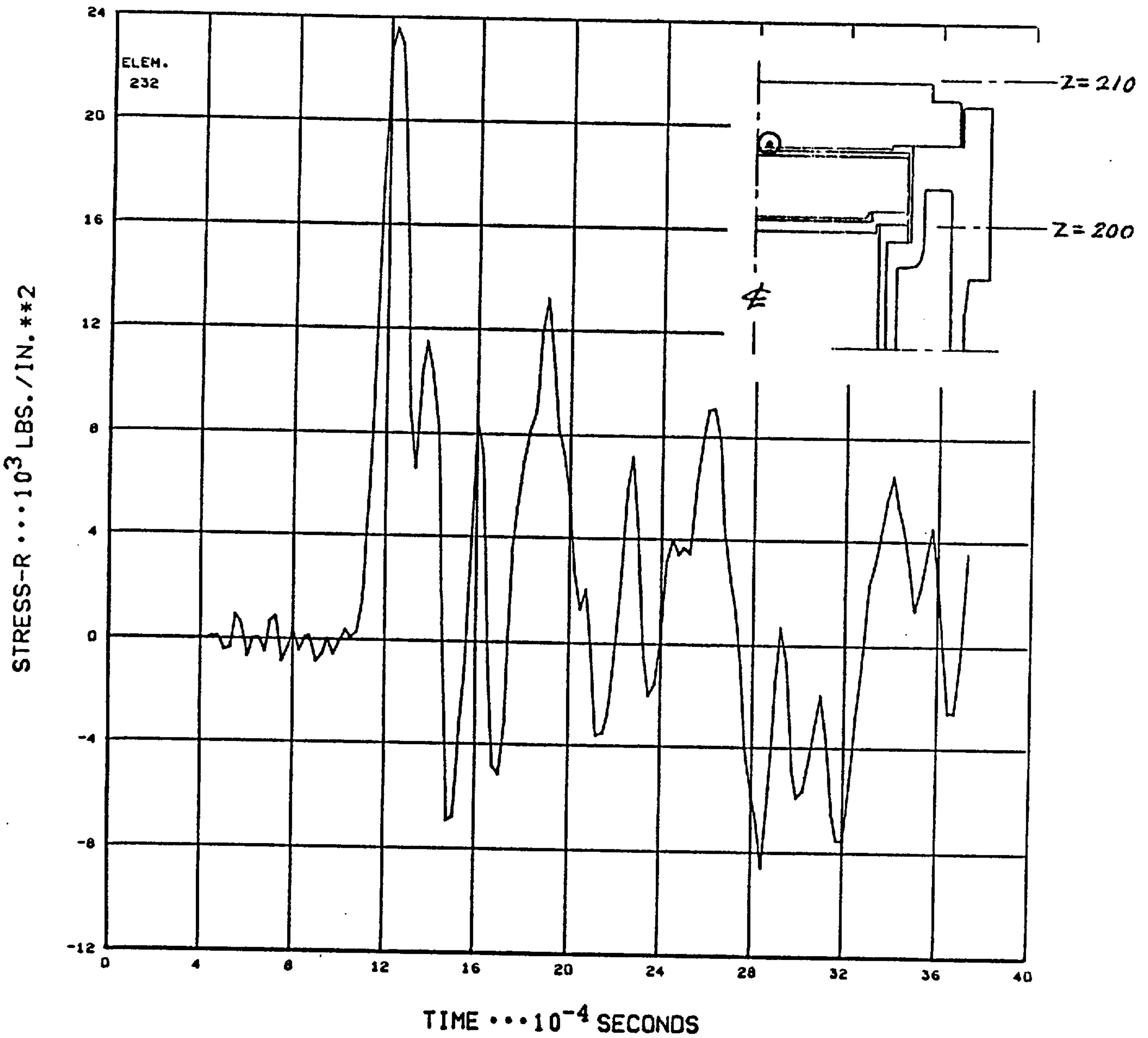

Figure 2-24

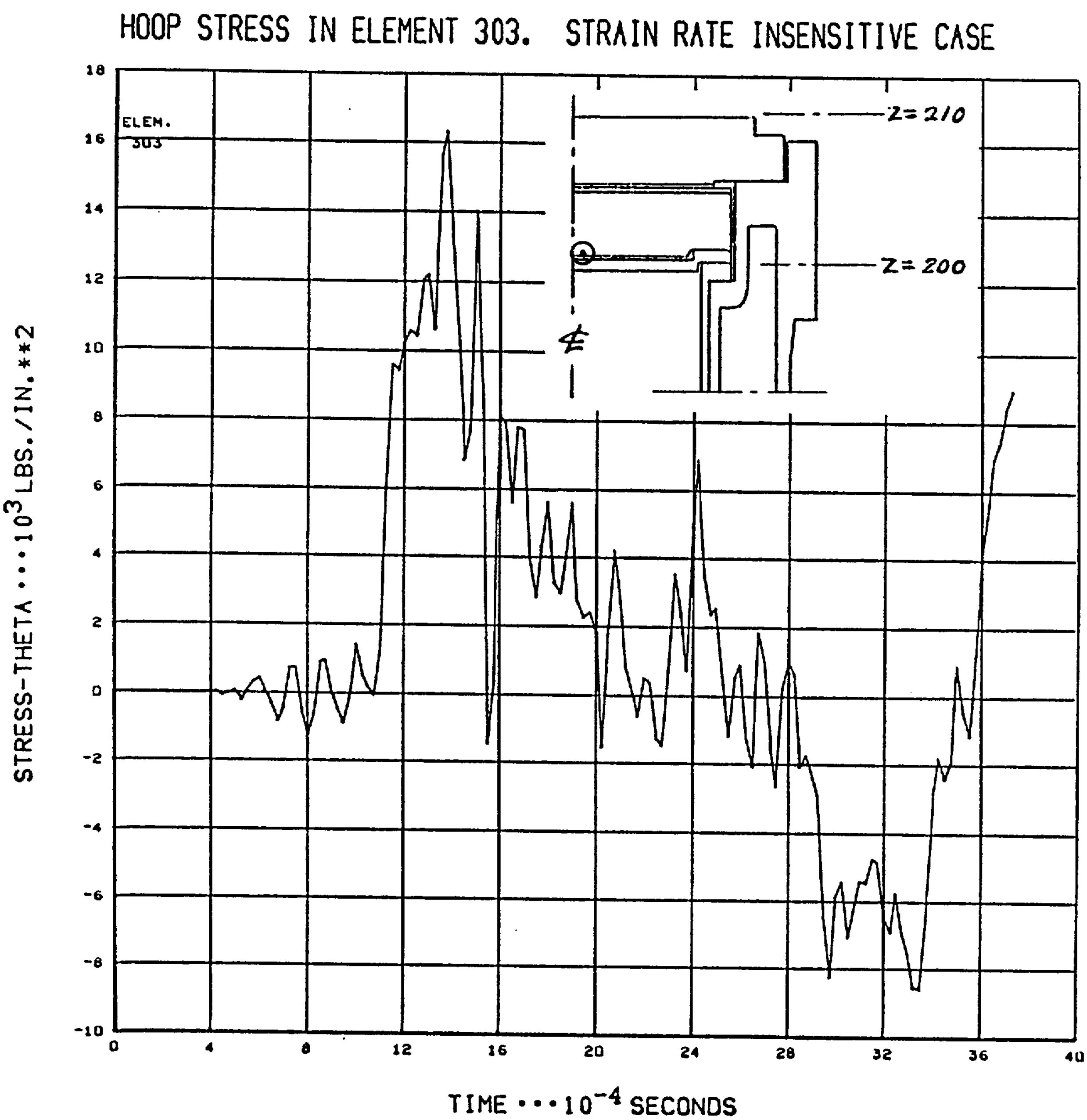
HOOP STRESS IN ELEMENT 303. STRAIN RATE INSENSITIVE CASE
ELEM. 303
Z= 210
Z= 200
STRESS-THETA ••• 10³ LBS./IN.**2
TIME ••• 10⁻⁴ SECONDS
18
16
14
12
10
8
6
4
2
0
-2
-4
-6
-8
-10
0
4
8
12
16
20
24
28
32
36
40

Figure 2-25

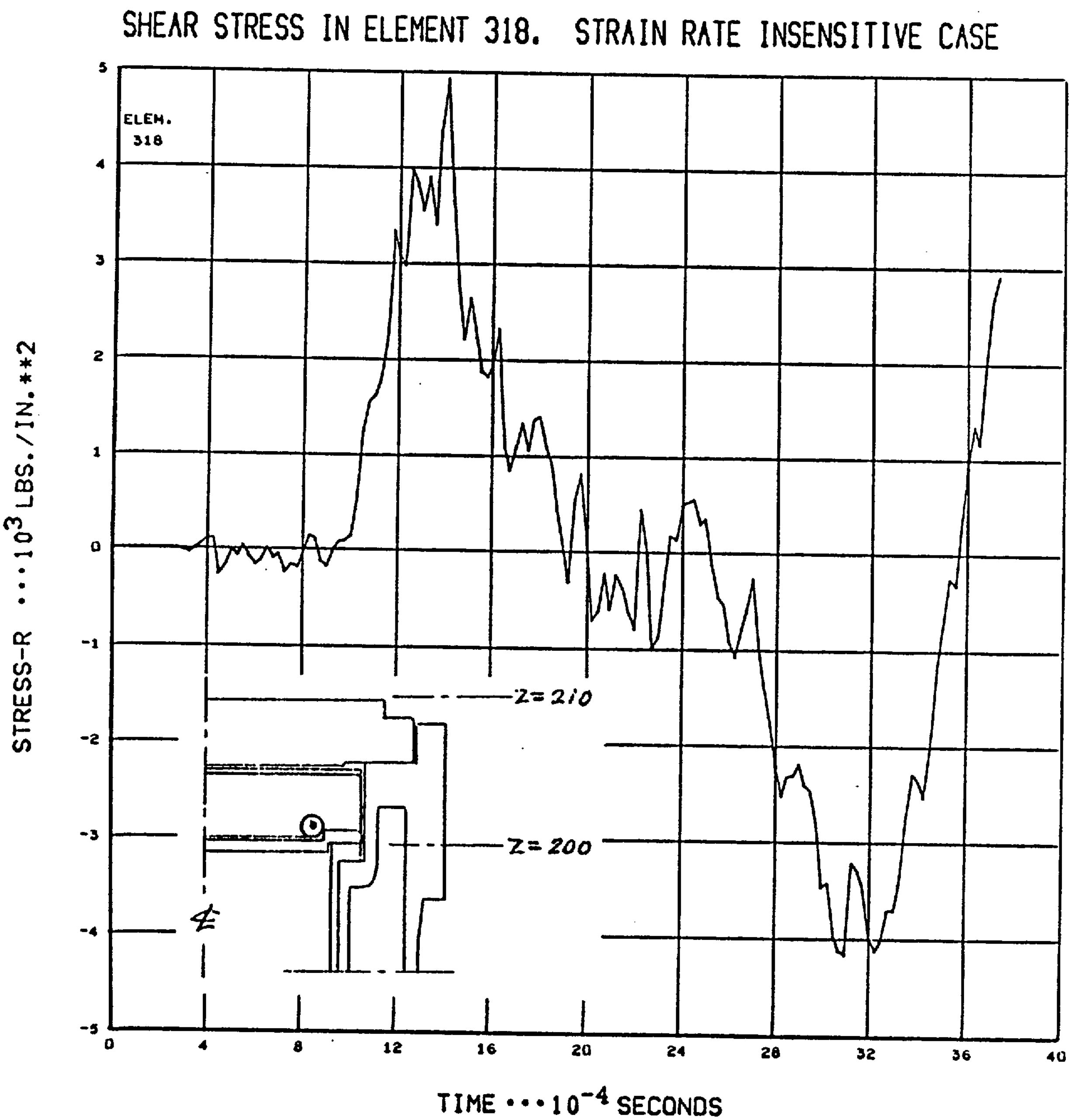
SHEAR STRESS IN ELEMENT 318. STRAIN RATE INSENSITIVE CASE
ELEM.
318
Z=210
Z=200
STRESS-R ···10^3 LBS./IN.**2
TIME ···10^-4 SECONDS
5
4
3
2
1
0
-1
-2
-3
-4
-5
0
4
8
12
16
20
24
28
32
36
40

Figure 2-26

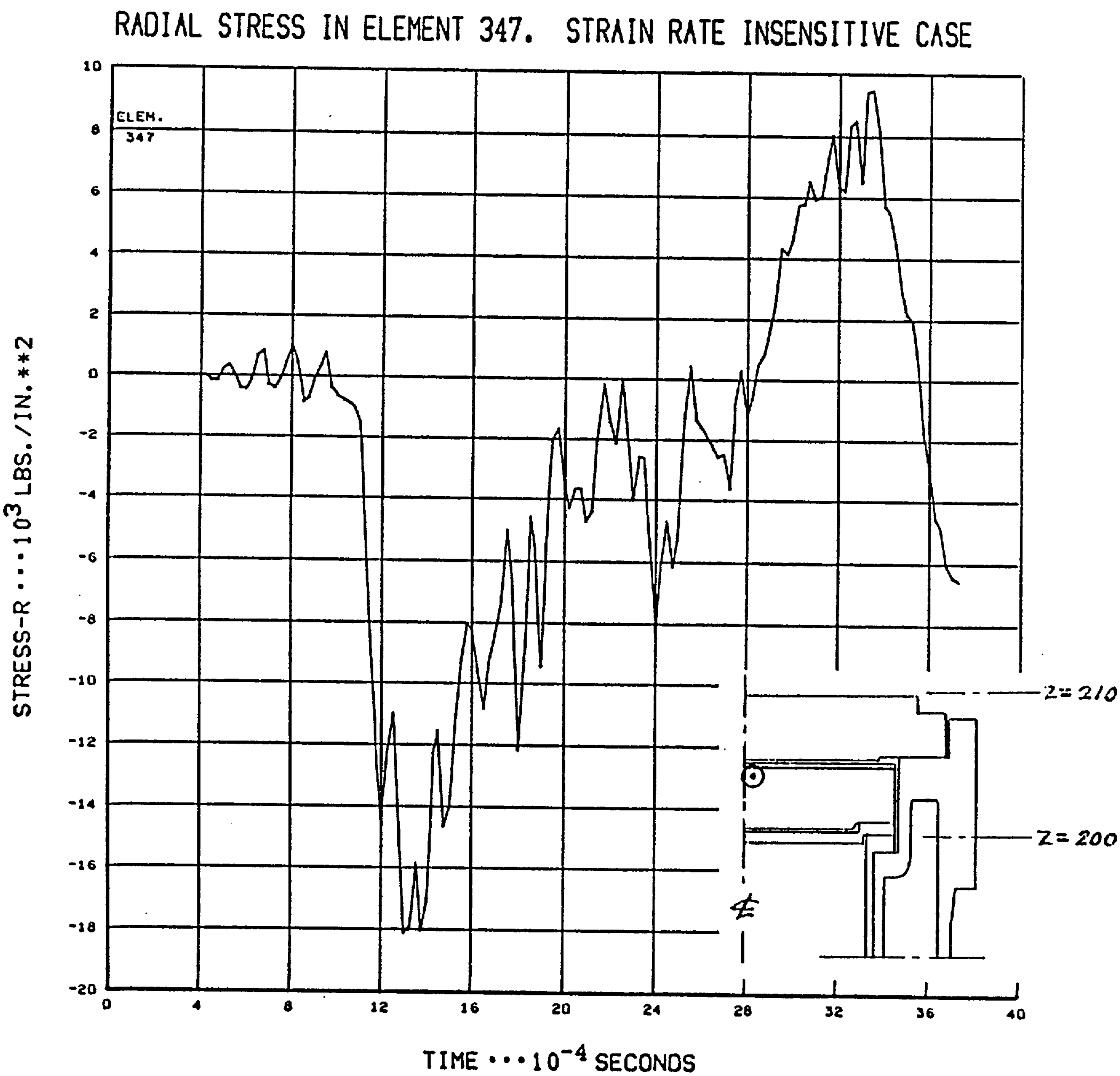
RADIAL STRESS IN ELEMENT 347. STRAIN RATE INSENSITIVE CASE
ELEM. 347
10
8
6
4
2
0
-2
-4
-6
-8
-10
-12
-14
-16
-18
-20
STRESS-R ··· 10^3 LBS./IN.**2
0
4
8
12
16
20
24
28
32
36
40
TIME ··· 10^{-4} SECONDS
Z= 210
Z= 200

Figure 2-27

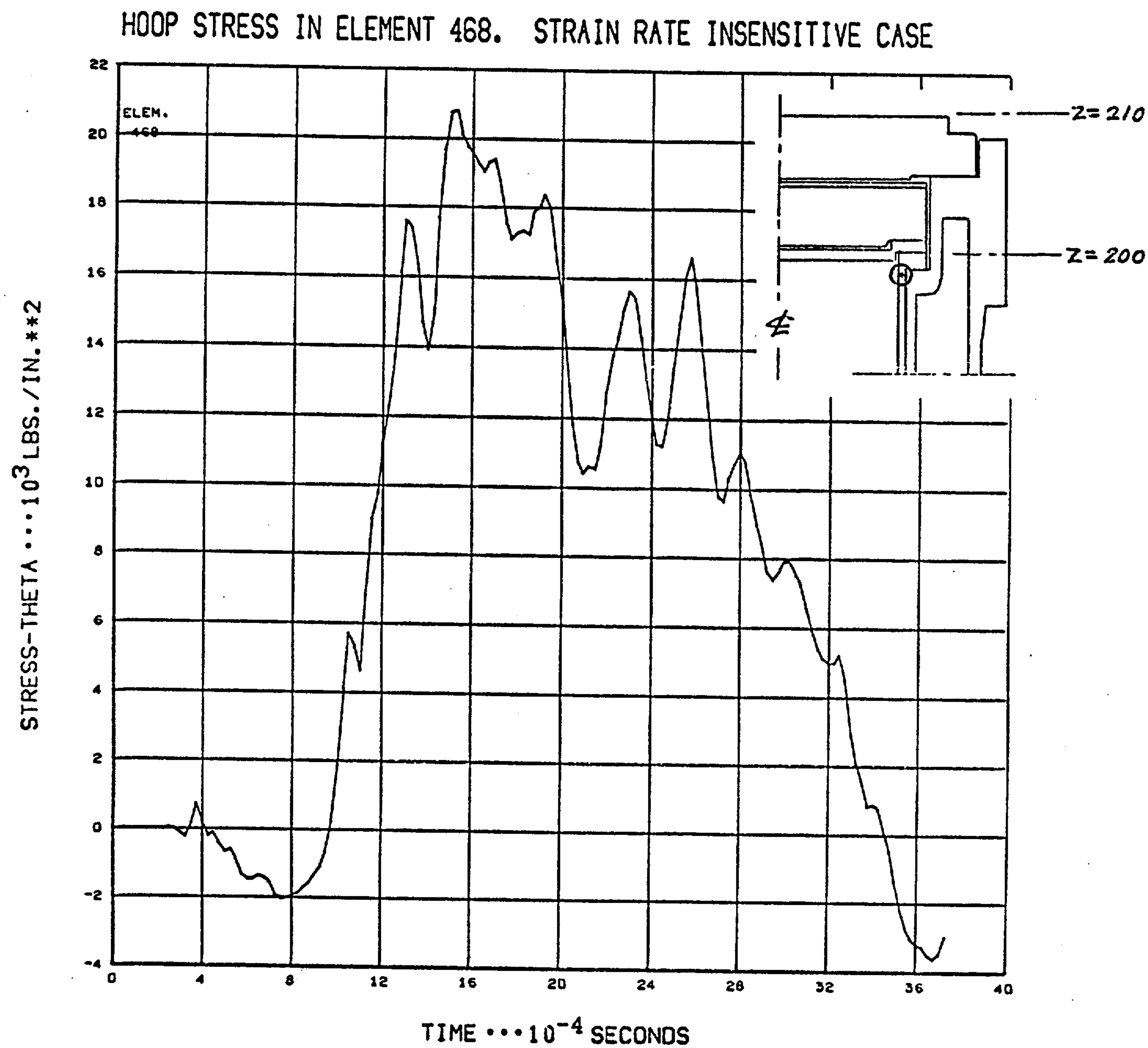
HOOP STRESS IN ELEMENT 468. STRAIN RATE INSENSITIVE CASE
ELEM. 468
Z=210
Z=200
22
20
18
16
14
12
10
8
6
4
2
0
-2
-4
0
4
8
12
16
20
24
28
32
36
40
STRESS-THETA ···10^3 LBS./IN.**2
TIME ···10^{-4} SECONDS

Figure 2-28

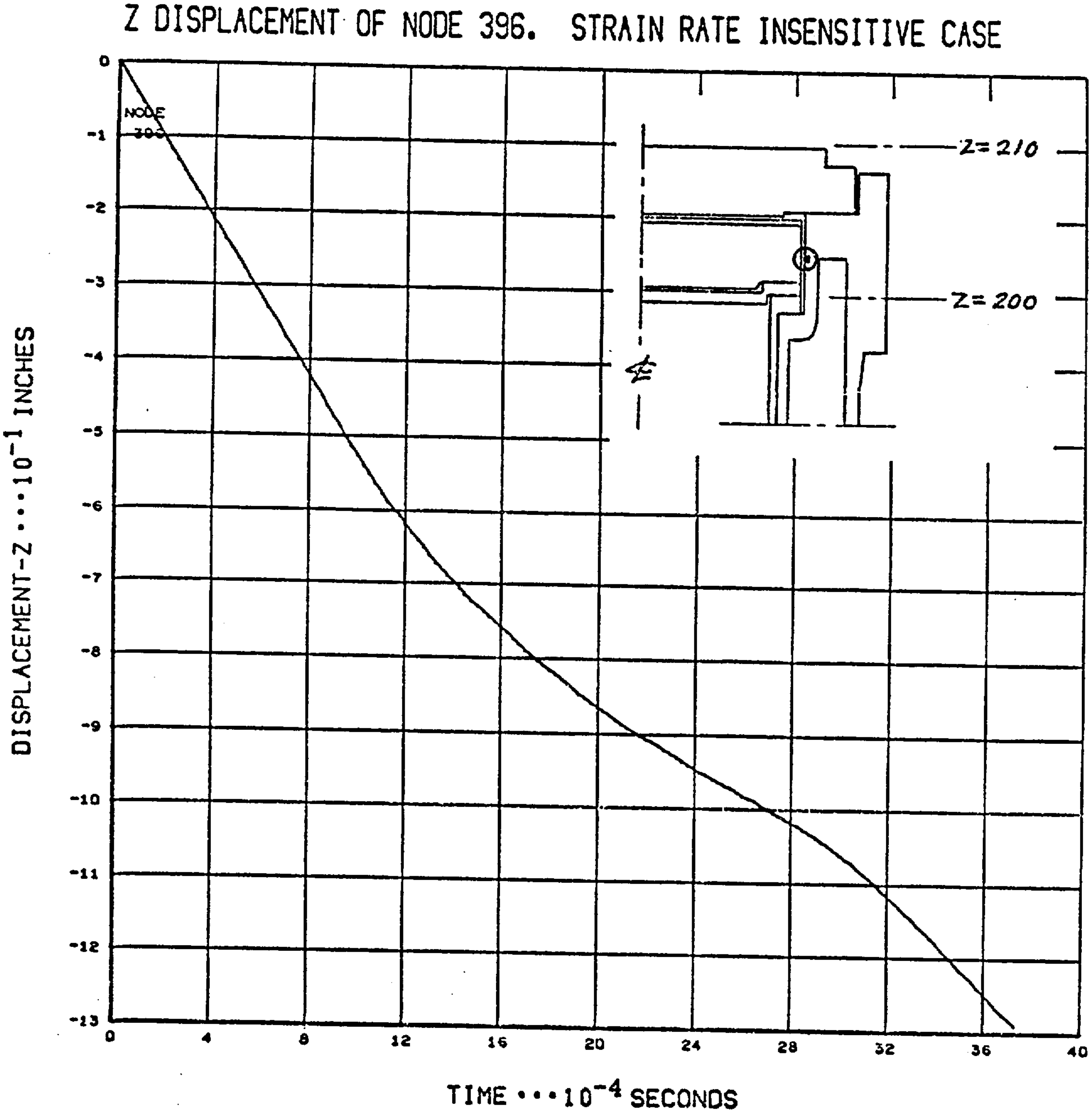
Z DISPLACEMENT OF NODE 396. STRAIN RATE INSENSITIVE CASE
0
-1
-2
-3
-4
-5
-6
-7
-8
-9
-10
-11
-12
-13
DISPLACEMENT-Z ···10^{-1} INCHES
0
4
8
12
16
20
24
28
32
36
40
TIME ···10^{-4} SECONDS
NODE
Z=210
Z=200

Figure 2-29

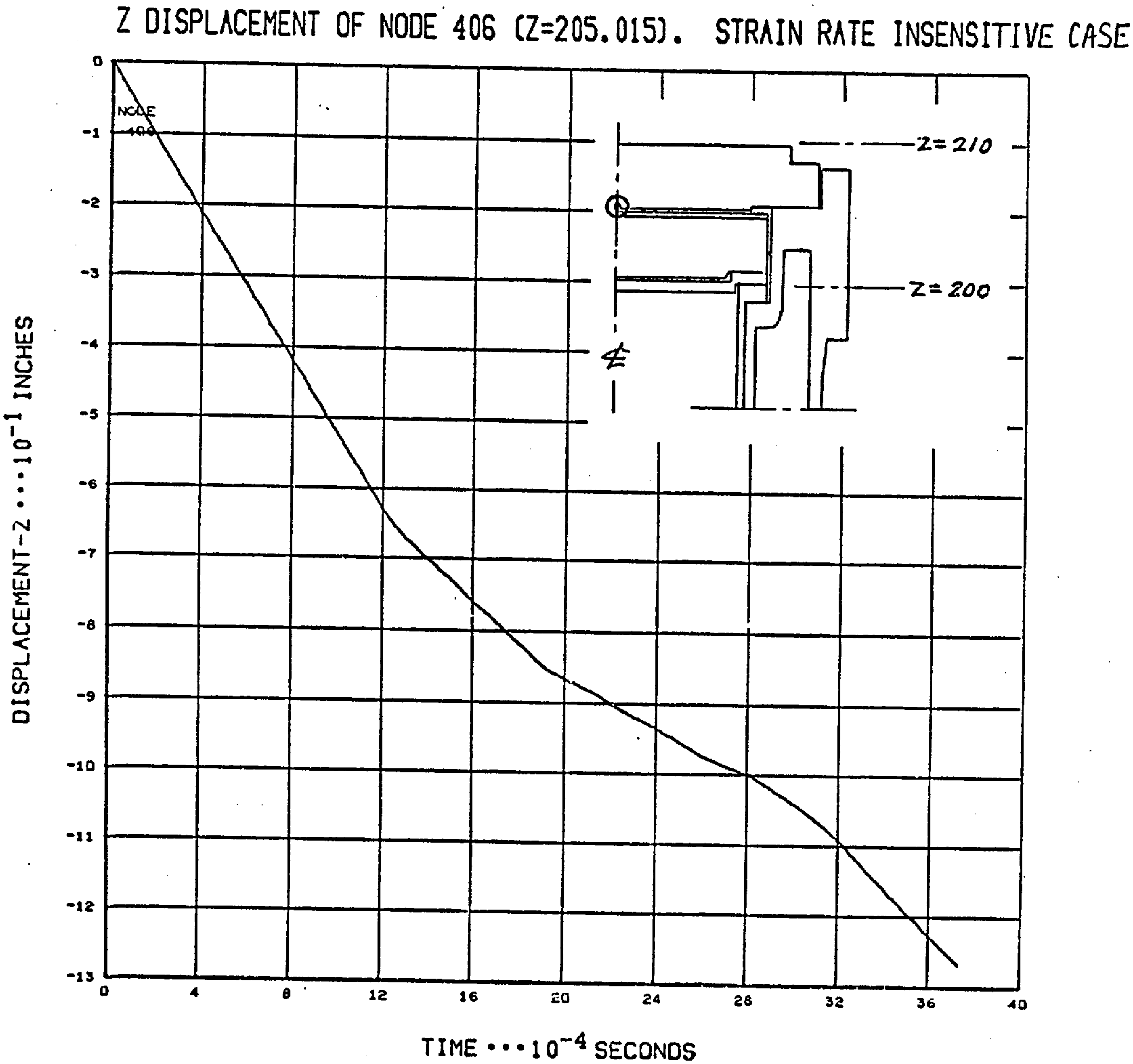
Z DISPLACEMENT OF NODE 406 (Z=205.015). STRAIN RATE INSENSITIVE CASE
NODE 406
Z=210
Z=200
DISPLACEMENT-2 ···10^{-1} INCHES
0
-1
-2
-3
-4
-5
-6
-7
-8
-9
-10
-11
-12
-13
0
4
8
12
16
20
24
28
32
36
40
TIME ···10^{-4} SECONDS

Figure 2-30

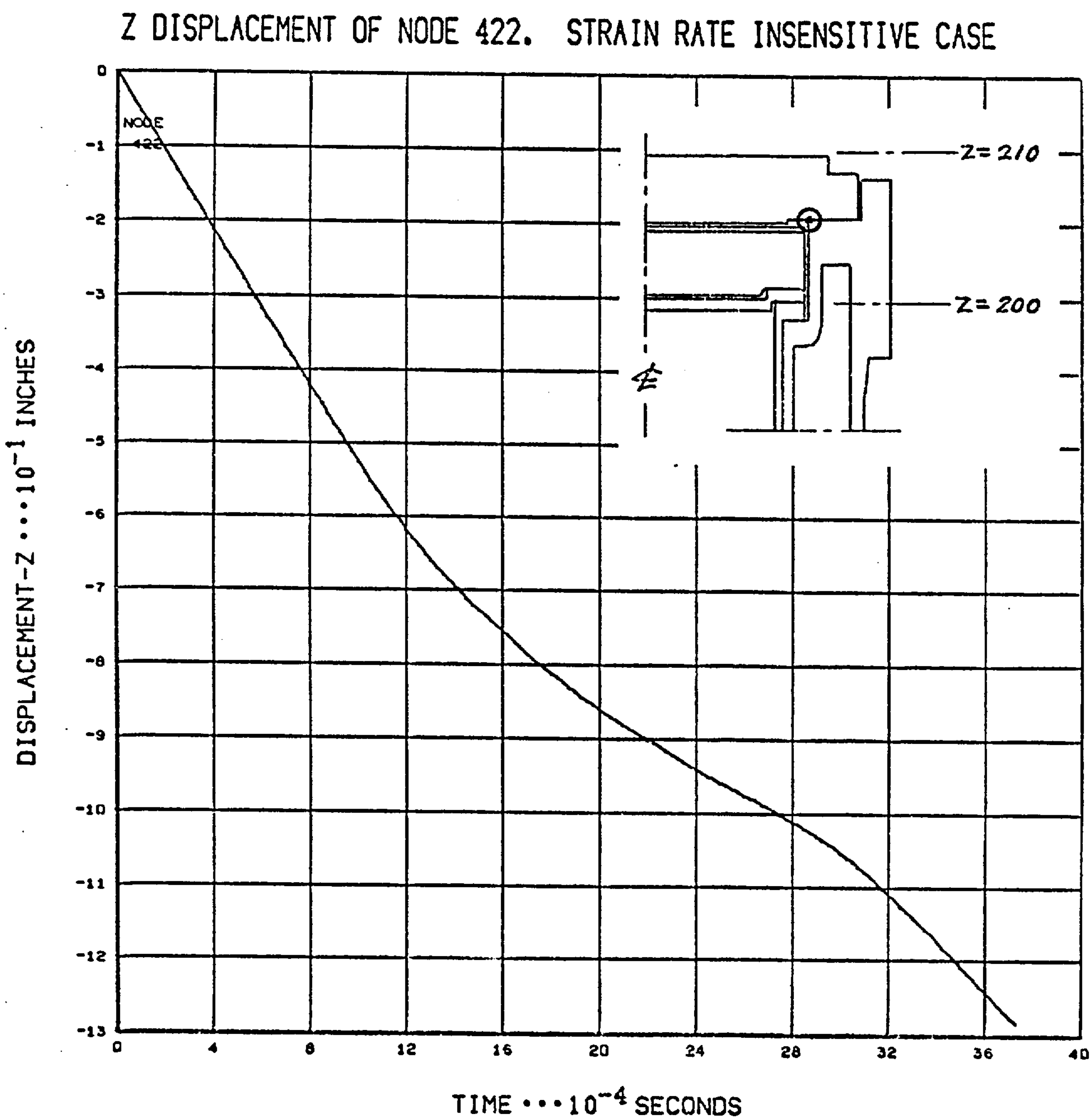
Z DISPLACEMENT OF NODE 422. STRAIN RATE INSENSITIVE CASE
NODE
422
Z=210
Z=200
DISPLACEMENT-Z ···10^{-1} INCHES
TIME ···10^{-4} SECONDS
0
-1
-2
-3
-4
-5
-6
-7
-8
-9
-10
-11
-12
-13
0
4
8
12
16
20
24
28
32
36
40

Figure 2-31

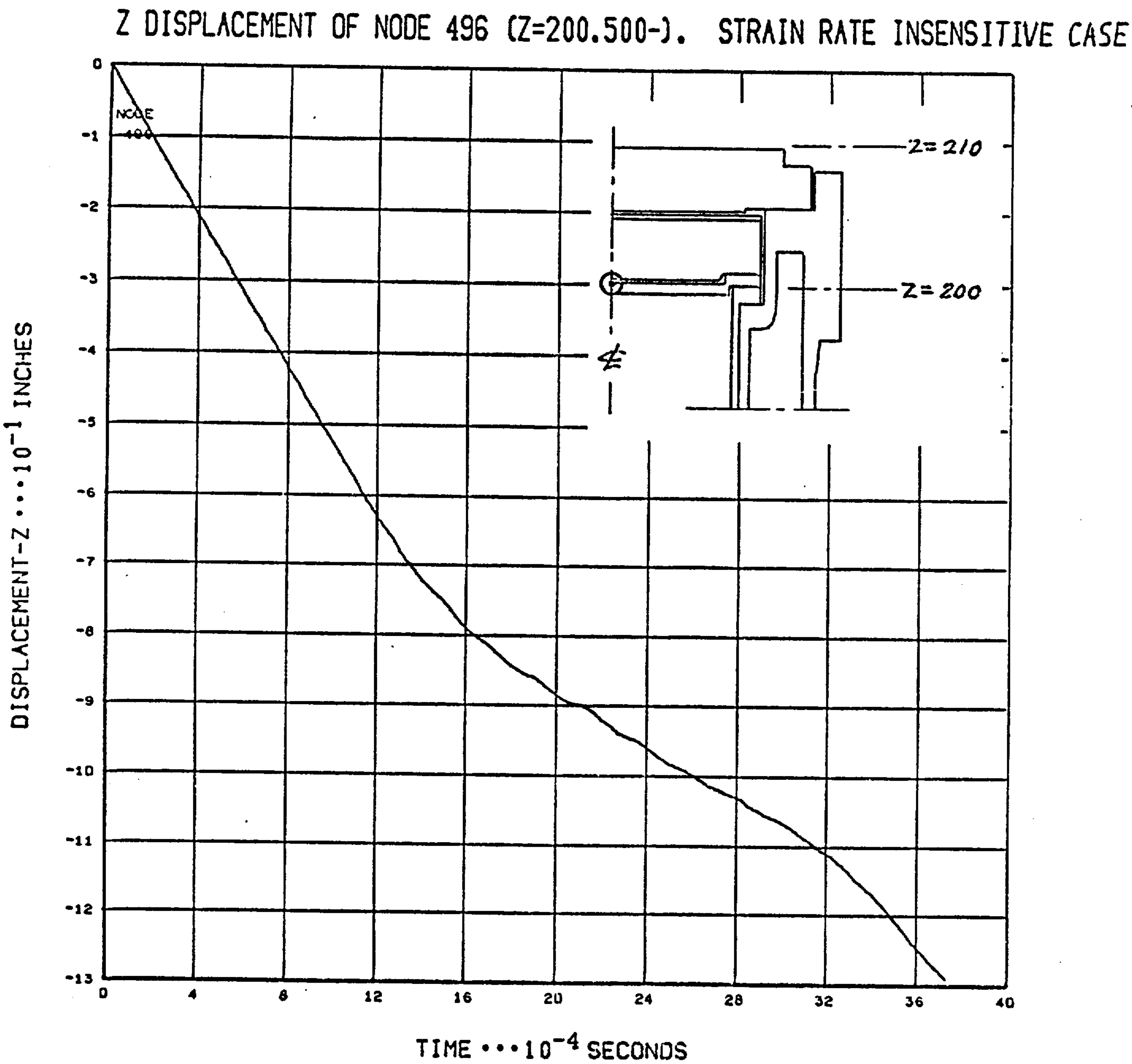
Z DISPLACEMENT OF NODE 496 (Z=200.500-). STRAIN RATE INSENSITIVE CASE
DISPLACEMENT-Z •••10^-1 INCHES
TIME •••10^-4 SECONDS
0
-1
-2
-3
-4
-5
-6
-7
-8
-9
-10
-11
-12
-13
0
4
8
12
16
20
24
28
32
36
40
NODE
Z=210
Z=200

Figure 2-32

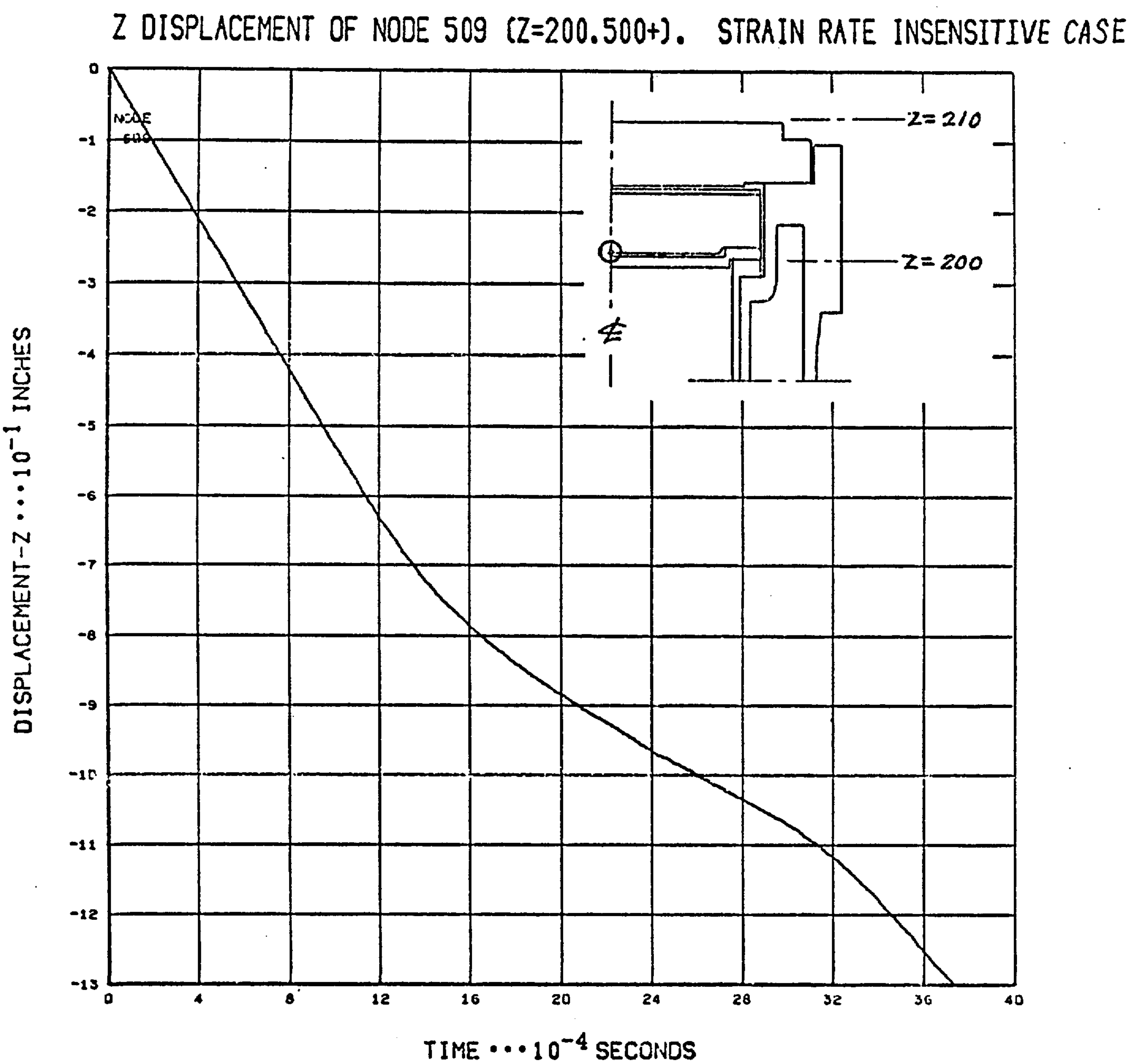
Z DISPLACEMENT OF NODE 509 (Z=200.500+). STRAIN RATE INSENSITIVE CASE
DISPLACEMENT-Z •••10^-1 INCHES
TIME •••10^-4 SECONDS
0
-1
-2
-3
-4
-5
-6
-7
-8
-9
-10
-11
-12
-13
0
4
8
12
16
20
24
28
32
36
40
Z=210
Z=200

Figure 2-33

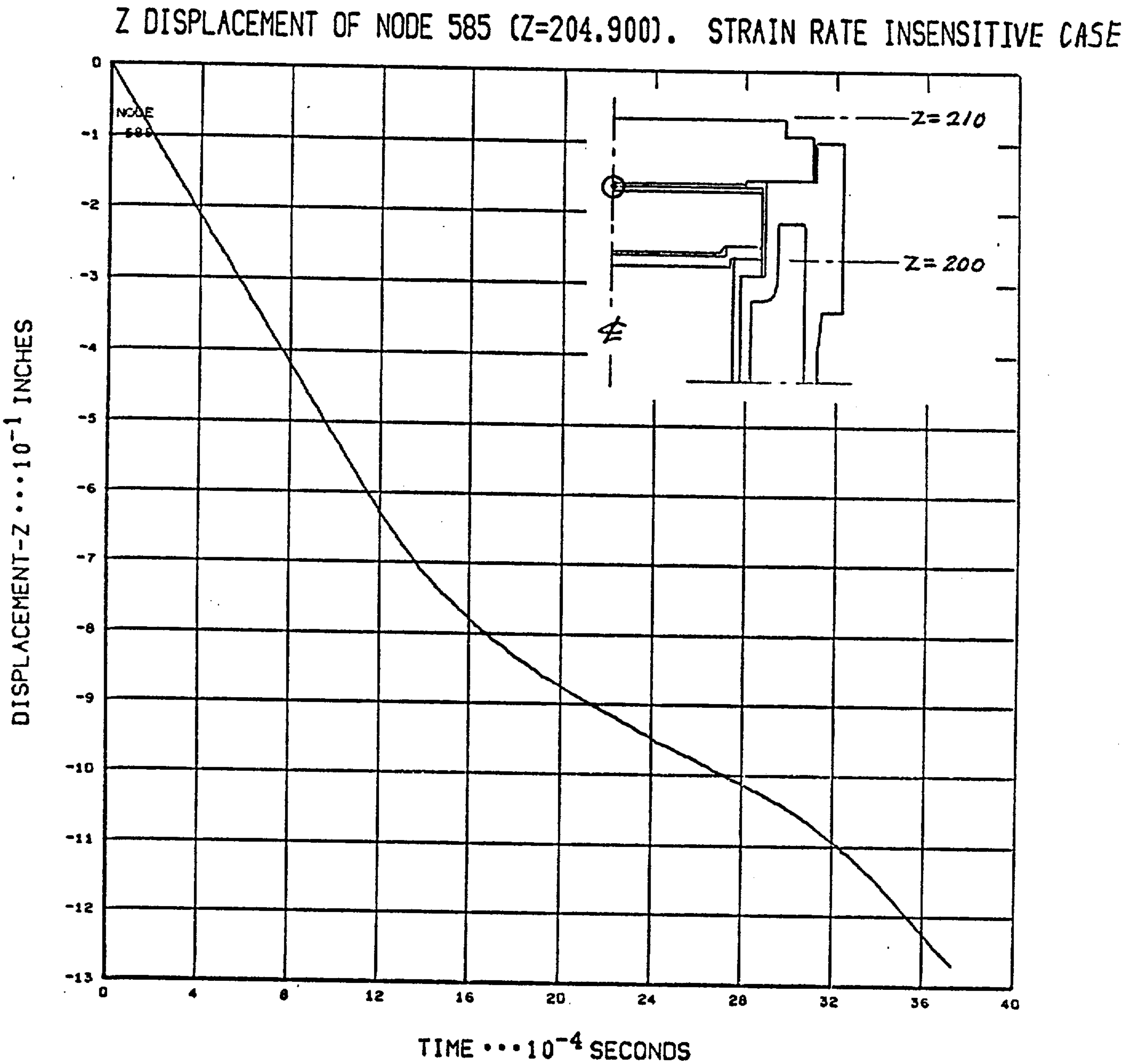
Z DISPLACEMENT OF NODE 585 (Z=204.900). STRAIN RATE INSENSITIVE CASE
NODE 585
Z=210
Z=200
DISPLACEMENT-Z ···10^-1 INCHES
TIME ···10^-4 SECONDS
0
-1
-2
-3
-4
-5
-6
-7
-8
-9
-10
-11
-12
-13
0
4
8
12
16
20
24
28
32
36
40

Figure 2-34

Z DISPLACEMENT AT TOP CENTER OF UPPER BULKHEAD. STRAIN RATE INSENSITIVE CASE

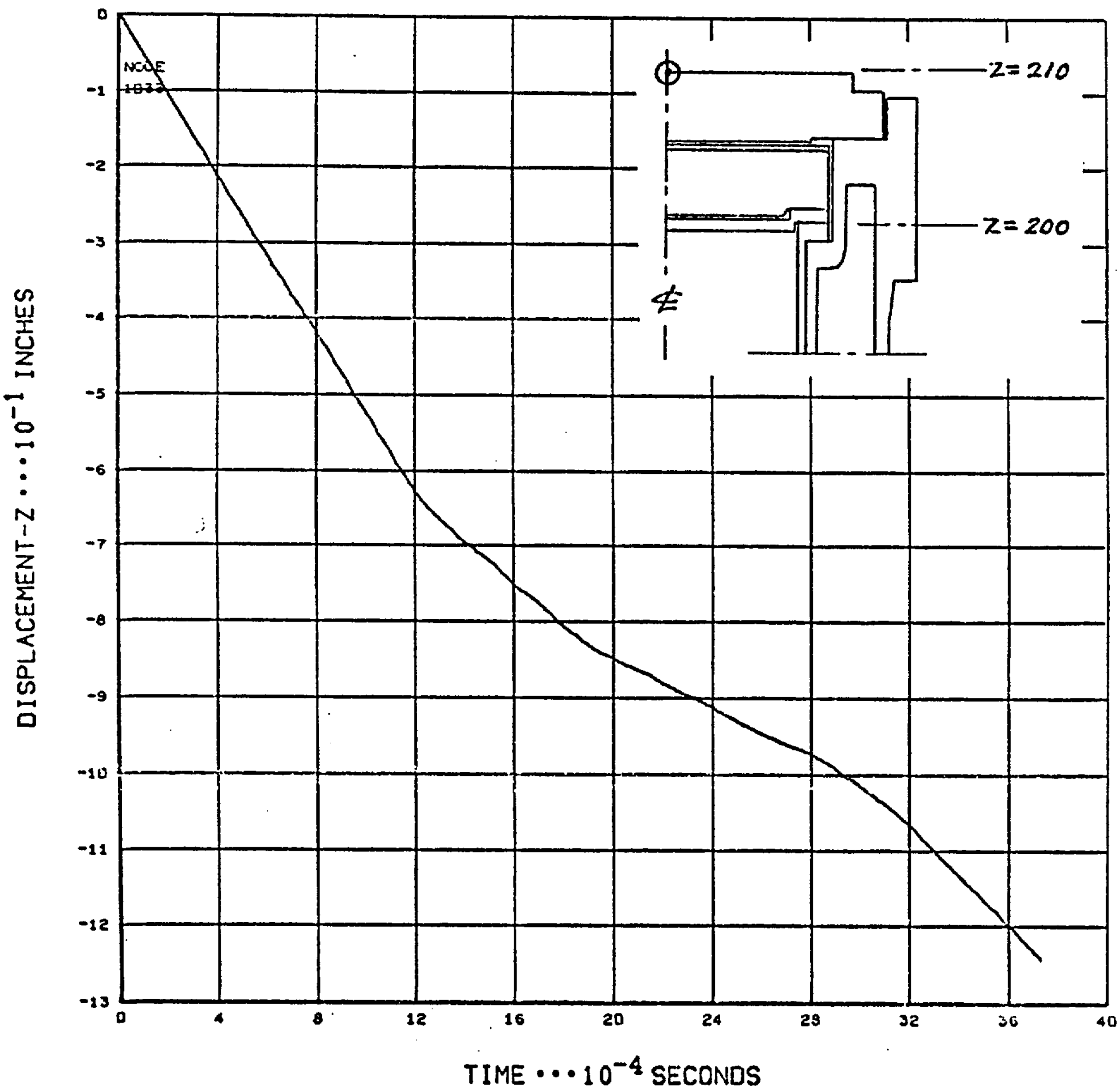

Figure 2-35

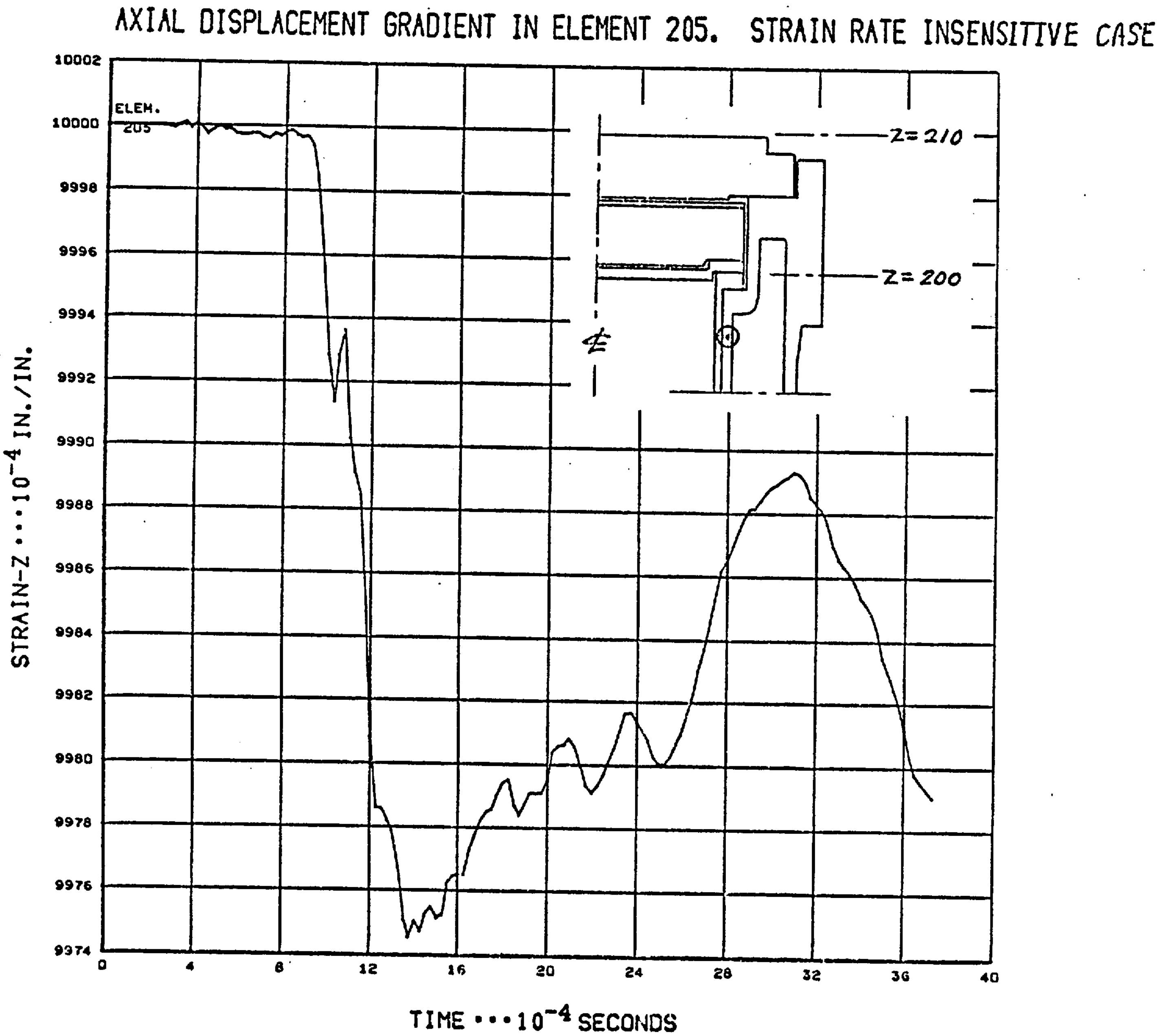
AXIAL DISPLACEMENT GRADIENT IN ELEMENT 205. STRAIN RATE INSENSITIVE CASE
ELEM. 205
10002
10000
9998
9996
9994
9992
9990
9988
9986
9984
9982
9980
9978
9976
9974
STRAIN-Z •••10^-4 IN./IN.
0
4
8
12
16
20
24
28
32
36
40
TIME •••10^-4 SECONDS
Z=210
Z=200

2.7.6.2 Discussion of HONDO Analysis

As stated in Section 2.7.6.1, the critical stresses are maximum for the strain rate sensitive case. For comparison with the stress summary in Section 2.7.6.1, Table 2-10 is provided for the strain rate insensitive case HONDO run.

Z-displacements depicted on Figures 2-14 through 2-20 and Figures 2-28 through 2-34 vary between approximately 0.7 in. and 1.3 in. for the time span considered.

Corresponding range of elongation based on a cask length of ~200 in.:

$$\frac{0.7}{200} < \varepsilon < \frac{1.3}{200}$$

or

$$0.35\% < \varepsilon < 0.65\%$$

which corresponds well to the 0.5% range used for construction of stress-strain diagrams in the materials data for HONDO input Section 2.7.4.

Materials

In order to clarify the validity of the materials data used, an additional HONDO run was made in December 1978 (Run No. BOT-08). The model for this run is identical to the original strain rate sensitive case model (Run No. BOT-02) with the exception of the lid uranium shield, for which strain rate insensitive behavior was input.

TABLE 2-10
MAX. ABSOLUTE STRESS SUMMARY PER C.P.O.
(STRAIN RATE SENSITIVE CASE. (RUN NO. BOT-03)

Component	Element No.	Time (10^{-4} sec.)	Predominant Stress Type(s)	Max. or Min. Principal Stress (psi)	Yield Strength at Temp. (psi)
4340 Stl. Bulkhead	232 (Bot. CL)	12.5	Rad & Hoop	23,520	150,000 (300°F)
0.2% Mo-U Alloy Shield, Lid	347 (Top CL) 303 (Bot. CL)	13.0 13.5	Rad & Hoop Rad & Hoop	-18,110 15,650	36,300 (300°F)
Top end of Cask	205 (Inner Cyl.)	12.0	Axial Compr.	-30,980	30,300 (250°F)
Top End of Container	468 Cylinder Below Flange	23.0	Axial Tens.	30,830	29,200 (300°F)
Container Lid Housing	281 (Bot. CL)	13.0	Rad & Hoop	18,260	29,200 (300°F)

As expected the stress and strain histories of all points outside of the lid are virtually identical for the two models. For the critical points (top and bottom centerline) of the lid shield results from Run No. BOT-08 are summarized in Table 2-11 (compare with Table 2-10).

TABLE 2-11
MAXIMUM ABSOLUTE STRESS SUMMARY PER C.P.O (RUN NO. BOT-08)
(STRAIN RATE SENSITIVE CASE, EXCEPT FOR LID SHIELD)

Component	Element No.	Time (10^{-4} sec.)	Predominant Stress Type(s)	Max. or Min. Principal Stress (psi)	Yield Strength at Temp. (psi)
0.2% Mo-U Alloy Shield Lid	347 (Top CL)	13.0	Rad & Hoop	-28,930	36,300 (300°F)
	303 (Bot CL)	13.5	Rad & Hoop	29,660	

Plots of the hoop stress in element 303 and the radial stress in element 347 vs. time for Run No. BOT-08 are shown on Figure 2-24 and 2-26 (compare with Figures 2-10 and 2-12.)

It is seen that for all three enveloping models (strain rate insensitive case, strain rate sensitive case, and strain rate sensitive with insensitive shield case) the maximum absolute stress in the uranium alloy lid shield will be below static ($\dot{\varepsilon} = 10^3$) yield strength at 300°F.

Run BOT-08 vertical displacements of bulkhead and lid are virtually identical to those depicted on Figures 2-15 and 2-19. The comments in Section 2.7.6.1 regarding possible interference are therefore still applicable.

For the strain rate sensitive case depicted on Figure 2-10 for elem. 303 there may theoretically be some plastic strain in the shield since a yield strength of 8180 psi is assumed at an extreme low strain rate of 10^{-6}. However, as shown below by a conservative calculation, the amount of plastic strain will be negligible.

For $\sigma \leq 8180$ psi: elastic strain regardless of strain rate.

Time span during which 8180 psi $< \sigma <$ 26,190 psi: $T = 6 \times 10^{-4}$ sec (Ref.: Figure 2-10 and Section 2.7.6.1).

Plastic strain may occur during this time span, provided the strain rate $\dot{\varepsilon} < 10^{-3}$.

If $\dot{\varepsilon}$ exceeds 10^{-3} the material will not yield at stresses below 28,000 psi (Ref. Table 2-5).

Total plastic strain $\varepsilon = \int_{T_1}^{T_2} (\dot{\varepsilon})\, dT$

where T_1 = time when σ first exceeds 8180 psi,

T_2 = time when σ drops below 8180 psi, and

$\dot{\varepsilon}$ = strain rate.

Consequently, for $\dot{\varepsilon} < 10^{-3}$:

$$\varepsilon < (10^{-3}) \int_{T_1}^{T_2} dt = (10^{-3})\ (T)$$

$$= (10^{-3})\ (6 \times 10^{-4}) = \underline{6 \times 10^{-7} \text{ in./in.}}$$

$$\sim 6 \times 10^{-5}\% = \underline{0.00006\%}$$

This amount of plastic strain is minute compared with the tested failure strain of the material and will not affect the integrity of the shield.

Properties input for the uranium shield, cylinder, material (material identication No. 3) are irrelevant for the analysis of the top head and lid of the cask. This is because the uranium cylinder is slip-fitted between the inner and outer container shells, and there is a 0.15 in. gap between the top of the shield and the stainless steel cavity containing it. The pressure wave from the ground impact will therefore travel through the stainless steel shells (Material No. 1) unaffected by the uranium shield. In other words: the HONDO stress-strain history of the cask closure system would have been the same regardless of what properties had been input for material no. 3.

The principal tension stress of 50,990 psi shown for element 468 in Table 2-8 is according to the computer output derived from the following stress components:

σ_r = -4,530 psi (radial stress)
σ_z = -50,850 psi (axial tension stress)
σ_T = -26,120 psi (hoop tension stress)
τ = 2,741 psi (shear stress)

Clearly the maximum principal stress in element 468 is oriented very close to the axial direction of the cask.

Ultimate tensile strength of material no. 1 is 70,000 psi min. at room temperature. According to the "International Nickel Company Stainless Steel Data Book, Sect. 2, Bulletin A (1963 Edition)," pg. 9, the nominal UTS varies from 78,000 psi @70°F to 55,000 psi @1000°F. Conservatively assuming a linear variation even at the lower end of the range from 70°F to 1000°F this corresponds to 78,000 - 55,000/1000 - 70 = 24.73 psi/°F. UTS at 300°F = 70,000 - (300-70)(24.73) = 70,000 - 5700 = 64,300 psi.

2.7.7 Evaluation of FSV-1 Configurations F and G

2.7.7.1 DISCUSSION

The complete structural evaluation of Model FSV-1 in Configurations E, F and G is presented in other parts of Section 2.0. This evaluation is applicable to Configurations F and G when used for the transport of irradiated hardware.

2.7.7.2 Evaluation

The 12-in. thick closure plug for the burial canister provides supplemental shielding for both the normal conditions of transport and the hypothetical accident conditions. During the normal conditions of transport, there are no forces which would move this closure plug from its installed position. The hypothetical accident condition most likely to apply forces tending to move the closure plug is the 30-ft drop onto an essentially unyielding surface. Neither a drop on the impact limiter nor a drop on the side would apply forces which would move the closure plug from its installed position. The drop from 30 ft onto the bottom end of the cask could apply a deceleration force of up to 905 times the force of gravity (905 g). The burial canister rests on the bottom of the cask cavity and the closure plug is supported on a shoulder at the open end of burial canister as shown on GADR-55-2-12 and GADR-55-2-13. As a result of the drop, the closure plug, which weighs 654 lb, will apply a force of 592,000 lb to the burial canister. The shoulder contact area between the burial canister and the closure plug is 11.2 in.^{2} and the burial canister wall has an area of 12.4 in.^{2} Therefore, the stress at the shoulder is:

$$\frac{592{,}000}{11.2} = 52{,}857 \text{ lb/in.}^2$$

and in the wall is:

$$\frac{592{,}000}{12.4} = 47{,}742 \text{ lb/in.}^2$$

The carbon steels used for these components of the burial canister have yield strengths of 30,000 to 35,000 lb/in.^{2} and ultimate strengths of 55,000 to 60,000 lb/in.^{2}. As a result of these stresses which are above yield for the materials involved, there will be some deformation until the available energy is expended. This deformation will be contained within the cask cavity and thus the displaced position of the closure plug will be such that its shielding effectiveness will be maintained.

The base plate of the burial canister as shown on GADR 55-2-12 and GADR 55-2-13 also provides supplemental shielding for both the normal conditions of transport and the hypothetical accident conditions. Only during the 30-ft drop onto the closure end of the cask would there be forces which would tend to move the base plate from its installed location. Because of the plywood impact limiter, the axial decelerating will not exceed 107 times the force of gravity (107 g). As a result of this deceleration, the base plate which weighs 165 lb, will apply a force of 17,655 lb to the burial canister wall. This wall has an area of 12.4 in.^{2} and the stress in the wall will be:

$$\frac{17,655}{12.4} = \underline{1,424} \text{ lb/in.}^2$$

This stress is well below the 30,000 to 35,000 lb/in.^{2} yield strength of the material and, therefore, the base plate will remain in place and provide the necessary shielding.

2.8 APPENDIX

2.8.1. Discussion

In an effort to obtain a preliminary indication of the ductility properties of uranium at subzero temperatures, a series of drop test was scheduled and conducted at National Lead Company's Albany branch. Samples of unalloyed depleted uranium were tested along with various samples of low alloys to serve as a basis for comparison.

Various diameters of as cast depleted uranium round bar were used; however, each round bar was cut to length such that the length to diameter ratio was 8 to 1 - this being approximately the same as the L/D ratio of the depleted uranium in Model FSV-1 in Configurations E, F and G.

Most drops were conducted from a height of 29 feet, 3 inches onto essentially unyielding surfaces of either steel or concrete. Two samples, also from a height of 29 feet 3 inches, were dropped on a sharp edged fulcrum. Temperature at the top of drop of all samples ranged between -55°F to -60°F.

Results of these preliminary drop test indicated that the unalloyed depleted uranium exhibited good ductility properties at low temperatures. Furthermore, it wasn't until the third 29 feet 3 inches drop of a test specimen that ductility failure occurred. A 1-3/16" diam by 9-1/2 inch long unalloyed depleted uranium round bar was dropped on a concrete impact surface with no visible failure resulting. The same test specimen was then dropped from the same height of 29 feet 3 inches and at the same temperature of -60°F on a steel plate. This time a slight bend in the bar was noted. On the third test, the specimen was dropped on the sharp edge of a steel angle. Along with a greater bend in the bar, it was noted that a small crack developed opposite the side of impact.

2.8.2 Results

See Table 2-12 on following page for the results of these tests.

2.8.3 Low Temperature 1/8 Scale Uranium Shell Impact Tests

2.8.3.1 Purpose of Tests

Experimental knowledge is required of the effects of impact loads as used in casks with uranium shielding and having relatively large L/D ratios. The experimental test specimen was subjected to several puncture tests to determine the amount of deformation and to observe the surface condition of the uranium in the impacted areas.

TABLE 2-12
RESULTS

Test No.	Specimen Drop No.	Material (As-Cast)	Diameter (in.)	Attitude at Impact	Impacting Surface	Test Results
1	1	U-2% Mo	1-1/4	Horizontal	Concrete	No failure
2	1	Unalloyed	1-3/16	Horizontal	Concrete	No failure
3	1	Unalloyed	1-3/16	Horizontal	Concrete	No failure
4	1	U-1% Mo, 1% Nb	0.6	Horizontal	Concrete	No failure
5	1	U-1% Mo, 1% W	0.6	45° Corner Drop	Concrete	No failure
6	1	U-1% Nb, 1% W	0.6	45° Corner Drop	Concrete	No failure
7	1	U-1% Ta, 1% W	0.6	Horizontal	Concrete	No failure
8	1	Unalloyed	0.6	Horizontal	Concrete	No failure
9	1	Unalloyed	0.6	Horizontal	Concrete	No failure
10	2	Unalloyed	1-3/16	Horizontal	Stl Plate	Slight Bend
11	2	Unalloyed	1-3/16	Horizontal	Stl Plate	Slight Bend
12	2	U-2% Mo	1-1/4	Horizontal	Stl Plate	No failure
13	2	U-1% Mo, 1% W	0.6	Horizontal	Stl Plate	No failure
14	2	Unalloyed	0.6	Horizontal	Stl Plate	Slight Bend
15	3	Unalloyed	1-3/16	Horizontal	90° Corner	Bent & Cracked
16	3	Unalloyed	1-3/16	Slight Angle Corner Drop	90° Corner	Bent

Test Conditions

Height of drop	29'3"
Temperature of specimens	-55°F to -60°F
Material Condition	As cast
Material Configuration	Round bars, L/D = 8:1

2.8.3.2 Material Used

An as cast 0.2% - 0.3% molybdenum-uranium cylindrical shell, 1/8 the size of the actual shielding in the shipping cask, was used for this series of tests.

Comparative dimensions and weights:

	1/8 Scale Cylindrical Shell	Full Size Uranium Shielding
Outside diameter	3-1/4"	26"
Inside diameter	2-3/8"	19"
Length	24-3/8"	194"
Weight	64 lb	32,800 lb

2.8.3.3 Test Procedures

Tests were conducted using the indoor drop test facilities of NLC, Wilmington branch.

An iron-constantan thermocouple was attached to the outer surface of the uranium cylindrical shell. The thermocouple extension leads were connected to a calibrated pyrometer indicator.

The test specimen was then submerged in a solution of acetone and dry-ice until it reached a temperature of approximately -60°F. With the thermocouple still attached, the uranium was connected to a quick release mechanism which, in turn, was attached to an overhead crane. The entire assembly was moved over the impact area which consisted of a 3/4 inch wide carbon steel fulcrum 4 inch deep and 12 inch long welded to a 12 inch x 12 inch x 3/4 inch carbon steel base plate. This weldment was resting on a steel anvil pad supported by a concrete foundation. With the use of a scaled line and plumb bob, the test specimen was raised to a height of 40 inches over the fulcrum. Its long axis was positioned level and perpendicular to the long axis of the fulcrum so that the center of gravity of the shell would impact against the fulcrum.

When the pyrometer indicator measured a surface temperature of -40°F the solenoid on the release mechanism was actuated, pulled a release pin and allowed the test specimen to free fall on the fulcrum.

This same test was conducted at 60 inches, 80 inches, 100 inches and 120 inches. Measurements were taken after each test of the outside diameter, inside diameter, length and angle of bend.

2.8.3.4 Results

Results of all free fall fulcrum tests proved negative. The test specimen experienced no dimensional changes or deformations.

The 120 inches drop test had a rebound after impact of 31-1/4 inches above the fulcrum--the test specimen remained level during the rebound. Although no damage occurred to the uranium, the 3/4 inch fulcrum received an indentation approximately 1/4 inch deep.

2.8.4. Uranium Weld Joint Study

2.8.4.1 Discussion

Successful completion of side puncture tests on a uranium casting scale model has prompted a review of impact condition analyses and has also allowed consideration of a type of joint for the uranium sections which permits a greatly reduced depth of welding.

The previous calculations for side wall puncture assumed the onset of plastic hinge deformation at 30,000 psi, and required that 83% of the kinetic energy of the 40 in. drop had to be absorbed by this mechanism. The new drop tests proved that more than double this height of drop did not produce any measurable permanent set. Obviously, justification of this performance requires that the calculated instantaneous peak bending stresses be allowed to reach for higher values and still be elastic.

The effects of this new performance are now investigated in regard to accident conditions, and include the behavior of the redesigned joints under such loadings.

According to the tests, separately reported, a drop height of 120 in., with a rebound of 31-1/4 in., can be credited, conservatively, with kinetic energy proportional only to a drop of 120 - 31-1/4 = 88-3/4 in. This means that energy 2.22 times the specified 40 in. drop was successful absorbed elastically.

2.8.4.2 Puncture Side Wall - 88-3/4 in. drop analysis.

The stainless steel outer shell, as the member directly exposed to penetration by the steel piston, is not critical. The piston merely cuts partly into the wall, due to the back-up effects of the uranium cylinder.

The uranium cylinder (as tested) is taken as a model, but calculations are now made on a full size cylinder analyzed as a separate body in an elastic drop up to 88-3/4 in.

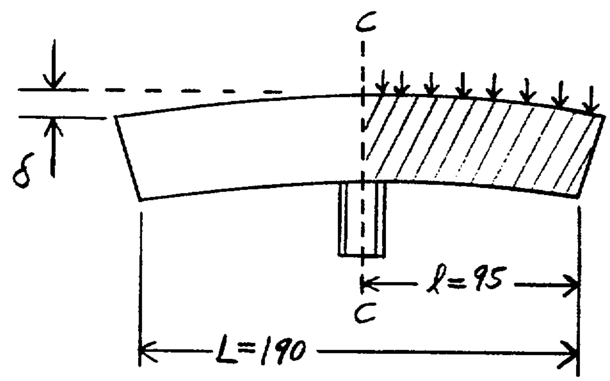

Consider 1G Load on Cantilever

D = 26 in., d = 19 in.

ℓ = 95 in., L = 190 in.

Vol. = (531-284) $in.^2$ (190 in.) = 46,930 $in.^3$ total

Wt = 46,930 (0.683) = 32,000 lb total

$I = 0.0491\ (26^4 - 19^4) = 16{,}041\ in.^4$

$Z = 16{,}041/13 = 1235\ in.^3$

$$M_c = \frac{w\ell}{2} = \frac{32{,}000}{2}\ \frac{95}{2} = 760{,}000\ \text{in. lb}$$

$$\delta = \frac{w\ell^3}{8EI} = \frac{16{,}000\ (95)^3}{8(29)\ 10^6\ (16{,}041)} = 0.0369\ \text{in.}$$

$$S_b = \frac{M_c}{Z} = \frac{760{,}000}{1235} = 615\ \text{psi}$$

From Marks Handbook, sixth edition, page 5-44:

$$U_{cantilever} = \frac{n^2}{m} \frac{K}{c}^2 \frac{S^2V}{2E} \text{ for uniform load}$$

$$n = 2 \quad m = 8 \quad K = \text{rad. gyr.} = \frac{\sqrt{D^2 + d^2}}{4} \text{ for tube section}$$

$$c = D/2$$

$$\therefore U_{cant.} = \frac{(2)^2}{8} \frac{4}{16} \frac{(D^2 + d^2)}{D^2} \frac{S^2V}{2E} = \frac{D^2 + d^2}{16D^2} \frac{S^2V}{E} \text{ for 1/2 beam lgth.}$$

$$U_B = \frac{D^2 + d^2}{8D^2} \frac{S^2V}{E} \text{ for full length beam as above}$$

$$= \frac{26^2 + 19^2}{8 \times 26^2} \frac{S^2(46,930)}{29\ (10^6)} = \frac{674 + 361}{8\ (676)} S^2 \frac{1615}{10^6} = \frac{310}{10^6} S^2$$

Now S = 615 psi for 1G load

$$U_B = \frac{310\ (615)^2}{10^6} = 117 \text{ in. lb} \quad \text{Note: } U_B \ \alpha \ S^2 \ \alpha \ (G's)^2$$

Line	G's	S psi	δ in.	(G's)²	U_B in. lb	Height Drop
1	1	615.	0.00369	1	117	
2	50	30,750	0.1845	2500	292,500	
3	104.5	64,300	0.386	10,920	1,280,000	40
4	156.	96,000	0.575	24,280	2,840,000	88-75

The stress of 96,000 psi is reached "instantaneously" and only at the top mid point of the beam. This peak is quite consistent with nominal properties of unalloyed cast uranium. Static compression, stress-strain curves for cast, unalloyed depleted uranium are shown in Figure 2-36.

The specification is limited to the values of Line 3. The joints are actually at positions B and the moment and stress is reduced to 4/9.

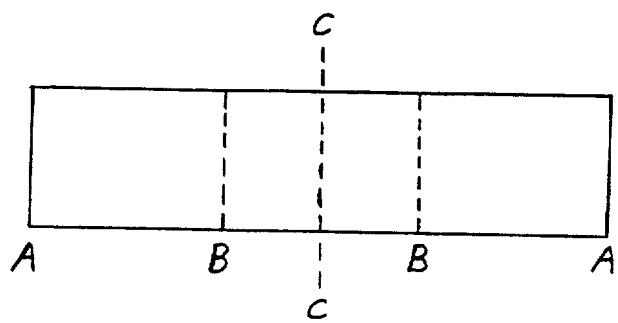

$$\frac{M_B}{M} = \frac{(2/3\ Wt)(2/3\ell)}{(Wt)(\ell)} = 4/9 \quad \therefore\ S_B = \frac{4}{9} S_B = \frac{4}{9}(64{,}300)$$

$$= \underline{28{,}600\ \text{psi}}$$

2.8.4.3 Results

Since the "solid" cylinder of the tests (equivalent to full depth penetration weld) has withstood at its midsection 96,000 psi, it would be theoretically possible to reduce the depth of an outside weld for position B so that Z for the weld area is only

$$Z_{B2} = \frac{28{,}600}{96{,}000} 1235 = \underline{368}$$

Figure 2-36.

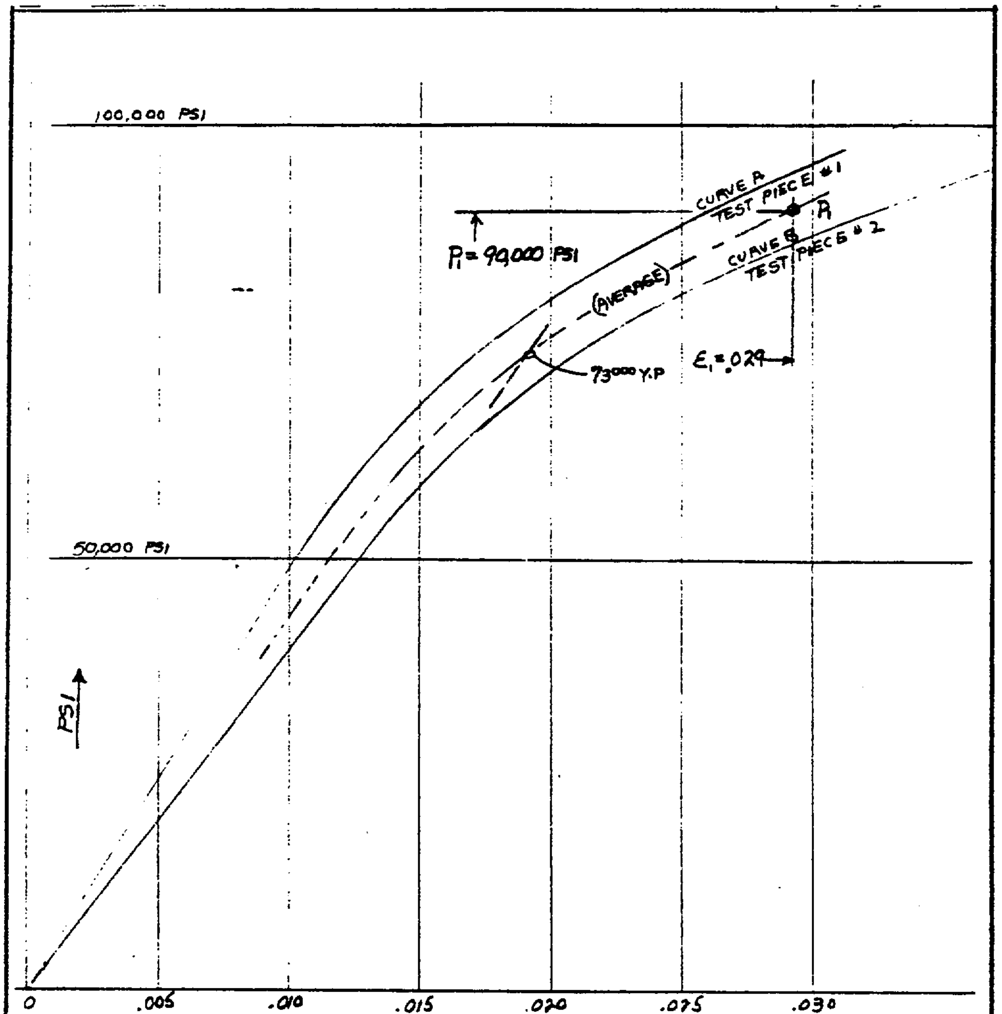

STATIC COMPRESSION STRESS-STRAIN CURVES
UNALLOYED DEPLETED URANIUM
"AS CAST" FOR SHIELDING - N.L.C. FEB. 1970
BACKOS

to find the i.d. which corresponds to this Z value, let

$$Z_{B2} = 368 = \frac{0.098}{26}(26^4 - d^4) = 0.00378\,[457{,}000 - d^4]$$

$$d^4 = \frac{1725 - 368}{0.00378} = 359{,}000$$

$$d = 24.5 \text{ in.} \quad \therefore\ t = \frac{26 - 24.5}{2} = \underline{3/4\text{-in. weld req'd min.}}$$

To be quite conservative, it is desirable to double this depth of weld, using 2 layers of 3/4-in. penetration welds (in offset relationship), providing continuous beam strength in an outer annulus 1-1/2 in. thick out of a total of 3-1/2-in. wall. The inner 2 in. would be machined with interlocking steps (four of 1/2-in. each) providing concentric shear rings and effective shielding pattern as illustrated.

Figure 2-37

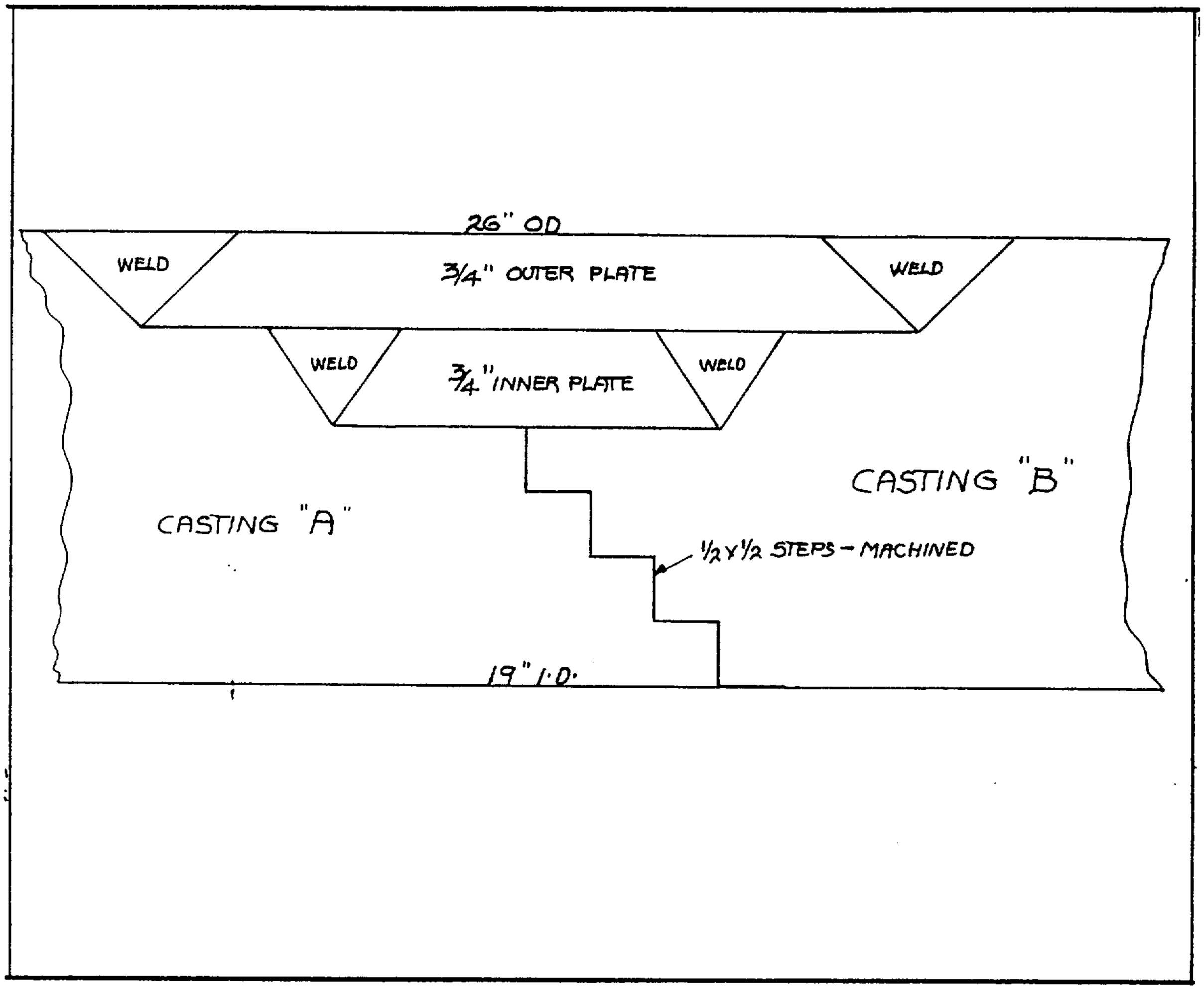
26" OD
WELD
3/4" OUTER PLATE
WELD
WELD
3/4" INNER PLATE
WELD
CASTING "B"
CASTING "A"
1/2 X 1/2 STEPS - MACHINED
19" I.D.

References

2-1. ASME Boiler and Pressure Vessel Code Section III - Nuclear Vessels, The American Society of Mechanical Engineers, United Engineering Center, NY, 1965.

2-2. ASME Boiler and Pressure Vessel Code Section IX - Welding Qualifications, The American Society of Mechanical Engineers, United Engineering Center, NY, 1965.

2-3. "Metallic O-Rings," United Aircraft Products, Inc., Bulletin No. 596191B, Dayton, Ohio, July 15, 1959.

2-4. "O-Ring Design Handbook," Plastic and Rubber Products Company, Ontario, California.

2-5. "Bolt, External Wrenching, Self-Retained by Washer," Standard Pressed Steel Company, Jenkintown, PA, Part Number and Specification 69241, Sheets 1, 2, and 3, March 6, 1968.

2-6. "Heli-Coil Screw-Lock Inserts," Heli-Coil Corporation, Danbury, Connecticut, Bulletin 900.

2-7. Aerospace Structural Metals Handbook, Dept. of Defense.

2-8. Clifford, C. B., "Design and Fabrication of a Prototype Laminated Uranium Metal Shipping Cask for Large Shipments of Co-60," USAEC Research and Development Report No. KY-521, Union Carbide Corporation, Nuclear Division, Paducah, KY, April 3, 1967.

2-9. Alloy Digest. HY-130 and HY-140(T) Steel Alloy, Filing Code: SA-280. Published by Engineering Alloys Digest Inc., September 1972.

2-10. Memo: FSV-ME:MLN:42:79, Nichols to Ketchen dated 4/3/79, "Summary of Plywood Evaluation Tests for the FSV-1 Shipping Cask Impact Limiter."

2-11. Handbook of the Engineering Sciences - Volume I, "The Basic Sciences."

2-12. Roark: "Formulas for Stress and Strain," 5th Edition.

2-13. Mantell, C. L., "Engineering Materials Handbook, 1958, McGraw.

2-14. Biggs, John M., "Introduction to Structural Dynamics," McGraw-Hill, 1964.

2-15. Clifford, C. B., "USAEC Research and Development Report Number KY-546," Union Carbide Corporation.

2-16. Lipp, Robert H., "Bolt Torque Factors," Design News Magazine, March 8, 1971 issue.

2-17. GAMD-9710. SAC Manual. Prepared by H.D. Shatoff. Dated 15 December 1969.

2-18. Parker Gask-O-Seal Handbook OSD 5411 (1977).

2-19. J. E. Shigley, "Mechanical Engineering Design," McGraw-Hill 1963.

2-20. Rack, H. J., "The Influence of Strain Rate and Temperature ___ Steele ___ Shipping Cask," SAND-75-0579. UC-79c, dated February 1976.

2-21. Burke, Colling, Gorum and Greenspan: "Physical Metallurgy of Uranium Alloys," First Ed. 1976.

2-22. SLA-74-0039, "HONDO - A Finite Element Computer Program" by S. W. Key April 1974.

2-23. Blasch, Stukenbroeker, Lusky, Bonilla, Berger: "The Use of Uranium as a Shielding Material," Nuclear Engineering and Design, Vol. 13 (1970), p. 146 and on.

2-24. Y-DA-3616, "Compilation of the Mechanical Properties of Dilute (5% maximum) Alloys of Uranium," Union Carbide Corp.

2-25. Steichen, J. M., "High Strain Rate Mechanical Properties of Type 304 stainless" HEDL-TME 71-145. Hanford Engineering Development Lab, dated September 1971.

2-26. Nuclear Systems Materials Handbook, Vol. 1. Design Data Part IV Nuclear Fuel Materials, Group 2 - Metals, Section 1 Uranium, Revision 1, 12/1/74.

2-27. Product Handbook, INCO Alloys International, Huntington, West Virginia, 1988 p. 11.